Earth-Science Reviews 224 (2022) 103875

Contents lists available at ScienceDirect

Earth-Science Reviews

journal homepage: www.elsevier.com/locate/earscirev

Evolution of the Laurentide and Innuitian ice sheets prior to the Last Glacial Maximum (115 ka to 25 ka)

April S. Dalton [a,b,*], Chris R. Stokes [a], Christine L. Batchelor [c]

[a] Department of Geography, Durham University, Durham, United Kingdom
[b] Department of Physical Geography and Geoecology, Charles University, Prague, Czech Republic
[c] School of Geography, Politics and Sociology, Newcastle University, Newcastle upon Tyne, United Kingdom

ARTICLE INFO

Keywords:
Wisconsinan Stade
Last Glacial Maximum
Keewatin Dome
Labrador Dome
Last glacial cycle

ABSTRACT

The Laurentide Ice Sheet was the largest global ice mass to grow and decay during the last glacial cycle (~115 ka to ~10 ka). Despite its importance for driving major changes in global mean sea level, long-term landscape evolution, and atmospheric circulation patterns, the history of the Laurentide (and neighbouring Innuitian) Ice Sheet is poorly constrained owing to sporadic preservation of stratigraphic records prior to the Last Glacial Maximum (LGM; ~25 ka) and a case-study approach to the dating of available evidence. Here, we synthesize available geochronological data from the glaciated region, together with published stratigraphic and geomorphological data, as well as numerical modelling output, to derive 19 hypothesised reconstructions of the Laurentide and Innuitian ice sheets from 115 ka to 25 ka at 5-kyr intervals, with uncertainties quantified to include best, minimum, and maximum ice extent estimates at each time-step. Our work suggests that, between 115 ka and 25 ka, some areas of North America experienced multiple cycles of rapid ice sheet growth and decay, while others remained largely ice-free, and others were continuously glaciated. Key findings include: (i) the growth and recession of the Laurentide Ice Sheet from 115 ka through 80 ka; (ii) significant build-up of ice to almost LGM extent at ~60 ka; (iii) a potentially dramatic reduction in North American ice at ~45 ka; (iv) a rapid expansion of the Labrador Dome at ~38 ka; and (v) gradual growth toward the LGM starting at ~35 ka. Some reconstructions are only loosely constrained and are therefore speculative (especially prior to 45 ka). Nevertheless, this work represents our most up-to-date understanding of the build-up of the Laurentide and Innuitian ice sheets during the last glacial cycle to the LGM based on the available evidence. We consider these ice configurations as a series of testable hypotheses for future work to address and refine. These results are important for use across a range of disciplines including ice sheet modelling, palaeoclimatology and archaeology and are available digitally.

1. Introduction

The North American ice sheet complex (consisting of the Laurentide, Cordilleran and Innuitian ice sheets; Fig. 1) was the largest global ice mass to grow and recede during the last glacial cycle (~115 ka to ~10 ka). Accordingly, its evolution played a fundamental role in many aspects of the Earth System, including the ability for humans to migrate to North America (Becerra-Valdivia and Higham, 2020; Bennett et al., 2021), global sea level change (Clark et al., 2009; Gowan et al., 2021), landscape evolution (Whipple et al., 1999; Wickert et al., 2013), the potential for carbon storage on the continent (Packalen et al., 2014; Treat et al., 2019) and atmospheric circulation (Löfverström and Lora, 2017; Tulenko et al., 2020). Specifically, the last glacial cycle (known as the Wisconsinan Stade in North America) comprised the growth, evolution and recession of continental ice that took place between the largely ice-free Marine Isotope Stage 5e (MIS 5e; ~125 ka) and the Holocene (~12 ka to present-day). The marine $\delta^{18}O$ record, used as a proxy for changes in sea level and continental ice volumes (Bintanja et al., 2005; Govin et al., 2015; Johnsen et al., 1992a; Linsley, 1996), suggests a waxing and waning of continental ice, with maximum ice build-up at the Last Glacial Maximum (LGM) around ~25 ka (Fig. 2; Clark et al., 2009; Lisiecki and Raymo, 2005). Best understood is the interval from ~25 ka to present-day, when the North American ice sheet complex deglaciated from its maximum LGM extent and left behind an abundance of sediments and landforms from which to reconstruct and date its recession (Dalton et al., 2020; Dyke, 2004; Dyke and Prest, 1987;

* Corresponding author at: Department of Physical Geography and Geoecology, Charles University, Prague, Czech Republic.
E-mail address: aprils.dalton@gmail.com (A.S. Dalton).

https://doi.org/10.1016/j.earscirev.2021.103875
Received 15 May 2021; Received in revised form 5 November 2021; Accepted 24 November 2021
Available online 2 December 2021

Fulton, 1989; Stokes, 2017).

Prior to the LGM, however, the history of continental ice over North America is very poorly constrained owing to sporadic preservation of evidence relating to the pre-LGM ice sheet activity. During that time, insolation at 60°N varied considerably (Fig. 2; Berger and Loutre, 1991) and the Greenland ice core record attests to rapid climate perturbations on the order of ~5°C in ~50 years (Dansgaard-Oeschger events; Dansgaard et al., 1993; Grootes et al., 1993; Johnsen et al., 1992b), suggesting the possibility of major changes to Northern Hemisphere ice extent. Estimates of sea level during this interval, although variable, also document shifts on the order of ±10s m, supporting periods of ice accumulation and decay on the continent (Fig. 2; Clark et al., 2009; Lambeck and Chappell, 2001; Pico et al., 2017; Spratt and Lisiecki, 2016).

Our understanding of pre-LGM continental ice over North America has progressed greatly over the past 100 years. One of the first depictions of the Laurentide Ice Sheet (the largest ice mass in the North American ice sheet complex; Fig. 1) suggested several independent glaciers (Tyrrell, 1898). Later, Flint (1943) proposed a model where large domes coalesced over Hudson Bay at the LGM. Following extensive mapping and geochronological efforts, largely led by the Geological Survey of Canada, a special issue of *Géographie physique et Quaternaire* in 1987 attempted to summarise knowledge on the Laurentide Ice Sheet spanning the last interglacial (~125 ka; St-Onge, 1987), early Wisconsinan (~90 ka; Vincent and Prest, 1987), middle Wisconsinan (~45 ka; Dredge and Thorleifson, 1987) and Late Wisconsinan (post-25 ka; Dyke and Prest, 1987). These papers reviewed available geologic, stratigraphic, and chronological data from the glaciated region and hypothesized ice sheet evolution over the continent during these broad intervals. In 1993, these data were incorporated into a major synthesis of the last glacial cycle (until the LGM) of the Laurentide and Cordilleran ice sheets (Clark et al., 1993). Since then, no comprehensive review of Wisconsinan ice sheets has taken place, despite significant advances in geochronology (notably the prominence of accelerator mass spectrometry and optically stimulated luminescence dating), and almost three decades of research, especially in the past ~10 years.

Here, we present a comprehensive review and analysis of geological and geochronological data to derive empirically constrained reconstructions on the extent of the Laurentide and Innuitian ice sheets. Results are a series of 19 reconstructions detailing the hypothesized extent of the ice sheets at 5-kyr intervals during the build-up phase of the last glacial cycle until the LGM (115 ka to 25 ka). Each map contains the most likely extent, given the available evidence, together with estimates of minimum and maximum ice extents for the given interval that capture uncertainties in the available evidence. The 57 ice margin reconstructions (ie. 'best', 'minimum' and 'maximum' ice estimates for

Fig. 1. Outline of North American ice extent at the Last Glacial Maximum (after Dalton et al., 2020) as well as locations discussed in the text. The Laurentide, Cordilleran and Innuitian ice sheets are shown, along with the two main sectors of the Laurentide (Keewatin and Labrador domes). The base layer shows modern-day coastlines, topography and political boundaries, with elevation data from the United States Geological Survey's Center for Earth Resources Observation and Science (EROS) (2010). The continental shelf (light blue <1000 m) is after http://www.naturalearthdata.com/. POW = Prince of Wales. Transects show where ice retreat rates between 60 ka and 45 ka were approximated (see Table 1).

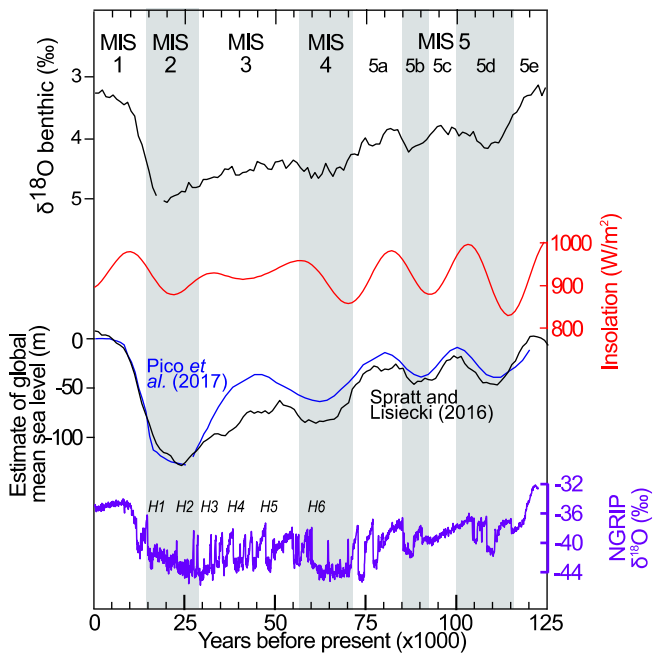

Fig. 2. Climate proxy data, orbital parameters, and sea level estimates through the last glacial cycle, known as the Wisconsinan Stade in North America. Note the discrepancy between estimates of global mean sea level during MIS 3, which partly contributes to large uncertainties in our ice sheet reconstructions through that interval.

each of the 19 time slices) are available as GIS shapefiles and in PDF format in Supplemental Information. Our focus is the Laurentide and the adjacent Innuitian ice sheet, as they were, by far, the largest in area and volume over North America during the last glacial cycle (Fig. 1; Dyke, 2004; Dyke and Prest, 1987; Fulton, 1989; Stokes, 2017; Tarasov et al., 2012). We exclude the Cordilleran Ice Sheet from our reconstructions because its complex topography (including plateaux and deep valleys) and high elevation are inherently difficult to reconcile with the geochronological record. To further add to the complexity, the Cordilleran may have remained glaciated even during some interglacial and interstadial times (Stokes et al., 2012). However, our maps would be potentially confusing (and indeed misleading) if we refrained from showing any ice cover in this region. Thus, we decided to include the broad Cordilleran Ice Sheet outlines from Batchelor et al. (2019). The same approach was taken for the Greenland Ice Sheet.

Our goal is to provide the most up-to-date understanding of North American ice sheets based on the available evidence (which is sometimes very scarce) and fully capture uncertainties associated with the geochronological, stratigraphic and modelling data. We stress that some ice outlines are only loosely constrained and therefore speculative, especially prior to 45 ka. Nevertheless, this work represents our most up-to-date understanding of the last glacial cycle in North America, and we consider these ice configurations as a series of testable hypotheses for future work to address, falsify and improve upon. This work comes at a time of renewed interest in Northern Hemisphere ice configurations through the Quaternary. Over the past decade, there have been several attempts to numerically model the build-up of North American ice cover (e.g. Carlson et al., 2018; Stokes et al., 2012), but this work has suffered from a lack of empirical data to help constrain and calibrate the models, which partly motivates our data-driven approach. Notably, a recent model of global ice extent over the past 80,000 years was published by Gowan et al. (2021), using global sea level records, glacioisostatic adjustment and ice sheet modelling. In that paper, less overall emphasis was placed on available geochronological and geological constraints; thus, it offers a timely independent analysis with which to compare our ice sheet reconstructions.

Prior to our work, Batchelor et al. (2019) presented the evolution of Northern Hemisphere ice sheets through the entire Quaternary, accomplished by integrating broad empirical evidence as well as numerical ice sheet models. Batchelor et al. (2019) focussed on ten key points during the last glacial cycle (MIS 5d ≈ 109 ka; MIS 5c ≈ 96 ka; MIS 5b ≈ 87 ka ; MIS 5a ≈ 82 ka; MIS 4 ≈ 60; 45 ka; 40 ka; 35 ka; 30 ka and LGM ≈ 25 ka). Here, however, our work is focused on improving the spatial and temporal resolution of the Laurentide and Innuitian ice sheets during the last glacial cycle until the LGM. We dedicate a large part of our work to dissecting the primary literature and compile an extensive geochronological dataset that was not available to Batchelor et al. (2019). We also link our reconstructions more explicitly to geomorphologic and chronostratigraphic constraints in the literature. Furthermore, we present our work in at 5-kyr time slices that are higher resolution than the MIS stages used in Batchelor et al. (2019). That said, we do refer to Batchelor et al. (2019) and we include their outlines for the Cordilleran and Greenland ice sheets for completeness when little other evidence is available to support an ice configuration at a given time.

2. Methods and approach

The Laurentide Ice Sheet was comprised of an eastern sector (Labrador Dome) and western sector (Keewatin Dome), separated in central Canada by Hudson Bay (Fig. 1). These ice domes remained distinct for much of the Quaternary, merging only during times of substantial continental ice extent, such as the LGM (Batchelor et al., 2019). Lying north of the Laurentide was the Innuitian Ice Sheet, which was centered over the Queen Elizabeth Islands (Fig. 1).

2.1. Geochronological dataset

We compile n = 939 geochronological data points from the glaciated region of North America spanning 125 ka to 25 ka. These data were extracted from a previous compilation of ages in the range of 60 ka to 30 ka (Dalton et al., 2019), a recent dataset of geochronological ages from the Great Lakes region (Heath et al., 2018) and supplemented with data spanning earlier intervals of the last glacial cycle (Supplementary Table 1). They comprise 799 radiocarbon ages, 103 luminescence ages and 37 U-series ages. All radiocarbon data were calibrated using the IntCal13 calibration curve (Reimer et al., 2013). Marine radiocarbon dates were not systematically compiled in this dataset because these data largely constrain the post-LGM recession. However, we consulted with the relevant marine literature when determining pre-LGM ice limits.

Using methods similar to Hughes et al. (2016) and Small et al. (2017), geochronological data were ranked according to reliability. We assign a low rank to data that we deem to have high uncertainties and are therefore inappropriate as control points for the ice margin. This includes, for example, shells >40 ka owing to the possibility of isotope fractionation from modern carbon which can cause artificially young dates (Pigati, 2002). Furthermore, infinite radiocarbon ages are not considered in our dataset. All ranks are provided in Supplemental Table 1. The result is n = 656 geochronological data points that we consider to be 'reliable' or 'somewhat reliable' control points for the ice margin (n = 532 radiocarbon ages, n = 89 luminescence ages and n = 35 U-series ages; Fig. 3). All other ages (n = 283) are excluded from further consideration. The majority (~80%) of the chronological data collected for this study have errors between 1 to 10%. However, in some extreme cases (<2% of data; typically luminescence ages) the error can exceed 20%. The errors are incorporated into our minimum and maximum ice estimates.

2.2. Reconstruction of ice margins

Our maps are based on empirical data (geochronological data,

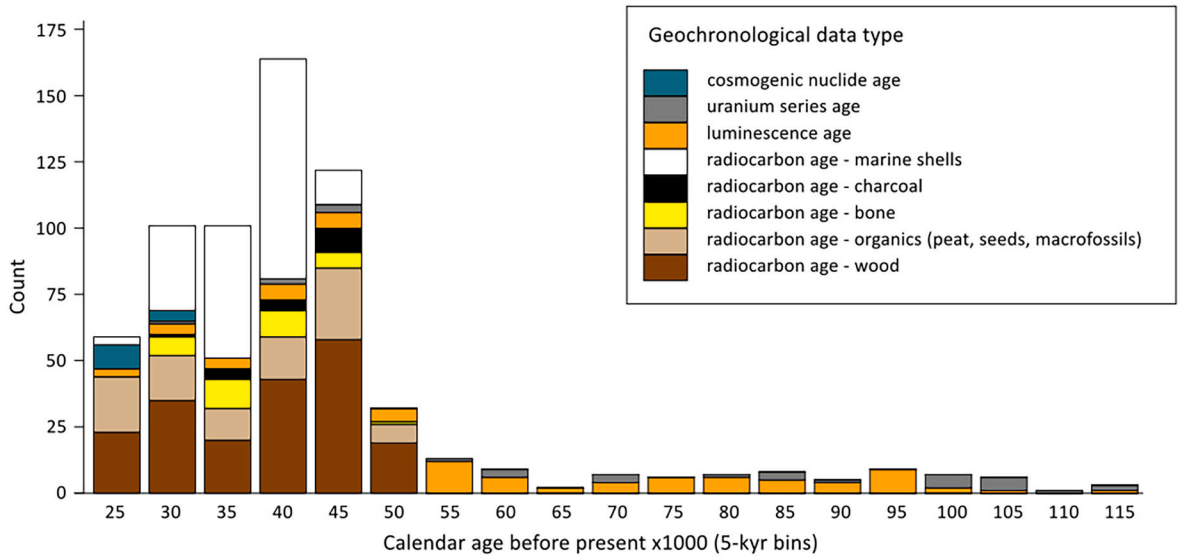

Fig. 3. Distribution of reliable geochronological data (n = 656) that constrain North American ice sheets during the last glacial cycle (115 ka to 25 ka).

stratigraphic data), numerical ice sheet modelling and estimates of global mean sea level (GMSL), alongside other palaeo-climate proxies (Fig. 2) to fully capture uncertainties in the ice margin positions through the build-up phase of the last glacial cycle until the LGM. A review of relevant literature and a rationale for each time-step is presented in Section 3. For each time-step, we integrate geochronological data (to constrain the timing and duration of ice-free areas), stratigraphic data (to provide constraints on the relative timing of glacial and non-glacial events in a given area) and geomorphological data (to show the likely flow direction of pre-LGM ice sheets). Flow set data (striae and landform) of Kleman et al. (2010), are assumed to represent the last glacial cycle owing to their preservation and the assumption that flow sets dating to earlier glacial cycles (e.g. MIS 6, >130 ka) would have presumably been eroded and/or overprinted by more recent glacial events.

Our ice reconstructions are also informed, qualitatively, by insolation values from the Northern Hemisphere in July (Berger and Loutre, 1991) as well as estimates of GMSL. For example, between 50 ka and 40 ka, insolation was higher than present-day and relatively stable, so we use this as support for reduced ice sheet extent at that time. Estimates of GMSL are derived from two sources: (1) a model of glacial isostatic adjustment of Pico et al. (2017), and (2) the principle component analysis of several $\delta^{18}O$ proxies (Spratt and Lisiecki, 2016). Similar to the insolation values, in the construction of our maps, an increase in GMSL was sometimes used qualitatively to justify a reduced ice sheet extent because the Laurentide Ice Sheet dominated sea level contributions during the last glacial cycle (Batchelor et al., 2019; Clark et al., 2009; Lambeck and Chappell, 2001; Stokes et al., 2012). Given that the amount and type of evidence varies through time, and to increase transparency, we include a pie chart on each map that broadly indicates the main lines of evidence used to produce each ice reconstruction (e.g. chronostratigraphic records, geomorphology, estimates of GMSL and numerical ice sheet model). We also include a measure of confidence (low, medium, high) in our ice reconstruction. Present-day ice in the Canadian Arctic is from http://www.naturalearthdata.com/.

We chose 5-kyr timesteps as a compromise between the spread of available geochronological data; higher resolution (e.g. 2.5-kyr intervals) would not be permitted because of a lack of geochronological data; lower resolution maps (e.g. 10-kyr intervals) would not take full advantage of what we know from geochronological dataset and stratigraphic records. We also present estimates of minimum and maximum ice extent at each time-step. These ice margins are largely based on uncertainties in geochronological data and the stratigraphic record and also consider trends and discrepancies in GMSL records. For example, an OSL age of 60 ± 15 ka, would be used primarily as evidence for local ice-free conditions at 60 ka. However, to account for the uncertainty, minimum/maximum timesteps from 45 ka through 75 ka are also influenced by this data point. Uncertainties also consider details from the stratigraphic record. For example, an ice advance that is clearly documented in the stratigraphic record but undated (or very widely constrained) would be assigned a particular age taking into consideration evidence from surrounding regions as well as the GMSL record. To account for the possibility that the advance occurred much earlier or later, we adjust the minimum/maximum ice extents for those time slices. When little information is available for the ice extents, we retain the generalized ice margins of Batchelor et al. (2019) or, rarely, use a template ice margin from the post-LGM record (Dalton et al., 2020) that corresponds to a similar palaeo-climate/GMSL record (Fig. 2).

3. Results

In the following subsections, we work from old to young, following the evolution of the Laurentide and Innuitian ice sheets. For simplicity, discussion of the Laurentide Ice Sheet is often broken into its domes (Keewatin and Labrador). Within each timestep, we review all relevant literature and geochronological evidence from the glaciated region. We also describe our best estimate of the ice margin, followed by estimates of minimum and maximum ice extents. Where applicable, we also present a brief comparison between our ice margin reconstructions and estimates of GMSL (Pico et al., 2017; Spratt and Lisiecki, 2016), as well as modelled work on North American ice sheet history, notably the work of Stokes et al. (2012), Bahadory et al. (2021) and Gowan et al. (2021). Heinrich Events are also discussed in relevant time-steps. Because our work integrates geochronological and stratigraphic datasets, these descriptions involve a combination of advance/retreat terminology as well as numerical time slices. A histogram showing the distribution of geochronological data within each time-step is presented in Fig. 3. Supplemental Information contains the 19 ice margin reconstructions as GIS shapefiles and in PDF format (Supplementary Fig. 1).

3.1. Laurentide and Innuitian ice sheets at 115 ka

Our 115-ka map shows the onset of Wisconsinan ice build-up over North America, based largely on numerical ice sheet modelling with some influence from geomorphology, estimates of GMSL and the chronostratigraphic record (Fig. 4A; low confidence). We show Keewatin ice covering most of Baffin Island, eastern Keewatin and an extension onto

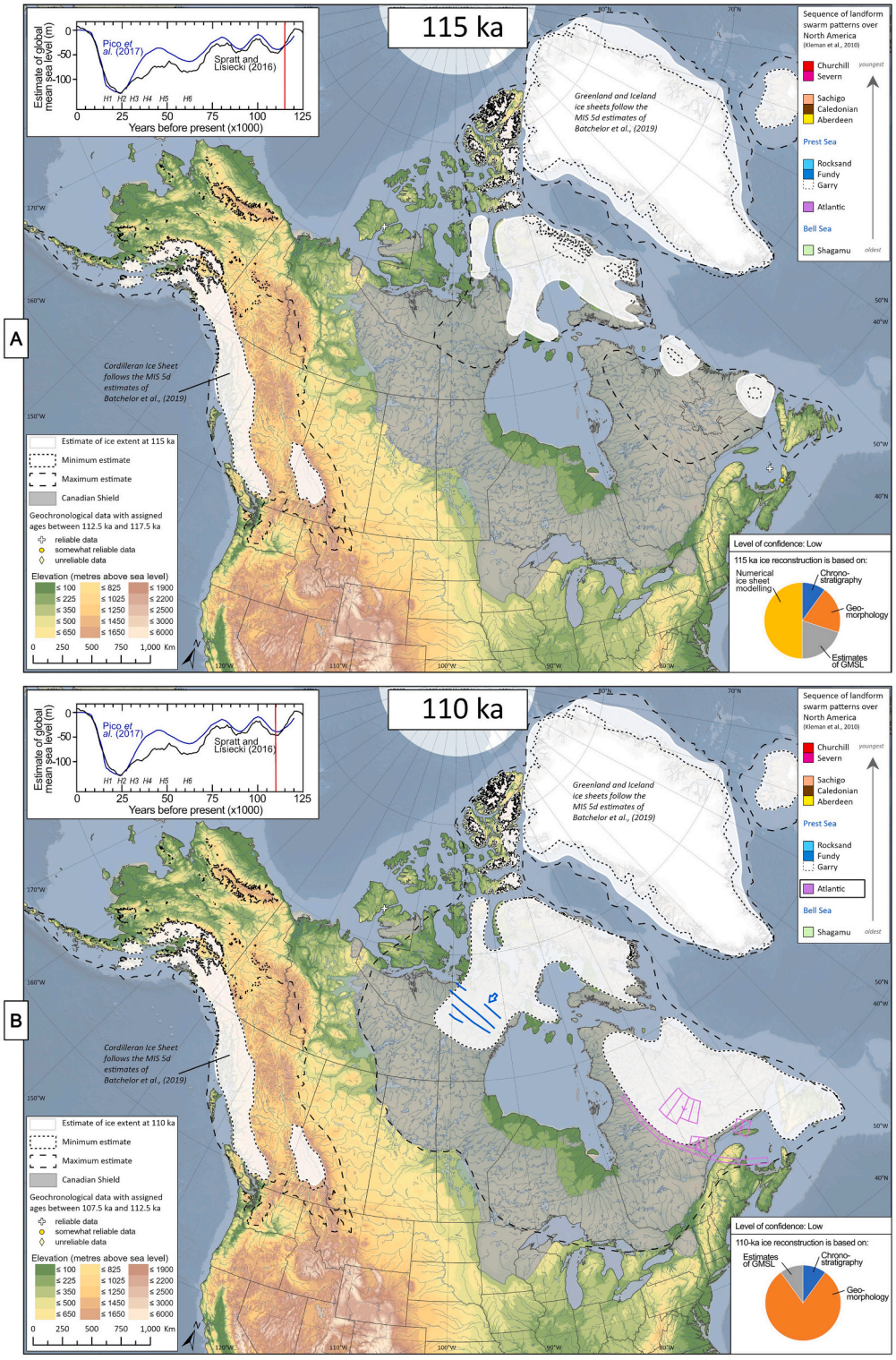

Fig. 4. Reconstructed North American ice at 115 ka (panel A) and 110 ka (panel B).

Somerset Island. This interval marked the onset of MIS 5d ice growth, and ice sheet modelling supports the likely location of nucleation centers in high-altitude regions of northern Québec and Labrador of glaciation (Bahadory et al., 2021; Marshall, 2002; Stokes et al., 2012). This ice depiction is in concordance with a longstanding body of work suggesting the inception of Wisconsinan ice occurred as the result of prolonged snow cover and increased precipitation in plateau areas of Baffin Island and eastern Keewatin (Andrews and Barry, 1978; Bahadory et al., 2021; Ives, 1957; Koerner, 1980; Marshall et al., 2000). Our ice configuration also takes into account evidence from the geomorphological record (Kleman et al., 2010) as well as GMSL that was between -25 m and -30 m compared to present-day (Pico et al., 2017; Spratt and Lisiecki, 2016). The sole geochronological constraints at 115 ka (Fig. 3) are from Banks Island, where a U-series age from shells in deltaic sediments suggests ice-free conditions (UQT-114, 113 ± 20 ka; Causse and Vincent, 1989), as well as Atlantic Canada, where an OSL age from a shoreline deposit

suggests an ice-free interval at 115 ± 8 ka (OSL51_feldspar; Rémillard et al., 2017).

The minimum ice extent at 115 ka shows a Keewatin Dome restricted to central and coastal Baffin Island (Fig. 4A). To depict this minimal ice configuration, we use the post-glacial 3 ka time-step for Baffin Island (Dalton et al., 2020 and references therein). We also show the minimum Labrador Dome as two very small nucleation centers over northern Québec and Labrador. This scenario could have presumably been possible because of a delay in MIS 5d ice build-up, following the much warmer and largely ice-free MIS 5e. On the other hand, our maximum ice extent at 115 ka assumes rapid onset of glacial build-up following MIS 5e. During this interval, we assign the maximum ice extent roughly to the footprint of the Canadian Shield northwest of Hudson Bay. Following Kleman et al. (2010), this maximum ice extent contains a northward extension onto Somerset Island, an eastward extension to Southampton Island, and a largely glaciated Baffin Island, except for some ice-free areas along the south coast. We show the maximum Labrador Dome following the outline of the Atlantic flow set (striae and landform data) of Kleman et al. (2010), an ice advance that likely occurred during a MIS 5 stadial (likely MIS 5d or MIS 5b). Similar to Batchelor et al. (2019), we reduce the southern margin of the maximal ice extent by ~100 to ~200 km to accommodate an ice-free interval in Atlantic Canada (de Vernal et al., 1986; Rémillard et al., 2017).

No geochronological data, stratigraphic data or modelling inference are available for the Innuitian Ice Sheet at 115 ka. We therefore assume present-day ice cover in the Queen Elizabeth Islands, where ice is restricted largely to upland areas of Ellesmere, Devon and Axel Heiberg islands (Fig. 4A). We consider this to be the minimum ice extent at that time, whereas the maximum ice extent shows Innuitian ice covering all the eastern Queen Elizabeth Islands, a scenario that could have been possible with enhanced moisture transport to this region.

3.2. Laurentide and Innuitian ice sheets at 110 ka

Our 110-ka map shows maximum MIS 5d continental ice over North America, based primarily on evidence from the geomorphology record, supported by estimates of GMSL and rare chronostratigraphic data (Fig. 4B; low confidence). We show Keewatin ice largely restricted to the Canadian Shield northwest of Hudson Bay. Following Kleman et al. (2010), this ice configuration contains a northward extension onto Somerset Island, an eastward extension to Southampton Island, and a largely glaciated Baffin Island, except for some ice-free areas along the south coast. This ice depiction aligns with glacial lineation flow set A (and possibly also B) of Boulton and Clark (1990) (blue lines on map) and maintains ice over the Keewatin nucleation centers as suggested by modelling (Bahadory et al., 2021; Marshall, 2002; Stokes et al., 2012). We show the Labrador Dome following the outline of the Atlantic flow set (striae and landform data) of Kleman et al. (2010), an ice advance that occurred during a MIS 5 stadial (likely MIS 5d or MIS 5b; Fig. 4B). Similar to Batchelor et al. (2019), we reduce the southern margin of the maximal ice extent by ~100 to ~200 km to accommodate an ice-free interval in Atlantic Canada (de Vernal et al., 1986; Rémillard et al., 2017). We assume that maximum MIS 5d ice occurred at 110 ka owing to the relative low point in GMSL (between -40 m and -46 m compared to present-day) at that time (Pico et al., 2017; Spratt and Lisiecki, 2016). The sole geochronological constraints at 110-ka stem from the work of Causse and Vincent (1989), who presented several U-series ages on a marine unit of 113 ka and 99.5 ka.

We consider the smallest possible ice configuration (minimum ice extent) to be equivalent to our best guess at 110 ka (Fig. 4B). On the other hand, our maximum ice extent for the Keewatin Dome assumes a much larger footprint, expanded northward to merge with the Innuitian Ice Sheet, westward to cover the entire Canadian Shield of Western Canada and eastward to join the Labrador Dome over Hudson Bay. Our maximum for the Labrador Dome assumes a dramatic response to glacierization, with ice extended mid-way to the continental shelf break along the Labrador coast, covering most of Atlantic Canada as suggested by numerical ice sheet modelling efforts (Ganopolski and Calov, 2011). The ice margin then roughly follows the Canadian Shield westward. The existence of moderately large ice masses (e.g. covering the entire Canadian Shield) over North America during this time is supported by modelling of benthic $\delta^{18}O$ records, orbital parameters, and CO_2 (Ganopolski and Calov, 2011). This maximum ice extent shows a partially glaciated Saint Lawrence Lowlands, allowing for the possible deposition of the Ste Anne Till at that time (Bernier and Occhietti, 1991). The age of the Ste Anne Till is inferred from underlying marine sediments dated to 98 ± 9 ka (La Pérade Clay).

Another consideration given to the maximum ice extent is the possible correlation with the Rocksand advance over the Hudson Bay Lowlands (Kleman et al., 2010; Veillette et al., 1999) although we find it more likely this ice advance occurred at ~60 ka (see Section 3.12). This unique SE-to-NW flow pattern occurred when the Labrador Dome was situated significantly farther south than later in the Wisconsinan, and it has been recognized as one of the oldest preserved flow sets over the broad Quebec and Labrador region (Veillette, 1995; Veillette et al., 1999; Veillette and Pomares, 1991). In the Hudson Bay Lowlands, Dalton et al. (2018) observed a similarly clast fabric-oriented till underlying non-glacial deposits dated between 73 ka and 60 ka, suggesting this ice advance must have occurred prior to MIS 4 or MIS 5 (Kleman et al., 2010; Thorleifson et al., 1992).

Regarding the Innuitian Ice Sheet, we show modern-day ice (Fig. 4B), although no geological constraints are available at 110 ka. We consider this to be the minimum possible ice extent, whereas the maximum ice extent shows Innuitian ice covering all the eastern Queen Elizabeth Islands.

3.3. Laurentide and Innuitian ice sheets at 105 ka

The 105-ka map shows the waning of MIS 5d continental ice over North America, based largely on numerical modelling with some influence from geomorphology, estimates of GMSL and the chronostratigraphic record (Fig. 5A; low confidence). We show Keewatin ice in a slightly reduced footprint compared to peak MIS 5d conditions (110 ka), largely restricted to the Canadian Shield northwest of Hudson Bay. This ice configuration has a northward extension onto Somerset Island, an eastward extension to Southampton Island, and a largely glaciated Baffin Island, except for some ice-free areas along the south coast (after Kleman et al., 2010). We assume that reduction of ice in eastern Keewatin followed the overall pattern of post-glacial retreat in that area (e.g. Campbell et al., 2013). This ice depiction maintains ice over the nucleation centers suggested by modelling (Bahadory et al., 2021; Marshall, 2002; Stokes et al., 2012). Regarding the Labrador Dome, we show ice restricted largely to upland areas of northern Quebec and Labrador and a separate ice cap over Newfoundland. This ice configuration follows striation data that suggest the early Wisconsinan Labrador Dome retreated to the northern Quebec and Labrador region (Veillette et al., 1999). The waning of MIS 5d ice also aligns with rising GMSL at that time between -30 m and -40 m compared to present-day (Pico et al., 2017; Spratt and Lisiecki, 2016).

Geochronological data for the 105-ka interval are uncommon (Fig. 3), offering little insight into the ice configuration at that time. Causse and Vincent (1989) reported a U-series age from Banks Island of 104.6 ± 15.2 ka (UQT-080). Ice was also likely absent from the eastern coast of Baffin Island as suggested by an OSL age from a lake sediment core (UIC1682IR; 105.35 ± 9.85 ka; Briner et al., 2007). In Atlantic Canada, two U-series ages from wood contained in a sub-till stratigraphic section (East Bay unit) suggest ice-free conditions at ~105 ka (UQT-108 and UQT-183; de Vernal et al., 1986). In the Hudson Bay Lowlands, wood contained in a sub-till stratigraphic sequence suggests the geographic center of the Laurentide Ice Sheet was ice-free at ~105 ka (U Series ages; 6N01B and 6N01C; Allard et al., 2012).

For the minimum ice extent at 105 ka, we show a Keewatin Dome

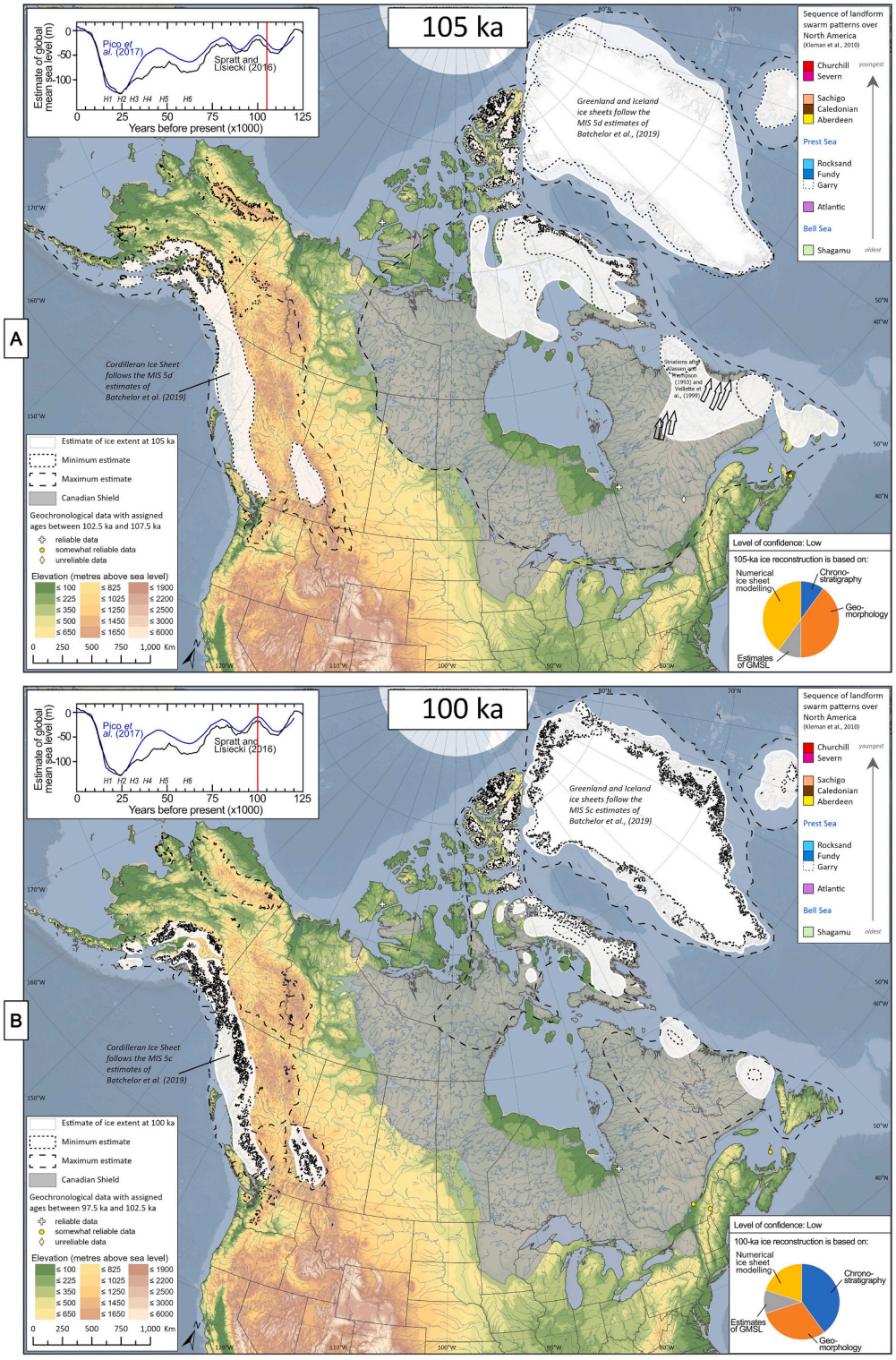

Fig. 5. Reconstructed North American ice at 105 ka (panel A) and 100 ka (panel B).

restricted to inland areas of Baffin Island while coastal areas are largely ice-free (Fig. 5A). The ice configuration over Baffin Island follows Hypothesis 2 of Dredge and Thorleifson (1987) for the mid-Wisconsinan. This minimum ice extent could have been possible at 105 ka if MIS 5d (110 ka) ice underwent rapid recession. As a minimum ice extent for the Labrador Dome, we show two ice nucleation centers in high-altitude regions of northern Quebec and Labrador (Bahadory et al., 2021; Marshall, 2002; Stokes et al., 2012). Our maximum ice extent assumes a sustained larger footprint of North American continental ice at 105 ka, with the Keewatin Dome potentially expanding to cover the entire Canadian Shield of western Canada and merged over Hudson Bay with the Labrador Dome. Moreover, our maximum ice extent assumes a dramatic response of the Labrador Dome to glacierization, with ice extended midway to the continental shelf break along the Labrador coast, covering most of Atlantic Canada, as suggested by numerical ice sheet modelling efforts (Ganopolski and Calov, 2011). The ice margin then roughly

follows the Canadian Shield westward. Identical to the Labrador estimate at 110 ka, this maximum ice margin is supported by benthic $\delta^{18}O$ records, orbital parameters, and CO_2 (Ganopolski and Calov, 2011). As described in the 110-ka timeslice, it takes into consideration a partially glaciated Saint Lawrence Lowlands, allowing for the possible deposition of the Ste Anne Till at that time (Bernier and Occhietti, 1991). Another consideration given to the maximum ice extent is the possible correlation with the Rocksand advance over the Hudson Bay Lowlands (Kleman et al., 2010; Veillette et al., 1999), although we find it more likely this ice advance occurred at ~60 ka.

No geochronological constraints are available for the Innuitian Ice Sheet at 105 ka. We therefore show the present-day ice extent over the Queen Elizabeth Islands which is restricted largely to upland areas of Ellesmere, Devon and Axel Heiberg islands (Fig. 5A). This is also the minimum ice extent, whereas the largest possible ice configuration (maximum ice extent) shows Innuitian ice covering all the eastern Queen Elizabeth Islands.

3.4. Laurentide and Innuitian ice sheets at 100 ka

The 100-ka map shows minimum MIS 5c continental ice over North America, based on the chronostratigraphic record, geomorphology, estimates of GMSL and numerical modelling (Fig. 5B; low confidence). We show the Keewatin Dome restricted to inland areas of Baffin Island while coastal areas are largely ice-free, following Hypothesis 2 of Dredge and Thorleifson (1987) for Baffin Island during the mid-Wisconsinan. This ice estimate is identical to the 115-ka interval, where GMSL was similarly in the range of -10 m and -20 m compared to present-day (Pico et al., 2017; Spratt and Lisiecki, 2016). We assume ice over two ice nucleation centers in high-altitude regions of northern Québec and Labrador (Bahadory et al., 2021; Marshall, 2002; Stokes et al., 2012). Overall, the 100-ka ice configuration is supported by seven geochronological constraints (Fig. 3); three U-series ages from shoreline deposits suggest the area of Banks and Victoria islands was ice-free from 107.8 ka to 99.5 ka (Causse and Vincent, 1989). In addition, ice retreat during this time likely exposed the eastern margin of Baffin Island, as suggested by OSL work at Lake CF8, where two OSL ages on sub-till lacustrine sediments suggest that the ice sheet retreated from this area between 105 ka and 97 ka (Briner et al., 2007). In Atlantic Canada, the Magdalen Islands were ice-free as suggested by the dating of lagoon sediments and organic materials at the Bassin site (U Series; de Vernal et al., 1986; Rémillard et al., 2017). Nearby, in the Saint Lawrence Lowlands, IRSL evidence suggests a local marine incursion (La Pérade Clay; Ferland and Occhietti, 1990) at 98 ± 9 ka (AP5; Occhietti et al., 1996). There is additional geomorphological evidence to suggest this region was ice-free at 102 ± 12 ka (Massawippi Formation; Caron, 2013). Finally, farther west in the Hudson Bay Lowlands, a sub-till sand unit interbedded with organic detritus at the Nottaway River Site was constrained via six age attempts to between 106 ka and 95 ka (OSL and U Series ages; Allard et al., 2012; Dubé-Loubert et al., 2013).

As a minimum ice extent at 100 ka, we assume a Keewatin Dome restricted to central and coastal Baffin Island (Fig. 5B). To depict this minimal ice configuration, we use the post-glacial 3 ka time-step for Baffin Island (Dalton et al., 2020 and references therein). This minimum ice extent could have been possible following a large-scale deglaciation at 100 ka, leaving ice only in nucleation centers. We show the minimum ice extent Labrador Dome as two very small nucleation centers over northern Québec and Labrador. On the other hand, for the maximum ice estimate, we show Keewatin ice that is largely restricted to the Canadian Shield area northwest of Hudson Bay. Following Kleman et al. (2010), this ice configuration contains a northward extension onto Somerset Island, an eastward extension to Southampton Island, and a largely glaciated Baffin Island, except for some ice-free areas along the south coast. Maximum ice extent for Labrador ice follows the outline of the Atlantic flow set (striae and landform data) of Kleman et al. (2010), an ice advance that likely occurred during a MIS 5 stadial (likely MIS 5d or MIS 5b). Similar to Batchelor et al. (2019), we reduce the southern margin of the maximal ice extent by ~100 to ~200 km to accommodate an ice-free interval in Atlantic Canada (de Vernal et al., 1986; Rémillard et al., 2017).

Owing to a lack of geochronological constraints, we show the present-day ice extent for the Innuitian Ice Sheet (Fig. 5B). Like the 105-ka interval, we consider this as the smallest possible ice extent at that time (minimum ice extent), whereas the largest possible ice configuration (maximum ice extent) shows Innuitian ice covering all the eastern Queen Elizabeth Islands.

3.5. Laurentide and Innuitian ice sheets at 95 ka

The 95-ka map shows the renewed onset of continental ice build-up over North America, based largely on geomorphological data, supported by evidence from estimates of GMSL and chronostratigraphy (Fig. 6A; low confidence). We show Keewatin ice covering a larger area compared to peak MIS 5c conditions (100 ka), largely restricted to the Canadian Shield northwest of Hudson Bay. This ice configuration has a northward extension onto Somerset Island, an eastward extension to Southampton Island, and a largely glaciated Baffin Island, except for some ice-free areas along the south coast (as in Kleman et al., 2010). We also show the Labrador Dome as retreated to the northern Quebec and Labrador region (Veillette et al., 1999). This ice configuration broadly aligns with GMSL between -30 m and -40 m compared to present-day (Pico et al., 2017; Spratt and Lisiecki, 2016), and follows the renewed onset of continental ice build-up over North America. Nine geochronological constraints support this ice configuration (Fig. 3). Along the eastern coast of Baffin Island, four OSL ages at Fog Lake suggest ice retreat and the development of subaerial conditions from 94 ka to 96 ka (Wolfe et al., 2000). Also on Baffin Island, sediments at Robinson Lake have been dated to 96 ka (Miller et al., 1999). In Atlantic Canada, a single OSL age from sand contained in a sub-till stratigraphic section suggests ice-free conditions at 96 ± 7 ka (OSL51; Rémillard et al., 2017). To the west, in the Hudson Bay Lowlands, an IRSL age from sand interbedded with organic detritus suggests the geographic center of the Laurentide Ice Sheet was ice-free at 95 ± 7 ka (06NO21; Dubé-Loubert et al., 2013).

As a minimum ice extent at 95 ka, we show the Keewatin Dome restricted to inland areas of Baffin Island while coastal areas are largely ice-free (Fig. 6A). The ice configuration over Baffin Island follows Hypothesis 2 of Dredge and Thorleifson (1987) for the mid-Wisconsinan. This scenario could have occurred because of a delay in MIS 5b ice build-up, following the largely ice-free MIS 5c at 100 ka. We assume minimum ice extent for Labrador ice restricted to two ice nucleation centers in high-altitude regions of northern Quebec and Labrador (Bahadory et al., 2021; Marshall, 2002; Stokes et al., 2012). Our maximum ice extent assumes a much larger footprint of the Keewatin Dome, expanded northward to merge with the Innuitian Ice Sheet, westward to cover the entire Canadian Shield of Western Canada and eastward to join the Labrador Dome over Hudson Bay. The maximum ice extent for Labrador ice is extended mid-way to the continental shelf break along the Labrador coast, covering most of Atlantic Canada and roughly following the Canadian Shield westward. This maximum ice extent is identical to the Labrador estimate at 110 ka, and takes into consideration a partially glaciated Saint Lawrence Lowlands, allowing for the possible deposition of the Ste Anne Till at that time (Bernier and Occhietti, 1991) as well as the possible correlation with the Rocksand advance over the Hudson Bay Lowlands, although we find it more likely this ice advance occurred at ~60 ka.

No geochronological constraints are available for the Innuitian Ice Sheet at 95 ka. Thus, similar to earlier intervals, we show present-day ice as the most likely scenario at 95 ka (Fig. 6A). We assume this to be the smallest possible ice extent (minimum ice extent) at that time. The largest possible ice configuration (maximum ice extent) assumes Innuitian ice covering all the eastern Queen Elizabeth Islands.

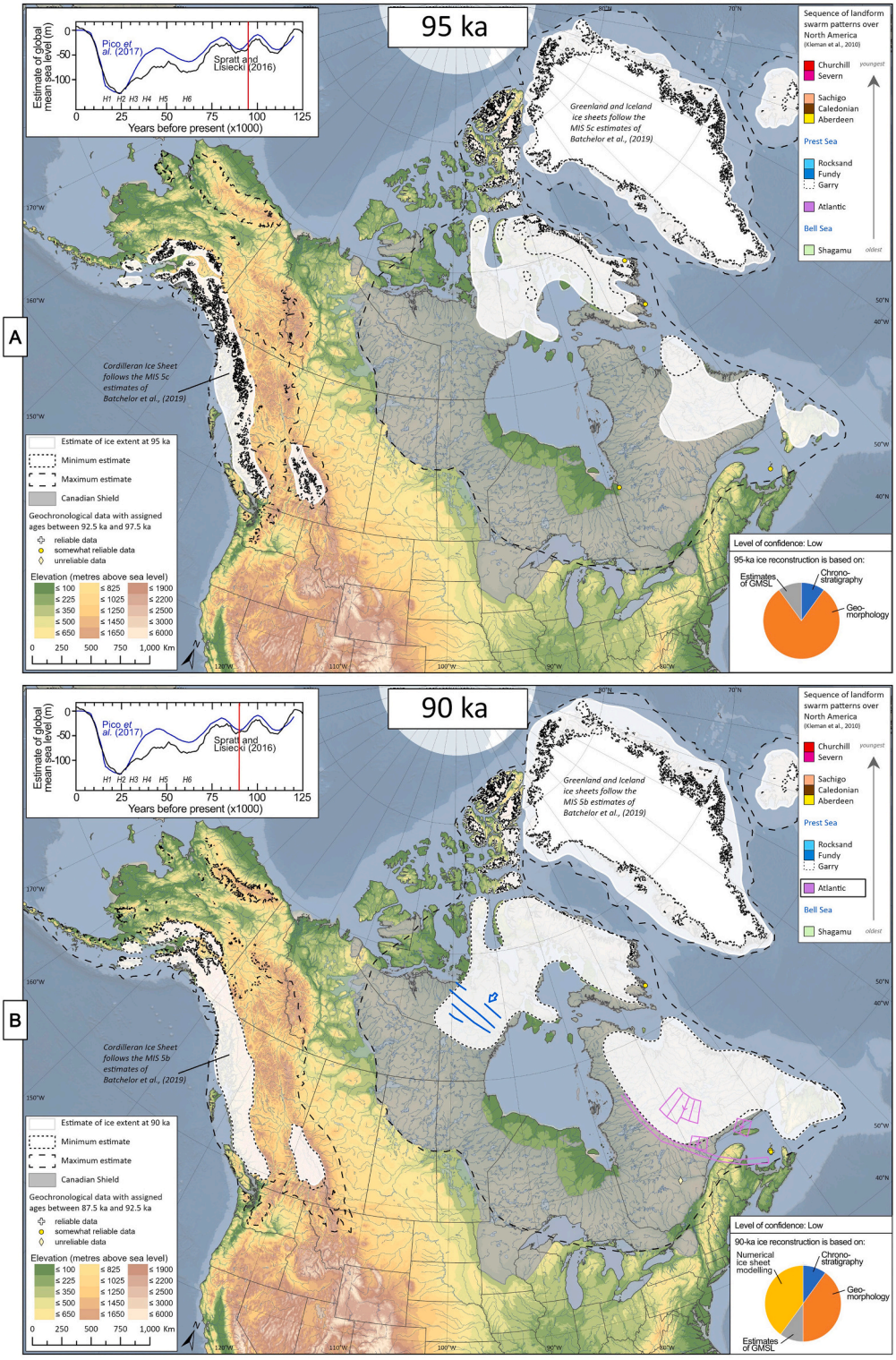

Fig. 6. Reconstructed North American ice at 95 ka (panel A) and 90 ka (panel B).

3.6. *Laurentide and Innuitian ice sheets at 90 ka*

The 90-ka map shows maximum MIS 5b continental ice over North America, based largely on numerical modelling and geomorphology, with some supporting evidence from chronostratigraphic records and estimates of GMSL (Fig. 6B; low confidence). We show Keewatin ice largely restricted to the Canadian Shield area northwest of Hudson Bay. Following Kleman et al. (2010), this ice configuration contains a northward extension onto Somerset Island, an eastward extension to Southampton Island, and a largely glaciated Baffin Island, except for some ice-free areas along the south coast. This ice depiction corresponds to the glacial lineation flow set A (and possibly also B) of Boulton and Clark (1990) (blue lines on map) and maintains ice over the nucleation centers suggested by modelling (Bahadory et al., 2021; Marshall, 2002; Stokes et al., 2012). We assume the Labrador Dome followed the outline of the Atlantic flow set (striae and landform data) of Kleman et al.

(2010), an ice advance that occurred during a MIS 5 stadial (likely MIS 5d or MIS 5b). Similar to Batchelor et al. (2019), we reduce the southern margin of the maximal ice extent by ~100 to ~200 km to accommodate an ice-free interval in Atlantic Canada (de Vernal et al., 1986; Rémillard et al., 2017). This moderate continental ice over North America corresponds to a GMSL of around -40 m compared to present-day (Pico et al., 2017; Spratt and Lisiecki, 2016). Geochronological data in the range of 90 ka are few (Fig. 3). Two IRSL ages from a sub-till lake sediment core in eastern Baffin Island (Robinson Lake) suggest ice-free conditions at 91 ka to 89 ka (OTL-551 and OTL-552; Miller et al., 1999). The sole 90-ka geochronological constraint for the Labrador Dome is from Atlantic Canada (Fig. 6B), on the Magdalen Islands, where three age constraints ranging from 92 ka to 89 ka support the development of wooded, subtidal and lagoon landscapes on this archipelago (de Vernal et al., 1986; Rémillard et al., 2017).

We assume our best estimate (above) as the minimum ice extent at 90

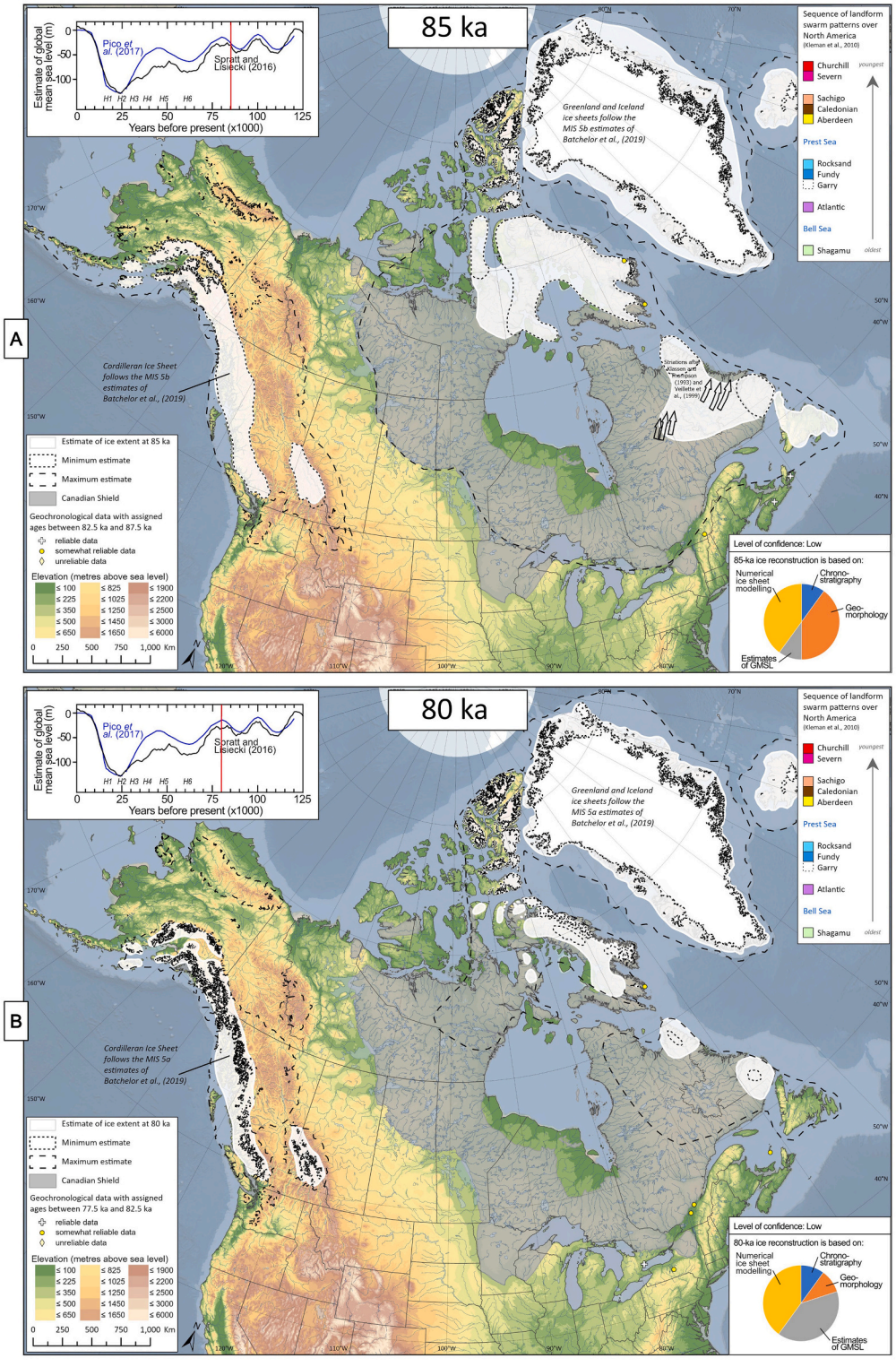

Fig. 7. Reconstructed North American ice at 85 ka (panel A) and 80 ka (panel B).

ka (Fig. 6B), given the low-point in GMSL at that time. Our maximum ice extent assumes a much larger footprint of the Keewatin Dome, expanded northward to merge with the Innuitian Ice Sheet, westward to cover the entire Canadian Shield of Western Canada and eastward to join the Labrador Dome over Hudson Bay. The maximum ice extent for Labrador ice assumes a dramatic response of the Labrador Dome to glacierization, with ice extended mid-way to the continental shelf break along the Labrador coast, covering most of Atlantic Canada and roughly following the Canadian Shield westward. This maximum ice extent is identical to the Labrador estimate at 110 ka, and takes into consideration a partially glaciated Saint Lawrence Lowlands, allowing for the possible deposition of the Ste Anne Till at that time (Bernier and Occhietti, 1991) as well as the possible correlation with the Rocksand advance over the Hudson Bay Lowlands, although we find it more likely this ice advance occurred at ~60 ka (see Section 3.12).

At 90 ka, we show modern-day Arctic ice for the Innuitian Ice Sheet (Fig. 6B). We assume the minimum ice extent is also equivalent to modern-day ice, whereas the maximum ice extent shows ice covering all the eastern Queen Elizabeth Islands.

3.7. Laurentide and Innuitian ice sheets at 85 ka

The 85-ka map shows the waning of MIS 5b continental ice over North America, based largely on numerical modelling and geomorphology, with some supporting evidence from chronostratigraphic records and estimates of GMSL (Fig. 7A; low confidence). Identical to the 105-ka interval, we show Keewatin ice in a slightly reduced footprint compared to peak MIS 5b conditions (90 ka), largely restricted to the Canadian Shield northwest of Hudson Bay. This ice configuration has a northward extension onto Somerset Island, an eastward extension to Southampton Island, and a largely glaciated Baffin Island, except for some ice-free areas along the south coast (as in Kleman et al., 2010). Reduction of ice in eastern Keewatin follows the overall pattern of post-glacial retreat in that area (e.g. Campbell et al., 2013) and this depiction maintains ice over the nucleation centers suggested by modelling (Bahadory et al., 2021; Marshall, 2002; Stokes et al., 2012). We also show ice restricted largely to upland areas of northern Quebec and Labrador and a separate ice cap over Newfoundland. This ice configuration is broadly aligned to a lowering of GMSL at that time (around -30 m compared to present-day; Pico et al., 2017; Spratt and Lisiecki, 2016), and it follows striation data that suggest the early Wisconsinan Labrador Dome retreated to the northern Québec and Labrador region (Veillette et al., 1999).

Seven geochronological constraints are available for the 85-ka interval (Fig. 3), all of which support ice-free conditions at least along the periphery of the glaciated region. On the east coast of Baffin Island, there are two OSL ages of ~85 ka and ~87 ka at Fog Lake (UIC-606; Wolfe et al., 2000) and two OSL ages spanning 87 ka to 83 ka at Robinson Lake (OTL-552 and OTL-548; Miller et al., 1999). In Atlantic Canada, two U-series ages on wood from a stratigraphic section suggest this region was ice-free and wooded between 85 ka and 84 ka (UQT-185 and UQT-186; de Vernal et al., 1986). Also, a U-series age on wood from East Bay Unit II, Nova Scotia, suggests ice-free conditions at 86.9 ± 6 ka (UQT-109; de Vernal et al., 1986).

We assume the smallest possible ice extent (minimum ice extent) at 85 ka to be a slightly reduced ice mass over eastern Keewatin (Fig. 7A). Our minimum ice extent shows a Labrador Dome restricted to two ice nucleation centers in high-altitude regions of northern Quebec and Labrador (Bahadory et al., 2021; Marshall, 2002; Stokes et al., 2012). On the other hand, our maximum ice extent assumes a much larger footprint of the Keewatin Dome, potentially expanding to cover the entire Canadian Shield of western Canada and merged over Hudson Bay with the Labrador Dome. Our maximum ice extent assumes a dramatic response of the Labrador Dome to glacierization, with ice extended mid-way to the continental shelf break along the Labrador coast, covering most of Atlantic Canada, as suggested by numerical ice sheet modelling efforts (Ganopolski and Calov, 2011). The ice margin then roughly follows the Canadian Shield westward. Identical to the Labrador estimate at 110 ka, this maximum ice extent is derived from the modelling of benthic $\delta^{18}O$ records, orbital parameters, and CO_2. As described in the 110-ka time-slice, it takes into consideration a partially glaciated Saint Lawrence Lowlands, allowing for the possible deposition of the Ste Anne Till at that time (Bernier and Occhietti, 1991). Another consideration given to the maximum ice extent is the possible correlation with the Rocksand advance over the Hudson Bay Lowlands (Kleman et al., 2010; Veillette et al., 1999), although we find it more likely this ice advance occurred at ~60 ka.

No geochronological constraints are available for the Innuitian Ice Sheet at 85 ka. Accordingly, we assume the modern-day ice extent as our best estimate for the Innuitian ice at 85 ka (Fig. 7A). We consider this to be the smallest possible ice extent (minimum ice extent) at that time. The largest possible ice configuration (maximum ice extent) shows Innuitian ice covering all the eastern Queen Elizabeth Islands.

3.8. Laurentide and Innuitian ice sheets at 80 ka

Our 80-ka map shows minimum MIS 5a continental ice over North America (Fig. 7B; low confidence), with Keewatin ice restricted to inland areas of Baffin Island while coastal areas are largely ice-free following Hypothesis 2 of Dredge and Thorleifson (1987) for the mid-Wisconsinan (Fig. 7B). This dramatic reduction in ice is informed by estimates of GMSL, which suggest high stands of -15 m to -30 m compared to present-day (Pico et al., 2017; Spratt and Lisiecki, 2016). Other estimates, based on speleothem encrustations from the Mediterranean, place GMSL at 80 ka close to or higher than present-day (Dorale et al., 2010). Overall, our ice sheet configuration at 80 ka follows modelling that suggests the probable location of two ice nucleation centers resulted from prolonged snow cover on plateaux and increased precipitation in these high altitude areas of northern Quebec and Labrador (Andrews and Barry, 1978; Bahadory et al., 2021; Ives, 1957; Koerner, 1980; Marshall et al., 2000; Stokes et al., 2012).

Seven geochronological constraints, which broadly support reduced North American ice sheets, are available for the 80-ka interval (Fig. 3). The eastern coast of Baffin Island was likely ice-free at this time as suggested by an IRSL age from sub-till lacustrine sediments from Robinson Lake (OTL-548; Miller et al., 1999). In Atlantic Canada an OSL age from lagoon sediments suggests that the Magdalen Islands were ice-free at 79 ± 7 ka (OSL101; Rémillard et al., 2017). In the Saint Lawrence Lowlands, stratigraphic and chronological data suggest ice-free conditions between 80 ka and 60 ka (Les Becquets interstade; Lamothe, 1989). Stratigraphically, this time interval is possibly represented by the Saint Pierre Sediments, a sequence of fluvial and organic-bearing units that document a prolonged ice-free interval. Age constraints on the Saint Pierre Sediments include three IRSL and TL determinations (between 82 ka and 61 ka; Balescu and Lamothe, 1994; Lamothe, 1984). A nearby IRSL age from varved sediments suggests an ice-marginal lake at 85 ± 2 ka (Caron, 2013). This ice-free interval may have lasted until ~51 ka (two OSL ages; Godfrey-Smith et al., 1988). Finally, near Lake Ontario, the Don Formation was dated using TL methods to 80 ± 19 ka (DVDF83-2; Berger and Eyles, 1994) and 78 ± 17 ka (DVDF-1; Berger and Eyles, 1994) suggesting ice-free conditions and the development of lacustrine environments. In nearby New York state, clay sediments at the Fernbank Site have been dated using TL to 81 ± 11 ka (Karrow et al., 2009), suggesting they are possibly related to the Don Formation.

As a minimum ice extent at 80 ka, we assume a Keewatin Dome restricted to central and coastal Baffin Island (Fig. 7B). We use the post-glacial 3-ka time-step for Baffin Island (Dalton et al., 2020 and references therein). This minimum ice extent could have been possible if GMSL was similar or higher than present-day (Dorale et al., 2010). The minimum ice extent for the Labrador Dome is two very small nucleation centers over northern Québec and Labrador. We show maximum Keewatin ice largely restricted to the Canadian Shield area northwest of

Hudson Bay. Following Kleman et al. (2010), this ice configuration contains a northward extension onto Somerset Island, an eastward extension to Southampton Island, and a largely glaciated Baffin Island, except for some ice-free areas along the south coast. The maximum ice extent for the Labrador Dome follows the outline of the Atlantic flow set (striae and landform data) of Kleman et al. (2010), an ice advance that likely occurred during a MIS 5 stadial (likely MIS 5d or MIS 5b). Similar to Batchelor et al. (2019), we reduce the southern margin of the maximal ice extent by ~100 to ~200 km to accommodate an ice-free interval in Atlantic Canada (de Vernal et al., 1986; Rémillard et al., 2017).

Owing to the lack of geochronological constraints for the Innuitian Ice Sheet, we assume present-day ice extent over the Queen Elizabeth Islands at 80 ka (largely upland areas of Ellesmere, Devon and Axel Heiberg islands; Fig. 7B). This is also our minimum ice extent, whereas the maximum ice extent shows Innuitian ice covering all of the eastern Queen Elizabeth Islands.

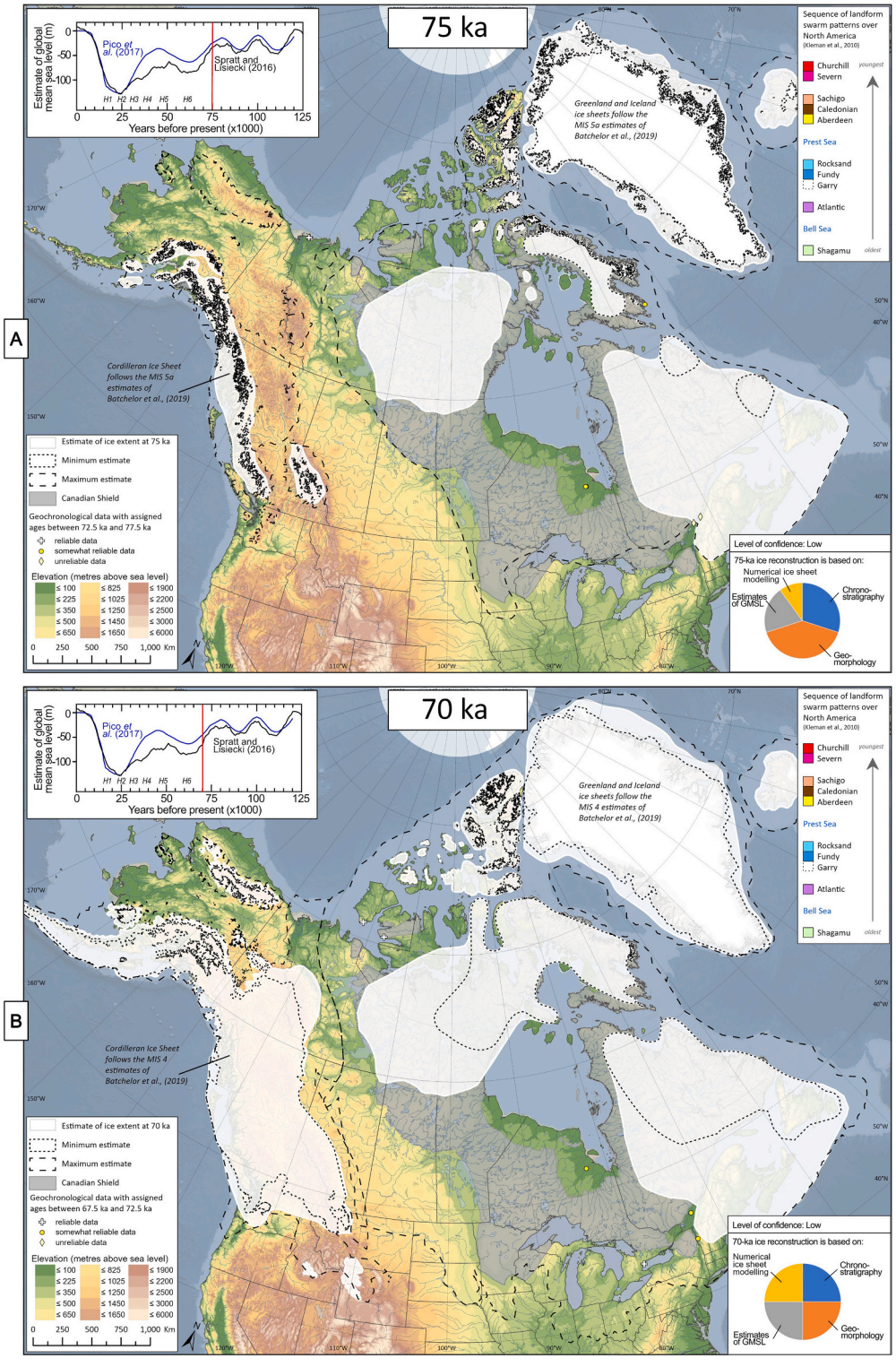

Fig. 8. Reconstructed North American ice at 75 ka (panel A) and 70 ka (panel B).

3.9. Laurentide and Innuitian ice sheets at 75 ka

Our 75-ka map shows a renewed build-up of continental ice over North America, informed largely by the chronostratigraphic record, estimates of GMSL and geomorphological data (Fig. 8A; low confidence). Following the mid-Wisconsinan Hypothesis 2 of Dredge and Thorleifson (1987), we assume Keewatin ice was restricted to the Canadian Shield, moderate in size, and covering much of mainland Nunavut and the Northwest Territories. Inland areas of Baffin Island are glaciated while coastal areas are largely ice-free. We further reduce the western margin of the Keewatin Dome to fit within the bounds of the Canadian Shield, and show a rapid onset of Labrador ice growth to cover most of Atlantic Canada including the continental shelf as suggested by the "Caledonia Phase" of Stea et al. (2011) and references therein. This ice configuration is informed by estimates of GMSL around -30 m compared to present-day (Pico et al., 2017; Spratt and Lisiecki, 2016).

Regarding the Labrador Dome, some chronostratigraphic constraints are also available for the 75-ka interval in the Saint Lawrence Lowlands and the region south of Hudson Bay. In the Saint Lawrence Lowlands, we show the southern margin of the Labrador Dome at the position of the Lévrard till (Lamothe et al., 1992) and the associated Deschaillons varves (Hillaire-Marcel and Page, 1981). This varved sedimentary unit of 20-m thickness occurred when the flow of the Saint Lawrence was blocked by a glacier and drainage was re-routed into the Hudson River (Clet and Occhietti, 1994). These varves have been dated using U-series methods to 79.8 ka (Hillaire-Marcel and Causse, 1989). Thus, they must have occurred during a dramatic ice advance immediately following MIS 5a (~80 ka). Elevation mapping of the hypothetical paleolake suggests it may have covered an extensive low-lying area spanning ~300 km to the southwest. Varve counting suggests ice may have remained in this position for 2500 years (Lamothe, 1985) to 4000 years (Hillaire-Marcel and Page, 1981). Finally, we show ice-free conditions around Hudson Bay as constrained by fluvial sediments dated via OSL in that region (BG4227 and BG4263; Dalton et al., 2018).

Regarding the Keewatin Dome, along the coastline of the northwest margin, stratigraphic records contain the remains of a pre-LGM river delta (Kilduit Formation; Rampton, 1988) and OSL dating suggests this area was ice-free between 76 ka and 73 ka (Shfd08142 and Shfd08150; Murton et al., 2017). This local ice-free interval likely lasted until the LGM (Murton et al., 2017). On Baffin Island, two TL ages from Robinson Lake suggest the east coast of Baffin Island was ice-free between 77 ka and 75 ka (OTL-552; Miller et al., 1999).

As a minimum ice extent at 75 ka (Fig. 8A), we assume ice was present in central Baffin Island while coastal areas are largely ice-free (as in Hypothesis 2 of Dredge and Thorleifson, 1987). Furthermore, we show two ice nucleation centers in high-altitude regions of northern Québec and Labrador (Bahadory et al., 2021; Marshall, 2002; Stokes et al., 2012). On the other hand, our maximum ice extent assumes rapid onset of glacial build-up following MIS 5a. Following the mid-Wisconsinan Hypothesis 2 of Dredge and Thorleifson (1987), we show maximum Keewatin ice broadly following the margin of the Canadian Shield and merged with the Labrador Dome over Hudson Bay. South of Manitoba, we also show an extension of this maximum ice into the continental United States to potentially account for the source of sediment in the Teneriffe Silt loess deposit in that region and elsewhere in the watershed of the Mississippi River (~77 ka; Forman et al., 1992). On the northwest margin, we show a maximum ice extent covering Victoria Island to align, within error, to an inter-till wood piece that was dated via U-Series to 71.8 ±10.4 ka (UQT-230_A0; Causse and Vincent, 1989). For the Labrador Dome, our maximum ice extent assumes a dramatic early build-up of ice toward peak MIS 4 conditions with the Labrador Dome merged with the Keewatin Dome over Hudson Bay (Stokes et al., 2012). We show the Labrador margin roughly following the continental shelf break along the Atlantic coast, bordering the southern Appalachian Range, into the Saint Lawrence Lowlands (drawn after Lamothe et al., 1992) and roughly following the outline of the Canadian Shield near the Great Lakes.

No geochronological constraints are available for the Innuitian Ice Sheet at 75 ka. Thus, our best estimate for Innuitian ice is the present-day ice extent (upland areas of Ellesmere, Devon and Axel Heiberg islands; Fig. 8A). We consider this to be the minimum possible ice extent at that time. The maximum ice extent shows Innuitian ice covering all the eastern Queen Elizabeth Islands to the present-day coastline (assumed).

3.10. Laurentide and Innuitian ice sheets at 70 ka

The 70-ka map assumes the continued build-up of continental ice over North America, supported by roughly equal weights of chronostratigraphic data, estimates of GMSL, numerical modelling and geomorphology (Fig. 8B; low confidence). We show a northward extension onto Somerset Island, an eastward extension to Southampton Island, and a largely glaciated Baffin Island. This ice depiction follows Kleman et al. (2010) merged with the mid-Wisconsinan Hypothesis 2 of Dredge and Thorleifson (1987), with the western Keewatin margin aligned to the Canadian Shield. This ice depiction assumes a correspondence to glacial lineation flow set A (and possibly also B) of Boulton and Clark (1990) (blue lines on map) and maintains ice over the nucleation centers suggested by modelling (Bahadory et al., 2021; Marshall, 2002; Stokes et al., 2012). Because at 70 ka GMSL had not yet reached its MIS 4 minimum, we assume a Keewatin Dome that is smaller than at peak MIS 4 (~60 ka). We also show a rapid onset of Labrador ice growth to cover most of Atlantic Canada including the continental shelf as suggested by the "Caledonia Phase" of Stea et al. (2011) and references therein. A key feature of our 70-ka ice estimate is the southern margin of the Labrador Dome in the Saint Lawrence Lowlands. This ice margin is derived from the position of the Lévrard till (Lamothe et al., 1992) and the associated Deschaillons varves (Hillaire-Marcel and Page, 1981). At this time, it is possible the Labrador Dome expanded southward and joined with ice expanding westward from the Appalachian Mountains, resulting in an extensive ice margin in the Saint Lawrence Lowlands (drawn after Lamothe et al., 1992).

Seven geochronological constraints are available for the 70-ka interval (Fig. 3). Data include three U-series ages from wood found on Banks and Victoria islands that date to the 72 to 68 ka interval (Causse and Vincent, 1989). In the Saint Lawrence Lowlands, a sand-bearing sub-till unit was dated via IRSL to 71 ± 7 ka (Balescu and Lamothe, 1994). Nearby in Vermont, OSL dating of cave sediments suggests the Champlain valley was not glaciated at 68 ± 10.8 ka (M002; Munroe et al., 2016). Near Lake Ontario, a TL age from the Don Formation yielded 67.6 ± 9 ka, suggesting a prolonged interval of ice-free conditions and the development of lacustrine environments (DVDF-7; Berger and Eyles, 1994). Finally, an OSL age from sub-till fluvial sediments along the Albany River suggests subaerial conditions in the Hudson Bay Lowlands at 67.6 ± 5.8 ka (BG4264; Dalton et al., 2018).

As a minimum ice extent at 70 ka, we assume Keewatin ice waslargely restricted to the Canadian Shield northwest of Hudson Bay (Fig. 8B). Following Kleman et al. (2010), this ice configuration contains a northward extension onto Somerset Island, an eastward extension to Southampton Island, and a largely glaciated Baffin Island, except for some ice-free areas along the south coast. We show the minimum ice extent for the Labrador Dome following the outline of the Atlantic flow set (striae and landform data) of Kleman et al. (2010), an ice advance that occurred during a MIS 5 stadial (likely MIS 5d or MIS 5b). Similar to Batchelor et al. (2019), we reduce the southern margin of the maximal ice extent by ~100 to ~200 km to accommodate an ice-free interval in Atlantic Canada (de Vernal et al., 1986; Rémillard et al., 2017). This minimum ice extent is identical to the ice estimate at 110 ka.

Our maximum ice extent at 70 ka assumes an early onset of MIS 4 conditions (Fig. 8B). Accordingly, similar to our estimate at peak MIS 4 (60 ka), we show the Keewatin Dome expanded dramatically to cover the entire southern Interior Plains into Montana, North Dakota and

South Dakota (ice margin drawn after Clayton and Moran, 1982). In Alberta, the westernmost extent of Keewatin ice is drawn after Jackson et al. (2011), who summarized the penultimate ice advance in this region (MIS 4) based on a review of regional stratigraphy. We show an westward extension of the ice margin following ice proxy evidence from sub-till glaciolacustrine sediments ("Grimshaw gravels"; Slomka and Hartman, 2018). Along the Atlantic coastline, the maximum ice extent roughly follows the continental shelf break and is based largely on seismic analyses and mapping of glaciomarine landforms (Josenhans et al., 1986; Piper and Macdonald, 2001; Shaw et al., 2006). In New England, the maximum ice extent follows the uppermost till unit (Sevon and Braun, 2000; Stone et al., 2005), and south of the Great Lakes, the maximum ice extent corresponds to the Shelbyville morainic system (Johnson et al., 1971) and Bloomington moraines (Frye et al., 1969).

No geochronological constraints are available for the Innuitian Ice Sheet at 70 ka. However, given the likelihood of Labrador/Keewatin ice

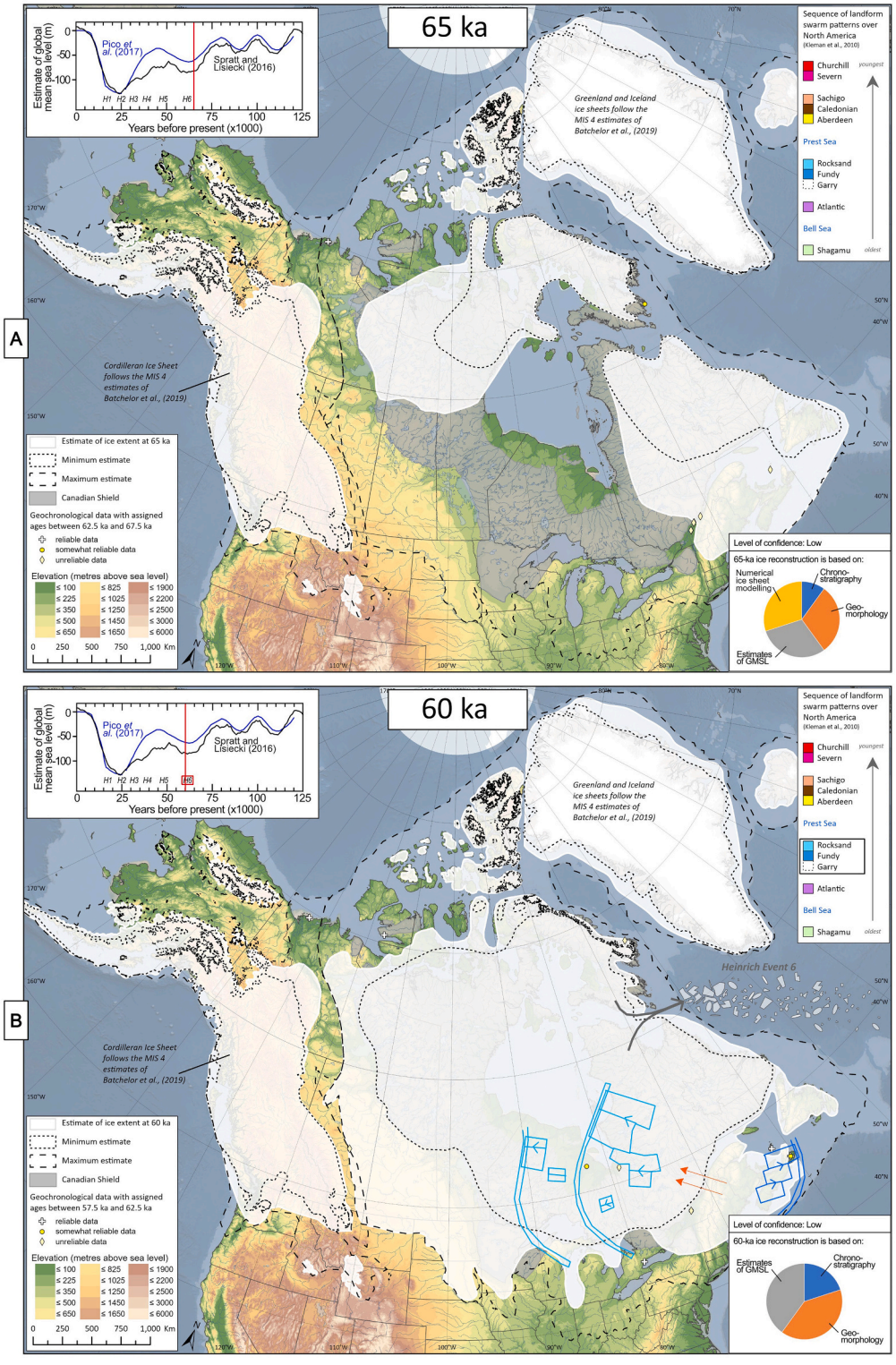

Fig. 9. Reconstructed North American ice at 65 ka (panel A) and 60 ka (panel B).

expansion at this time, it is probable that the Innuitian Ice Sheet was also expanding. To hypothesize this growth, we borrow the 10.3 ka time of post-LGM deglaciation (see 9 ka yrs 14C in Dalton et al., 2020), where ice covers all of Ellesmere, Axel Heiberg and Devon islands (Fig. 8B). Farther west, we assume small ice caps on Melville and Prince Patrick islands. As a minimum ice extent of Innuitian ice extent, we assume present-day ice extent over the Queen Elizabeth Islands, which is restricted largely to upland areas of Ellesmere, Devon and Axel Heiberg islands. As a maximum ice extent, we show Innuitian Ice at the continental shelf edge. This scenario would have been possible with an early and dramatic growth corresponding to MIS 4.

3.11. Laurentide and Innuitian ice sheets at 65 ka

The 65-ka map shows the continued build-up of continental ice over North America, broadly informed by falling GMSL between -60 m and -80 m compared to present-day (Pico et al., 2017; Spratt and Lisiecki, 2016). Owing to the scarcity of constraints on the ice margin, our estimate of the 65-ka ice margin is identical to the 70-ka margin (Fig. 9A; low confidence). As described in the earlier time-slice, we show Keewatin ice expanded to cover the entire western region of the Canadian Shield, north to merge with the Innuitian Ice Sheet, and east to cover Hudson Bay (after Dredge and Thorleifson, 1987; Kleman et al., 2010). We show ice covering most of Atlantic Canada including the continental shelf as suggested by the review of Stea et al. (2011) and references therein. We trace the "Caledonia Phase" ice margin of Stea et al. (2011). We also show the southern margin of the Labrador Dome in the Saint Lawrence Lowlands. This ice margin is derived from the position of the Lévrard till (Lamothe et al., 1992) and the associated Deschaillons varves (Hillaire-Marcel and Page, 1981). Only two chronological data points are available at 65 ka (Fig. 3); these data are an OSL age from the northwest margin suggesting an extensive fluvial deposit at 62.6 ± 3.4 ka (Shfd02060; Bateman and Murton, 2006) and ice-free conditions on the eastern coast of Baffin Island as suggested by OSL data from Robinson Lake at 66 ± 7 ka (OTL-552; Miller et al., 1999).

As a minimum ice extent at 65 ka, we assume Keewatin ice was largely restricted to the Canadian Shield area northwest of Hudson Bay (Fig. 9A). Following Kleman et al. (2010), this ice configuration contains a northward extension onto Somerset Island, an eastward extension to Southampton Island, and a largely glaciated Baffin Island, except for some ice-free areas along the south coast. This minimum ice extent could have been possible following a delayed response of ice build-up toward peak MIS 4 conditions (~60 ka). As a minimum ice extent for the Labrador Dome at 65 ka, we assume ice followed the outline of the Atlantic flow set (striae and landform data) of Kleman et al. (2010) and we reduce the southern margin of the maximal ice extent by ~100 to ~200 km to accommodate an ice-free interval in Atlantic Canada (de Vernal et al., 1986; Rémillard et al., 2017).

Our maximum ice extent at 65 ka assumes an early onset of MIS 4 conditions (Fig. 9A). Accordingly, we show the maximum ice extent for the Keewatin Dome expanded to cover the entire southern Interior Plains into Montana, North Dakota and South Dakota (ice margin drawn after Clayton and Moran, 1982). In the northwestern sector, we show a significant expansion of the Keewatin Dome to almost LGM extent. In Alberta, the westernmost extent of Keewatin ice is drawn after Jackson et al. (2011) and we show a westward extension of the ice margin following ice proxy evidence from sub-till glaciolacustrine sediments ("Grimshaw gravels"; Slomka and Hartman, 2018). Along the Atlantic coastline, the maximum ice extent roughly follows the continental shelf break and is based largely on seismic analyses and mapping of glaciomarine landforms (Josenhans et al., 1986; Piper and Macdonald, 2001; Shaw et al., 2006). In New England, the maximum ice extent follows the uppermost till unit (Sevon and Braun, 2000; Stone et al., 2005), and south of the Great Lakes, the maximum ice extent corresponds to the Shelbyville morainic system (Johnson et al., 1971) and Bloomington moraines (Frye et al., 1969).

No geochronological constraints are available for the Innuitian Ice Sheet at 65 ka. Therefore, like the 70-ka interval, we borrow the 10.3 ka time of post-LGM deglaciation (see 9 ka yrs 14C in Dalton et al., 2020), where ice covers all of Ellesmere, Axel Heiberg and Devon islands (Fig. 9A). We assume small ice caps were present on Melville and Prince Patrick islands. As a minimum ice extent of Innuitian ice extent, we show the present-day ice configuration over the Queen Elizabeth Islands, which is restricted largely to upland areas of Ellesmere, Devon and Axel Heiberg islands. As a maximum ice extent, we show Innuitian ice at the continental shelf edge. This scenario would have been possible with an early and dramatic growth corresponding to MIS 4.

3.12. Laurentide and Innuitian ice sheets at 60 ka

The 60-ka map shows maximum MIS 4 continental ice over North America (Fig. 9B; low confidence), as broadly informed by estimates of GMSL between -65 m and -85 m compared to present-day (Pico et al., 2017; Spratt and Lisiecki, 2016). We first discuss the Keewatin Dome; based largely on the chronostratigraphic records, we show the southern Keewatin margin expanded dramatically to cover the entire southern Interior Plains into Montana, North Dakota and South Dakota to reflect an ice advance to its maximum MIS 4 position (60 ka ice margin drawn after Clayton and Moran, 1982). This mid-Wisconsinan ice advance (the Burke Lake advance) is well-documented in the stratigraphic record throughout the Interior Plains. In Alberta, this till has been traced westward to at least Birch Mountains (Pine Point; Paulen et al., 2005); in the United States, this till has been traced to almost the LGM position (Napoleon drift of Clayton and Moran, 1982) and potentially as an extensive, weathered pre-LGM till documented in westernmost Ontario (Bajc, 1991). Most workers assign the Burke Lake advance to MIS 4 based on its stratigraphic position (e.g. Evans and Campbell, 1992). However, its age is unknown. We therefore assume the Burke Lake advance occurred at 60 ka based on stratigraphic position and low GMSL at that time. This ice depiction corresponds to the glacial lineation flow set C1 of Boulton and Clark (1990). In the northwestern sector, we show a significant expansion of the Keewatin Dome to cover most of the mainland Northwest Territories (mid-Wisconsinan hypothesis 2 of Dredge and Thorleifson, 1987). In Alberta, the westernmost extent of Keewatin ice is drawn after Jackson et al. (2011) and we show an westward extension of the ice margin following ice proxy evidence from sub-till glaciolacustrine sediments ("Grimshaw gravels"; Slomka and Hartman, 2018).

Regarding the Labrador Dome at 60 ka (Fig. 9B), we show Labrador ice extending over Hudson Bay and merged with the Keewatin Dome. This 60-ka ice advance likely represented the Rocksand advance (Kleman et al., 2010), characterized by a westward expansion of the Labrador Dome with an inception point at a significantly more southern area than later in the Wisconsinan (Veillette et al., 1999). Parent et al. (1995) documented a similar northwest-trending ice flow to the east of Hudson Bay, which is likely correlative to this 60-ka ice advance. We do not consider this to be in conflict with OSL data from the Hudson Bay Lowlands (BG4228 and BG4262; Dalton et al., 2018) owing to the relatively low precision of those ages. We also assume that Labrador ice covered all of Québec and eastward to Atlantic Canada. In Atlantic Canada at 60 ka, we show a significant calving bay into the Laurentian Channel (following the "Mid Wisconsinan" ice exent of Stea et al., 2011). We widen the calving bay to show an ice-free Magdalen Islands to align with OSL data from that area (OSL54; Rémillard et al., 2017). However, the ice likely extended to the shelf break in some areas during peak MIS 4 as suggested by wedge-shaped units in the marine stratigraphic record that have been constrained to that interval by Mosher et al. (1989). Stratigraphic data suggest that ice advanced westward from the Appalachian Mountains over the Saint Lawrence Lowlands (orange arrows on map; Lamothe et al., 1992). This anomalous westward-trending till suggests the potential for a significant ice cap over Atlantic Canada, which subsequently combined with the Labrador Dome (Veillette et al.,

1999). Near Lake Ontario, we show ice following position "D" of Mulligan and Bajc (2018). This ice position is derived from the Scarborough Formation, a sequence of rhythmically bedded lacustrine and deltaic sediments that conformably underlie the Don Formation (Eyles and Williams, 1992). These sediments are likely the result of ice advance into the eastern Lake Ontario outlet, causing damming of drainage and rising of lake levels to >45 m (possibly >100 m) above present-day (Karrow, 1967). This proto-Lake Ontario may have extended northward along the ice margin and drainage must have been diverted to the Atlantic Ocean (via Rome outlet; see Mulligan and Bajc, 2018). Pollen, plant macrofossils and insects found in the Scarborough Formation suggest it was deposited during cooler climate conditions than present-day, perhaps boreal forest or tundra environment (Terasmae, 1960), which supports the nearby presence of an ice sheet. Also, in the Great Lakes region, we show ice covering all of Lake Michigan. It is possible that this ice advance was the source of the deposition of the Glenn Shores till on the eastern coast of Lake Michigan (Monaghan and Larson, 1986; Monaghan et al., 1986). However, the only constraint on this till is that it underlies an extensive organic-bearing deposit that has been assigned to ~65 ka to ~30 ka (Athens Subepisode; Colgan et al., 2015), thus it is possible that it represents an earlier advance.

Overall, available geochronological data (n = 9; Fig. 3) for the 60-ka interval are sparse and largely restricted to ice marginal areas. An OSL age from the northwest margin supports ice-free conditions at 58 ± 4.6 ka (Shfd08146; Murton et al., 2017). In that region, a sub-till wood piece on Victoria Island was dated via U-series to 61.8 ± 8.8 ka (Causse and Vincent, 1989). In Atlantic Canada, OSL data suggest the Magdalen Islands were ice-free with a shallow marine environment at 60 ± 4 ka (OSL54; Rémillard et al., 2017). Nearby, on Cape Breton Island, a wood piece at a sub-till site was constrained to 62.1 ka and 60.8 ka using U-series methods (UQT-179 and UQT-179; de Vernal et al., 1986). In the Saint Lawrence Lowlands, a single TL age from the Pierreville site 98 suggests that this region was ice-free at 61.1 ± 9.2 ka (RS-2000; Lamothe, 1984; Lamothe and Huntley, 1988). Near Lake Ontario, several TL ages on the sub-till Scarborough Formation constrain the deposition of extensive clays to 59.8 ± 8.5 ka (DVSF-10a; Berger and Eyles, 1994). Finally, in the Hudson Bay Lowlands, two OSL ages from sub-till fluvial deposits suggest ice-free conditions at 59.1 ± 5.6 ka and 59.7 ± 5.5 ka (BG4228 and BG4262; Dalton et al., 2018).

Regarding the minimum ice extent at 60 ka, we show Labrador and Keewatin ice roughly following the outline of the Canadian Shield and joined over Hudson Bay (Fig. 9B). We consider the maximum ice extent at 60 ka to be the MIS 4 ice extent. Along the northwest margin, our maximum ice extent is compatible with marine geomorphological evidence, and tentative age estimates, that suggest the ice streams of the western Canadian Arctic Archipelago may have fed an ice shelf that grounded along the Beaufort Sea continental slope and across the Chukchi Borderlands during MIS 4 (Engels et al., 2008; Polyak et al., 2007). As a maximum ice extent at 60 ka, along the Atlantic coastline, the ice margin roughly follows the continental shelf break and is based largely on seismic analyses and mapping of glaciomarine landforms (Josenhans et al., 1986; Piper and Macdonald, 2001; Shaw et al., 2006). In New England, the maximum ice extent follows the uppermost till unit (Sevon and Braun, 2000; Stone et al., 2005), and south of the Great Lakes, the maximum ice extent corresponds to the Shelbyville morainic system (Johnson et al., 1971) and Bloomington moraines (Frye et al., 1969).

Owing to a lack of geochronological constraints for the Innuitian Ice Sheet at 60 ka, we borrow the 10.3 ka time of post-LGM deglaciation (see 9 ka yrs 14C in Dalton et al., 2020), where ice covers all of Ellesmere, Axel Heiberg and Devon islands (Fig. 9B). Farther west, small ice caps are present on Melville and Prince Patrick islands. As a minimum ice extent of Innuitian ice extent, we show the present-day ice configuration over the Queen Elizabeth Islands, which is restricted largely to upland areas of Ellesmere, Devon and Axel Heiberg islands. As a maximum ice extent, we show Innuitian ice at the continental shelf edge.

On Fig. 9B, we also show Heinrich Event 6, which took place at ~60 ka (Hemming, 2004). It remains unclear whether Heinrich Event 6 was a true increase in ice rafted debris or simply an interval where foraminiferal dissolution occurred (Gwiazda et al., 1996; Hemming, 2004). Nevertheless, our 60-ka map shows expansion of continental ice over Hudson Bay and Hudson Strait, a scenario that would provide ample ice cover to drive ice-rafting events into the North Atlantic.

3.13. Laurentide and Innuitian ice sheets at 55 ka

Our 55-ka map maintains large-scale MIS 4 continental ice over North America (Fig. 10A; low confidence), informed largely by estimates of GMSL between -50 m and -70 m compared to present-day (Pico et al., 2017; Spratt and Lisiecki, 2016). We show Keewatin ice restricted to the Canadian Shield region, leaving the southern Interior Plains ice-free (Fig. 10A). Ice covers Hudson Bay, all of Québec and eastward to Atlantic Canada. In Atlantic Canada, we show a significant calving bay into the Laurentian Channel (following the "Mid Wisconsinan" ice exent of Stea et al., 2011). We widen the calving bay to show an ice-free Magdalen Islands to align with OSL data from that area (OSL54; Rémillard et al., 2017). Nearby, in the Saint Lawrence Lowlands, we show a detailed ice configuration. In that region, stratigraphic data suggest the combined Laurentide/Appalachian ice may have retreated slightly to the west (Malone till, see Prest and Hode-Keyser, 1977) and to the east (Chaudière till; Lamothe et al., 1992) allowing for the development of an ice marginal lake in the intervening area (Glacial Lake Gayhurst). This lake was characterized by rhythmically bedded silt and sand, and varve-counting suggests it was present for ~4000 years (McDonald and Shilts, 1971; Shilts, 1981). Paleoelevation mapping of this ice marginal lake suggests that it must have drained through New York and New Hampshire (MacDonald, 1971). We draw the ice margin in the Saint Lawrence Lowlands after McDonald and Shilts (1971).

In the Great Lakes region at 55 ka, there is evidence to suggest an ice advance into the Lake Ontario Basin (Guildwood phase; Karrow et al., 2000). This is documented by a thin till (Sunnybrook Till) that overlies the Scarborough Formation along the Lake Ontario shoreline (Terasmae, 1960). The extent of ice advance over the region is debated (in particular, whether Toronto was over-ridden by ice; Eyles and Eyles, 1983). However, it is possible that the ice margin approximated the Niagara Escarpment, since there is evidence of a till at Paris, Ontario (correlative with "Canning" till?; Karrow, 1963) and Gondwana, New York (correlative with "brown" till?; Calkin et al., 1982). There are two additional TL ages of 41.2 ± 8 ka and 45.9 ± 9 ka (SPSD84-1 and WCSD; Berger and Eyles, 1994). Based on the stratigraphic position of the Sunnybrook Till, it may have been deposited between ~55 ka and ~50 ka, which is within 2-sigma error on these age estimates. Palynological analyses of nearby non-glacial deposits suggest that the area around Lake Ontario had a moist and cool climate during the deposition of the Sunnybrook Till (Berti, 1975). We assume ice margin "E" of Mulligan and Bajc (2018). Ice in this position would have created widespread pooling of water in the Lake Ontario area, shifting the drainage of the Great Lakes Basin to the Mississippi River via the Chicago outlet (Mulligan and Bajc, 2018). In the Great Lakes region, between 60 ka and 55 ka, we show ice advancing into Lake Michigan. It is possible that this ice advance was the source of the Glenn Shores till on the eastern coast of Lake Michigan (Monaghan and Larson, 1986; Monaghan et al., 1986). However, the only constraint on this till is that it underlies an extensive organic-bearing deposit that has been assigned to ~65 ka to ~30 ka (Athens Subepisode; Colgan et al., 2015), thus it is possible that it represents an earlier advance.

Available geochronological data for the 55-ka interval (n = 13; Fig. 3) are sparse and largely restricted to ice marginal areas. Three OSL ages from the northwest margin support ice-free conditions between 57 ka and 53 ka (Murton et al., 2017). Nearby, on Banks Island, a U-series age from re-worked deltaic sediments suggests that this area was ice-free at 52.5 ± 6.8 ka (Causse and Vincent, 1989). In Atlantic Canada, an OSL

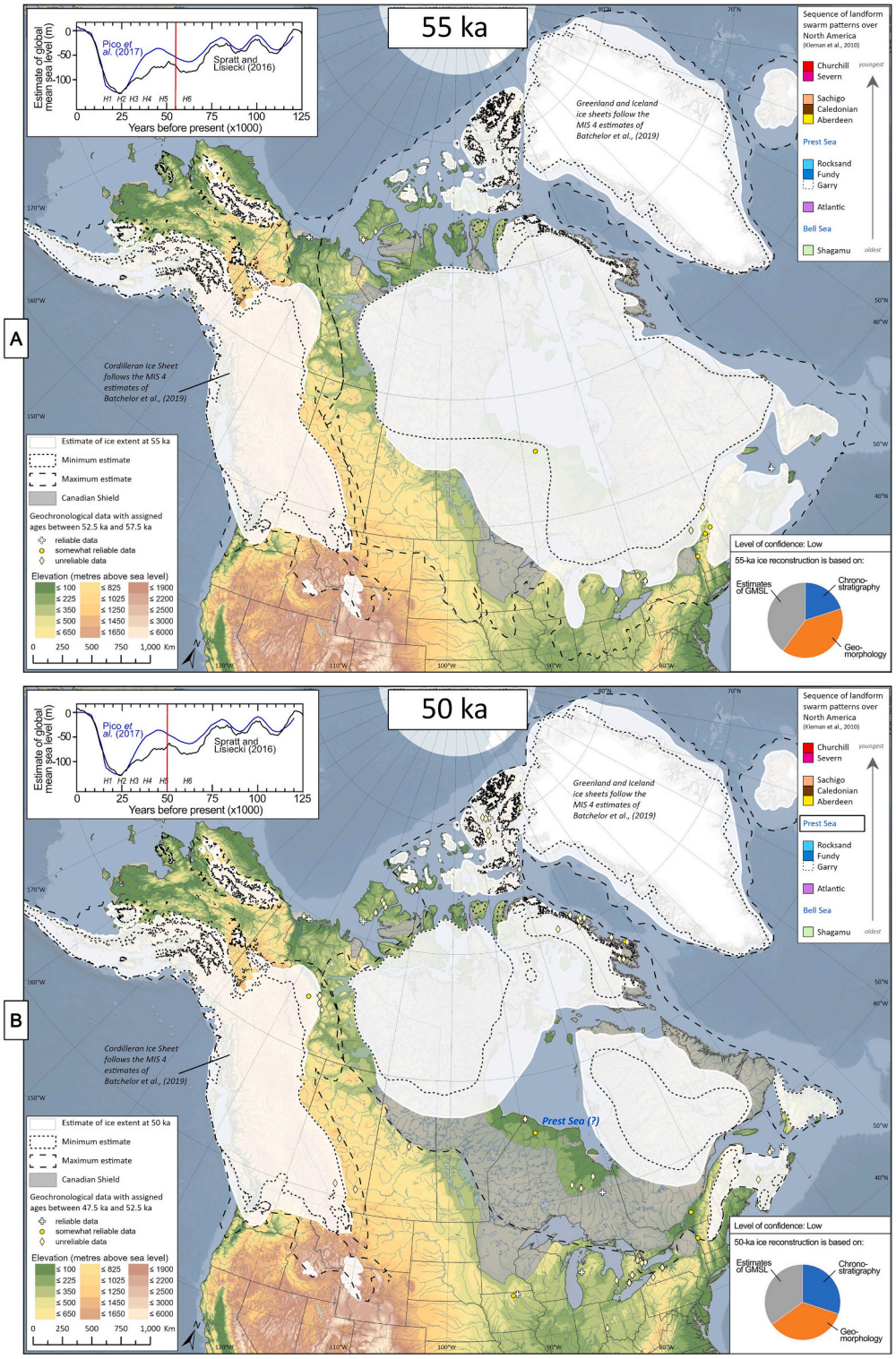

Fig. 10. Reconstructed North American ice at 55 ka (panel A) and 50 ka (panel B).

age from the Magdalen Islands suggests a shoreline deposit at 55 ± 5 ka (OSL53; Rémillard et al., 2017). Nearby, in the Saint Lawrence Lowlands, two IRSL ages suggest a varved lake may have been present at some point between 56 ka and 55 ka (Caron, 2013) and an OSL age from sub-till fluvial sediments suggests ice-free conditions at 53 ± 16 ka (SPSC_2; Godfrey-Smith et al., 1988). Near Lake Ontario, TL ages on the sub-till Scarborough Formation constrain the deposition of extensive clays between 55 ka and 54 ka (CPSF87-1 and DVSF-10b; Berger and Eyles, 1994). Finally, in the Hudson Bay Lowlands, geochronological data suggest the area became ice-free soon after 55 ka. Notably, a sub-till marine shoreline deposit was dated to 52.5 ± 5 ka (BG3807; Dalton et al., 2016).

As a minimum ice extent estimate at 55 ka, we assume the Keewatin Dome covered the entire Canadian Shield of western Canada, extending eastward to cover Baffin Island except for coastal areas (Fig. 10A). This minimum ice extent also shows the Keewatin and Labrador domes

merged over Hudson Bay, with parts of the western Hudson Bay Lowlands ice-free to accommodate, within error, marine sediments dated via OSL to ~60 ka (BG4228 and BG4262; Dalton et al., 2018). The minimum ice estimate also takes into account preliminary cosmogenic nuclide dating in the Torngat Mountains, which suggests potentially ice-free conditions at some point between 56 ka and 36 ka, with the most probably age, corrected for burial, to be 56 ka (dating of wave-cut benches, suggestive of an ice-dammed lake; Pico et al., 2021). Our maximum ice extent assumes a delayed peak of MIS 4 conditions. Identical to the 60-ka time slice, we show maximum Keewatin ice expanded dramatically to cover the entire southern Interior Plains into Montana, North Dakota and South Dakota (ice margin drawn after Clayton and Moran, 1982).

No geochronological constraints are available for the Innuitian Ice Sheet at 55 ka. Thus, we use the 10.3 ka time of post-LGM deglaciation (see 9 ka yrs 14C in Dalton et al., 2020), that shows ice covering all of Ellesmere, Axel Heiberg and Devon islands (Fig. 10A). Farther west, small ice caps are present on Melville and Prince Patrick islands. As a minimum ice extent of Innuitian ice extent, we show the present-day Innuitian ice extent over the Queen Elizabeth Islands (upland areas of Ellesmere, Devon and Axel Heiberg islands). As a maximum ice extent, we show Innuitian ice at the continental shelf edge.

3.14. Laurentide and Innuitian ice sheets at 50 ka

Our 50-ka map shows the reduction of MIS 4 ice over North America (Fig. 10B; low confidence), with an ice-free Hudson Bay and Labrador/Keewatin domes reduced in size from their MIS 4 extent. At that time, GMSL was between -45 m and -70 m compared to present-day (Pico et al., 2017; Spratt and Lisiecki, 2016). We show Keewatin ice expanded to the entire western region of the Canadian Shield. To better align with evidence for an ice-free Hudson Bay during MIS 3 (discussed next) we separate the Keewatin and Labrador domes. The updated Keewatin Dome covers much of eastern Keewatin and eastward to Baffin Island. Because the 50-ka interval represents the likely removal of MIS 4 ice from Hudson Bay, we assume this ice configuration was similar to the post-LGM deglaciation of Hudson Bay at ~9 ka (8 ka uncalibrated) (see Dalton et al., 2020 and references therein). Ice-free condition in the Hudson Bay Lowlands follow several geochronological constraints in that area (Dalton et al., 2016; Stroup et al., 2013). Under this scenario, this low-lying region was likely isostatically depressed, resulting in a marine incursion (Prest Sea? Thorleifson et al., 1992). Because the 50-ka interval represents the likely removal of MIS 4 ice from Hudson Bay, we show the western and northern margin of the Labrador Dome resembling post-LGM deglaciation of that region (e.g. ice margin near the Sakami moraine, see Dalton et al., 2020 and references therein). In Atlantic Canada, we show a significant calving bay into the Laurentian Channel (following the "Mid Wisconsinan" ice exent of Stea et al., 2011). We further widen the calving bay to show an ice-free Magdalen Islands (see OSL work of Rémillard et al., 2017) as well as an ice-free Saint Lawrence Lowlands (see OSL work of Godfrey-Smith et al., 1988; Munroe et al., 2016). Various geochronological constraints from around the Great Lakes offer confirmatory evidence of ice-free conditions around 50 ka, known locally as the Port Talbot Phase (Karrow et al., 2000).

At the 50-ka interval, 32 chronological constraints are available (Fig. 3). Two radiocarbon ages from wood pieces contained in sub-till organic-bearing sediments suggest the region between the Keewatin Dome and Cordilleran Ice Sheet area was ice-free at 48.9 ± 1.3 ka (TO-1187; Smith, 1992) and 47.7 ± 1.5 ka (TO-195; Hughes et al., 1993). On the northwest margin, one OSL age from the coastline suggests this area was ice-free at 52 ± 3.1 ka (Shfd08145; Murton et al., 2017). Nearby on Banks Island, shells contained in deltaic sediments were dated to 52.5 ± 6.8 ka (UQT-145_A0; Causse and Vincent, 1989). Farther east, on Baffin Island, two radiocarbon ages on organic material preserved in sub-till lacustrine sediments suggest ice-free conditions at 49.2 ± 1 ka (OS-18067; Fréchette et al., 2006) and 47.8 ± 2.3 ka (CAMS-28655; Steig et al., 1998). In Atlantic Canada, sand contained in a stratigraphic section was dated via OSL to 51 ± 4 ka (OSL55; Rémillard et al., 2017). Nearby, in the Saint Lawrence Lowlands, an OSL age from a sub-till silt unit suggests ice-free conditions at 51.4 ± 14 ka (SPSC_1; Godfrey-Smith et al., 1988). An ice-free Saint Lawrence Lowlands is supported by an OSL age from cave sediments in Vermont (M016_quartz; Munroe et al., 2016). Farther south, near Lake Ontario, four radiocarbon ages from an extensive sub-till organic unit suggest ice-free conditions at ~50 ka (borehole records; Mulligan and Bajc, 2018). Nearby, this is supported by six radiocarbon ages on wood and organic material, re-worked into till and outwash sediments, suggesting ice-free conditions south of Lake Ontario (Genesee Valley site; Young and Burr, 2006). A TL age from a sediment lens in till suggests the ice margin was nearby at 50.9 ± 8.8 ka (SPSF87-2; Berger and Eyles, 1994). In addition, north of Lake Erie, several radiocarbon ages on wood contained in a channel-fill sequence suggest ice-free conditions at ~50 ka (Zorra Quarry site; Bajc et al., 2015). Finally, in the Hudson Bay Lowlands, three radiocarbon ages from sub-till organic material have been dated to the ~50 ka interval (Dalton et al., 2016; Stroup et al., 2013) and sub-till marine sediments were dated via OSL to 52.5 ± 5 ka (BG3807; Dalton et al., 2016).

As a minimum ice extent at 50 ka, we show Keewatin ice restricted to the Canadian Shield, moderate in size, and covering much of mainland Nunavut and the Northwest Territories (Fig. 10B). Inland areas of Baffin Island are glaciated while coastal areas are largely ice-free, following the mid-Wisconsinan Hypothesis 2 of Dredge and Thorleifson (1987). The minimum Keewatin Dome also largely follows this hypothesis but with a further reduction of the western margin to fit within the bounds of the Canadian Shield. Our minimum ice extent shows a moderately sized Labrador Dome, along with smaller independent ice masses in Atlantic Canada (mid-Wisconsinan Hypothesis 2 of Dredge and Thorleifson, 1987). On the other hand, our maximum Keewatin ice extent shows ice largely restricted to the Canadian Shield and joined with the Labrador Dome over Hudson Bay to account for a late removal of MIS 4 ice from Hudson Bay. Our maximum ice extent of Labrador ice at 50 ka is similar to the 55-ka interval. In Atlantic Canada, we show a significant calving bay into the Laurentian Channel (following the "Mid Wisconsinan" ice exent of Stea et al., 2011). We widen the calving bay to show an ice-free Magdalen Islands to align with OSL data from that area (OSL55; Rémillard et al., 2017). This maximum ice configuration is extended into the Lake Ontario basin to account for large uncertainties in the timing of the Sunnybrooke Till between 55 ka and 50 ka (Guildwood phase; Karrow et al., 2000). This maximum ice extent, showing long-lasting ice cover over central Canada, satisfies criticisms of MIS 3 geochronological data from the Hudson Bay Lowlands (Miller and Andrews, 2019).

A single reliable radiocarbon age from Ellesmere Island helps to constrain the Innuitian Ice Sheet at 50 ka; a radiocarbon age from wood located in detrital sand dated to 47.7 ± 1.8 ka (Bell, 1992). To depict Innuitian ice at 50 ka, we use the 10.3 ka time of post-LGM deglaciation (see 9 ka yrs 14C in Dalton et al., 2020), where ice covers all of Ellesmere, Axel Heiberg and Devon islands (Fig. 10B). Farther west, small ice caps are present on Melville and Prince Patrick islands. As a minimum ice extent, we show the present-day ice extent over the Queen Elizabeth Islands, which is restricted largely to upland areas of Ellesmere, Devon and Axel Heiberg islands. As a maximum ice extent, we show Innuitian ice at the continental shelf edge.

3.15. Laurentide and Innuitian ice sheets at 45 ka

Based largely on evidence from the chronostratigraphic record and estimates of GMSL, our 45-ka map shows moderate ice over North America, with distinct Keewatin and Labrador domes and the Hudson Bay region ice-free (Fig. 11A; medium confidence). During this interval, we assume Keewatin ice was restricted to the Canadian Shield, moderate in size, and covered much of mainland Nunavut and the Northwest Territories, similar to the mid-Wisconsinan Hypothesis 2 of Dredge and

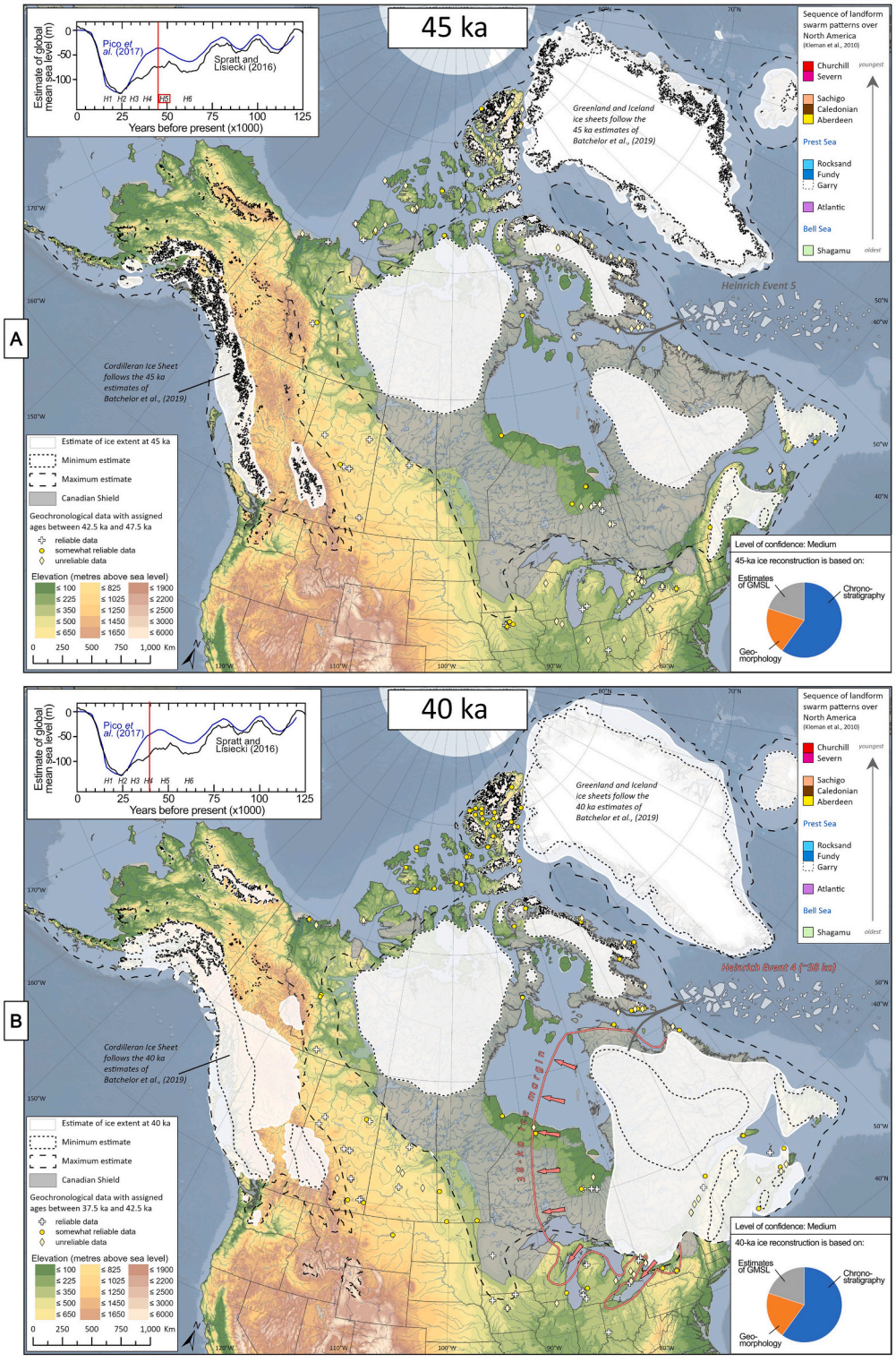

Fig. 11. Reconstructed North American ice at 45 ka (panel A) and 40 ka (panel B), with an ice advance at ~38 ka shown as a pink line.

Thorleifson (1987). We further reduce the western margin to fit within the bounds of the Canadian Shield. We show Labrador ice centered over Quebec, with smaller ice masses over Newfoundland, the Appalachian Range and Atlantic Canada (Fig. 11 upper; following mid-Wisconsinan Hypothesis 2 of Dredge and Thorleifson, 1987). This 45-ka ice configuration is informed by estimates of GMSL between -35 m and -75 m compared to present-day (Pico et al., 2017; Spratt and Lisiecki, 2016). However, our ice configuration leans more toward the higher estimate of GMSL (-35 m) because this estimate was recently reconciled with the geochronological record from the Hudson Bay Lowlands (Dalton et al., 2019). The following three paragraphs outline the evidence in support of this ice configuration.

Our ice configuration at 45 ka aligns with numerous geochronological data from the southern Interior Plains, northwest margin and eastern Keewatin suggesting ice-free conditions at ~45 ka. Eight radiocarbon ages from charcoal, wood and bones suggest ice-free

conditions in the Southern Interior Plains at ~45 ka (Bélanger et al., 2014; Jass and Beaudoin, 2014; Lowdon and Blake, 1975; Shapiro et al., 2004; Young et al., 1994). In the Northern Interior Plains, wood and bark contained in stratigraphic sections also constrain ice-free conditions at ~45 ka (UCIAMS-23866 and UCIAMS-26790; Huntley et al., 2008). Also in that region, along the northwest margin, sand from an aeolian dune (Kittigazuit Fm) was dated to 43.4 ± 2.4 ka based on OSL methods (Shfd02061; Bateman and Murton, 2006). Nearby, Banks and Prince of Wales islands were ice-free at ~43 ka as suggested by two radiocarbon ages from shells (UCI-60271 and GSC-4322; Lakeman, 2012; McNeely and McCuaig, 1991). Moreover, on the western coast of Banks Island, bone fragments located in marine sands suggest ice-free conditions at 45.3 ± 1.5 ka (TO-2294; McNeely and Jorgensen, 1992). Finally, in eastern Keewatin, two radiocarbon ages from shells located in the Rae Isthmus ice stream were dated at 42.6 ± 0.63 ka and 42.9 ± 0.7 ka (Beta-339718 and Beta-315076; McMartin et al., 2019) and a TL age from fluviolacustrine sediments in northern Manitoba was dated to 46 ± 4 ka (EKN-8; Berger and Nielsen, 1990).

A reduced Labrador Dome is also supported by the chronostratigraphic record. This ice configuration aligns with the "Mid Wisconsinan" ice extent (Stea et al., 2011), showing a significant calving bay into the Laurentian Channel. In Atlantic Canada, an OSL age from a shoreline deposit on the Magdalen Islands suggest this region was ice-free at 44 ± 4 ka (OSL04; Rémillard et al., 2016). Ice-free conditions on Cape Breton Island are supported by U-series and radiocarbon ages on wood contained at the Bay St Lawrence site of ~48 and ~47 ka (UQT-178 and GSC-3636; Blake, 1984; de Vernal et al., 1986). In the Appalachian region, a radiocarbon age of 44.7 ± 2.5 ka on wood from a lacustrine sediment core (OS-3468; Dorion, 1997) and an IRSL age from a possible ice marginal delta of 45.5 ± 5 ka (Caron, 2013) suggest local ice-free conditions. To the south, key evidence from Lake Ontario comes from seven radiocarbon dates from organic material contained in borehole records in the range of 47 ka to 43 ka (Mulligan and Bajc, 2018). South of Lake Ontario, 35 radiocarbon ages on wood and plant fragments in sub-till lacustrine sediments suggest ice-free conditions at between 47 ka and 42 ka (Genesee Valley and Sixmile Creek sites; Karig and Miller, 2013; Young and Burr, 2006). Additional radiocarbon ages on wood and plant matter support ice-free conditions near Lake Erie (deVries and Dreimanis, 1960; Dreimanis et al., 1966; McNeely and Jorgensen, 1993; Vogel and Waterbolk, 1972) and in Michigan (Colgan et al., 2015; Rieck and Winters, 1980) at ~45 ka.

Finally, an ice-free Hudson Bay Lowlands at 45 ka is supported by three radiocarbon ages on organic material from the Albany and Moose river sites (TO-1752, UOC-0594 and UOC-0597; Dalton et al., 2016; Dalton et al., 2018). Nearby, Stroup et al. (2013) reported a radiocarbon age of 45.5 ± 0.7 ka (OS-67639) on wood contained in the sand unit of a lake core, and McNeely and Jorgensen (1993) report wood from a drill core dating to 43.1 ± 2.5 ka (GSC-4837). Confirmatory evidence for an ice-free Hudson Bay Lowlands is provided by an OSL age from sub-till fluvial sediments of 42.8 ± 3.8 ka (BG3800; Dalton et al., 2016). Moreover, an ice-free Hudson Bay ~45 ka helps to reconcile isostatic adjustment, local marine records and far afield shoreline deposits that have been constrained to this time (Dalton et al., 2019; Pico et al., 2017).

Our minimum ice extent of North American ice at 45 ka (Fig. 11A) follows mid-Wisconsinan Hypothesis 2 of Dredge and Thorleifson (1987). On the other hand, our maximum Keewatin ice extent shows ice largely restricted to the Canadian Shield with the western margin based on Hypothesis 2 of Dredge and Thorleifson (1987). Keewatin ice is shown merged with the Labrador Dome over Hudson Bay, and the ice sheet is extended to the shelf break (Rashid et al., 2019). This maximum ice extent, showing long-lasting coverage over central Canada, satisfies criticisms of MIS 3 geochronological data from the Hudson Bay Lowlands (Miller and Andrews, 2019). Our maximum ice extent also considers evidence suggesting a short-lived, dramatic extension of the Keewatin Dome southward into the continental United States via a low-lying topographic corridor in Manitoba. The timing and extent of this advance into Iowa (known as the Fort Dodge Advance) is constrained to between 45 ka and 39 ka based on several radiocarbon dates on wood contained within, overlying and underlying a local till unit associated with the Keewatin Dome (Kerr et al., 2021). In Atlantic Canada, the maximum ice extent of Labrador ice at 45 ka shows the ice margin at midway between the present-day coastline and the continental shelf break. We also show the Labrador and Keewatin domes joined over Hudson Bay. This maximum ice extent, showing long-lasting coverage over central Canada, satisfies criticisms of MIS 3 geochronological data from the Hudson Bay Lowlands (see Section 4.2; Miller and Andrews, 2019).

Regarding the Innuitian Ice Sheet, a single reliable geochronological constraint is available at 45 ka. On Ellesmere Island, a radiocarbon age from a wood piece is located in a re-worked stony silt unit and dated to 44.7 ± 0.8 ka (TO-113; Blake, 1993). We therefore assume present-day ice extent over the Queen Elizabeth Islands (upland areas of Ellesmere, Devon and Axel Heiberg islands). We consider this to be the minimum ice extent at that time, whereas the maximum ice extent shows Innuitian ice covering all the eastern Queen Elizabeth Islands and merged with the Keewatin Dome farther south (assumed).

In Fig. 11A, we also show Heinrich Event 5m which took place at ~45 ka (Hemming, 2004). This event was characterized by a pronounced increase in ice rafted debris from the general area of Hudson Strait into the North Atlantic (Hemming, 2004). Our 45-ka map shows a greatly reduced Labrador Dome with no ice over Hudson Bay, a scenario that would be unlikely to provide sufficient ice to drive rafting events into the North Atlantic. However, given the resolution of our maps (5-ka time-steps), any rapid ice growth/recession would not be represented here. Another possible explanation is a slightly delayed removal of MIS 4 ice from the Hudson Bay/Strait from ~50 ka to closer to 45 ka (~48 ka as suggested by terrestrial data? see Asmerom et al., 2010; Wang et al., 2001). Both scenarios are taken into consideration in our generous minimum and maximum uncertainties for the 45-ka interval.

3.16. *Laurentide and Innuitian ice sheets at 40 ka*

Our 40-ka map relies largely on chronostratigraphic data, with some inferences from the geomorphic record and estimates of GMSL. We show the persistence of independent ice domes over Keewatin and Labrador, while Hudson Bay (Fig. 11B; medium confidence). Our 40-ka estimate shows Keewatin ice restricted to the Canadian Shield, moderate in size, and covering much of mainland Nunavut and the Northwest Territories (Fig. 11B), similar to the mid-Wisconsinan Hypothesis 2 of Dredge and Thorleifson (1987), with the western margin fitted to the boundary of the Canadian Shield. The southern, western and eastern Keewatin margins are aligned with geochronological data suggesting ice-free conditions. At 40 ka, we assume the Labrador Dome extended 200 to 600 km from the mid-Wisconsinan margin proposed by Dredge and Thorleifson (1987) because of evidence for an ice margin near the Great Lakes (see below). This ice configuration is broadly informed by estimates of GMSL between -40 m and -85 m compared to present-day (Pico et al., 2017; Spratt and Lisiecki, 2016). Chronostratigraphic evidence in support of this ice configuration is detailed below.

At 40 ka, 122 chronological constraints are available from the glaciated region of North America (Fig. 3). Radiocarbon ages on charcoal from a paleosol in central Saskatchewan provide evidence for ice-free conditions in the Southern Plains continuously between ~50 and ~32 ka (Bélanger et al., 2014). This ice-free configuration is supported by nine radiocarbon ages from bones contained in pre-LGM valley fill deposits in Alberta (Lowdon and Blake, 1975; Shapiro et al., 2004; Young et al., 1994). Several other radiocarbon ages from organic materials in this region offer confirmatory evidence for ice-free conditions between 42 ka and 38 ka, including dates from wood in lake sediments (Fisher et al., 2009), bones from a sub-till prairie dog burrow (Young et al., 1999), wood contained in a sub-till silt unit (I-2615; Lowdon and Blake, 1970), wood contained in a gravel and sand unit (AECV-428C;

Liverman et al., 1989) and wood found at the base of a till unit dated to 40.2 ± 0.8 ka (Beta-249392; Paulen et al., 2019). Along the northwest margin, two U-series ages on shells in re-worked deltaic sediments on Banks Island suggest local ice-free conditions between 42 ka and 38 ka (UQT-220_A0, A1; Causse and Vincent, 1989). Nearby, Murton et al. (2017) presented an OSL age on fluvial sediments (Kidluit Fm) yielding ages of 41 ± 2.9ka (Shfd06063). In eastern Keewatin, three radiocarbon ages from shells located in the Rae Isthmus ice stream were dated between 42 ka and 40 ka (Beta-339713, Beta-339717 and Beta-339715; McMartin et al., 2019) and a TL age from fluviolacustrine sediments in northern Manitoba was dated to 38 ± 3 ka (EKN-7; Berger and Nielsen, 1990).

Geochronological constraints are also available for Baffin Island and the eastern sector of the Keewatin Dome. On southernmost Baffin Island adjacent to the Labrador Strait, Manley and Jennings (1996) presented two radiocarbon ages on shells in till yielding ages of ~42 ka, suggesting ice-free conditions in the Labrador Strait at this time. Also in this region, three radiocarbon ages from shells on till yielded ages of ~39 ka (AA-11451, GSC-426 and AA-6298; Kaufman and Williams, 1992; Lowdon et al., 1967; Manley and Jennings, 1996) and three radiocarbon ages from shells on till yielded ages of ~38 ka (AA-7899, AA-12608 and AA-10646; Manley and Jennings, 1996). With respect to the Labrador Dome, a radiocarbon age on a shell in till suggests ice-free conditions along the southern Labrador Strait at 42.1 ± 2.1 (AA-10232; Manley and Jennings, 1996) and two radiocarbon ages from shells in a similar context suggest coastal Labrador was ice-free between 42 ka and 37.5 ka (GSC-3950 and GSC-4189; McNeely and McCuaig, 1991). In Atlantic Canada, a deglaciated Anticosti Island is suggested by two radiocarbon ages from shells in glacial sediments (till and glaciomarine sediment) dated to between 40 ka and 39 ka (UQ-514 and UQ-553; Gratton et al., 1984). Nearby, on Magdalen Islands, two OSL ages from sub-till beach sediments suggest ice-free conditions at 41 ± 4 ka and 38.3 ± 3 ka (OSL03 and OSL08; Rémillard et al., 2016). Ice-free conditions in mainland Atlantic Canada between 41 ka and 38 ka are also suggested by radiocarbon ages from shells and sub-till wood (GSC-1440, GSC-4018, I-3236 and GSC-3848 HP; Blake, 1984; Blake, 1986; MacNeill, 1969; McNeely and McCuaig, 1991). It is also possible that the Saint Lawrence Lowlands were ice-free at ~40 ka, as suggested by a radiocarbon age from shell fragments in an estuary deposit dated to 38 ± 1.1 ka (TO-3990; Dionne and Occhietti, 1996) as well as wood dated to 38.7 ± 3.5 ka from a stratigraphic section (UL-11; Brodeur and Allard, 1985).

Geochronological constraints for the 40-ka interval are also available for the Great Lakes region and the Hudson Bay Lowlands. Key evidence from near Lake Ontario comes from radiocarbon dates from organic material contained in borehole records in the range of ~42 ka (Mulligan and Bajc, 2018). South of Lake Ontario, 14 radiocarbon ages on wood and plant fragments in sub-till lacustrine sediments suggest ice-free conditions between 42 ka and 38 ka (Genesee Valley and Sixmile Creek sites; Karig and Miller, 2013; Young and Burr, 2006). Two additional radiocarbon ages on wood in till support ice-free conditions on the northern shore of Lake Erie (Dreimanis et al., 1966; Vogel and Waterbolk, 1972) and eight radiocarbon ages constrain an ice-free Michigan at ~40 ka (Buckley and Willis, 1972; Colgan et al., 2015; Gephart et al., 1982; Kehew et al., 2005; Rieck and Winters, 1980; Winters and Rieck, 1991). To the north, an ice-free Hudson Bay Lowlands is supported by three separate wood pieces from stratigraphic sections dated to between 42 ka and 38 ka (ISGS A2460, TO-1751 and TO-1753; Dalton et al., 2016). Confirmatory evidence for an ice-free Hudson Bay Lowlands is provided by an OSL age from sub-till fluvial sediments of 42.2 ± 4 ka (BG3808; Dalton et al., 2016).

In Atlantic Canada, we show a significant calving bay into the Laurentian Channel (following the "Mid Wisconsinan" ice exent of Stea et al., 2011). We widen the calving bay to show an ice-free Magdalen Islands as well as a deglaciated Anticosti Island following three radiocarbon ages from shells in glacial sediments (till and glaciomarine sediment) that suggest regional ice-free conditions at ~40 ka (GSC-4018, UQ-514 and UQ-553; Blake, 1986; Gratton et al., 1984). In the Great Lakes region, we show the ice margin located within Lake Ontario and Lake Huron following ice margin "F" of Mulligan and Bajc (2018). Finally, following geochronological data from the Hudson Bay Lowlands (Dalton et al., 2016), we maintain ice-free conditions surrounding Hudson Bay.

We assume the mid-Wisconsinan Hypothesis 2 of Dredge and Thorleifson (1987) to be the minimum ice extent at 40 ka (Fig. 11B). On the other hand, our maximum Keewatin ice extent assumes ice largely restricted to the Canadian Shield with the western margin based on Hypothesis 2 of Dredge and Thorleifson (1987). Keewatin ice is shown merged with the Labrador Dome over Hudson Bay, and the ice sheet is extended to the shelf break (Rashid et al., 2019). This maximum ice extent, showing ice coverage over central Canada, satisfies criticisms of MIS 3 geochronological data from the Hudson Bay Lowlands (Miller and Andrews, 2019). Our maximum ice extent also considers evidence suggesting a short-lived, dramatic extension of the Keewatin Dome southward into the continental United States via a low-lying topographic corridor in Manitoba. The timing and extent of this advance into Iowa (known as the Fort Dodge Advance) is constrained to between 45 ka and 39 ka based on several radiocarbon dates on wood contained within, overlying and underlying a local till unit associated with the Keewatin Dome (Kerr et al., 2021).

Regarding the maximum extent of the Labrador Dome, we assume an ice margin along the Atlantic coast at approximately midway between the present-day coastline and the continental shelf break. In Hudson Strait, we show ice-free conditions extending westward to accommodate shells from eastern Keewatin (McMartin et al., 2019). Near Lake Ontario, the maximum estimate assumes scenario "F" of Mulligan and Bajc (2018). We also show the Labrador and Keewatin domes joined over Hudson Bay. This maximum ice extent, showing almost complete ice coverage over central Canada, satisfies criticisms of MIS 3 geochronological data from the Hudson Bay Lowlands (see Section 4.2; Miller and Andrews, 2019).

Regarding the Innuitian Ice Sheet, there are more than 30 radiocarbon ages in the range of ~42 ka to ~38 ka from the coastal areas of Ellesmere and Axel Heiberg islands (Bednarski, 1995; England, 1990; England, 1996; England et al., 2000; Ó Cofaigh et al., 2000; Smith, 1999). To the west, on Melville Island, several radiocarbon dates on shells in till also suggest sub-aerial conditions at ~42 ka (England et al., 2009). We therefore show the present-day ice extent over the Queen Elizabeth Islands (upland areas of Ellesmere, Devon and Axel Heiberg islands; Fig. 11B). We assume this to be the minimum ice extent at that time. The maximum ice extent shows Innuitian ice covering all the eastern Queen Elizabeth Islands.

3.16.1. *Rapid advance of the Labrador Dome at ~38 ka and Heinrich Event 4*

Also included in Fig. 11B is a rapid 38-ka expansion of Labrador ice westward over the Hudson Bay Lowlands and southward into the Great Lakes (pink line and arrows). South of Lake Ontario, this event likely resulted in the rapid formation (40 m of deposition) of a proglacial lake in Sixmile Creek, dated between ~39 ka to ~38 ka (Karig and Miller, 2013). We assume the ice margin extended into the Lake Ontario basin, where it remained from ~39 ka to ~36 ka (known as both the Brimley Phase and Cherry Tree Stadial; Karrow et al., 2000). This oscillating ice margin was possibly responsible for depositing the extensive, silt-rich buried moraines (also known as "overridden moraines") that characterize the stratigraphic record around Lake Erie (e.g. Bleuer, 1974; Totten, 1969; White et al., 1969) and formed the Mogadore, Titusville, Millbrook and Jelloway tills (Frolking and Szabo, 1998; White, 1968; White, 1984; White et al., 1969). We also assume the rapid 38-ka expansion of Labrador ice extended into Wisconsin. This advance fits with evidence of an ice advance over Lake Michigan at some point between 39.1 ± 0.4 ka and 30.4 ± 0.9 ka (Carlson et al., 2018) and the subsequent abandonment of a moraine in Michigan at 35 ka (discussed

in the 35-ka timeslice; Ceperley et al., 2019). Heinrich Event 4 took place at ~38 ka (Hemming, 2004) and is likely associated with rapid ice advance in the vicinity of Hudson Bay and/or Hudson Strait.

3.17. Laurentide and Innuitian ice sheets at 35 ka

Our 35-ka map shows a build-up of ice toward the LGM (Fig. 12A; medium confidence), informed largely by the various geochronological and geomorphology datasets, as well as estimates of GMSL. At that time, GMSL was between -60 m and -100 m compared to present-day (Pico et al., 2017; Spratt and Lisiecki, 2016), which supports ice expansion. We show the Keewatin Dome largely constrained to the Canadian Shield, moderate in size, and covering much of mainland Nunavut and the Northwest Territories. This ice margin follows the "late MIS 3" ice extent of Kleman et al. (2010) but we assume it did not extend beyond the 30 ka ice limit of Dyke et al. (2002). The growth of the Keewatin Dome at 35 ka

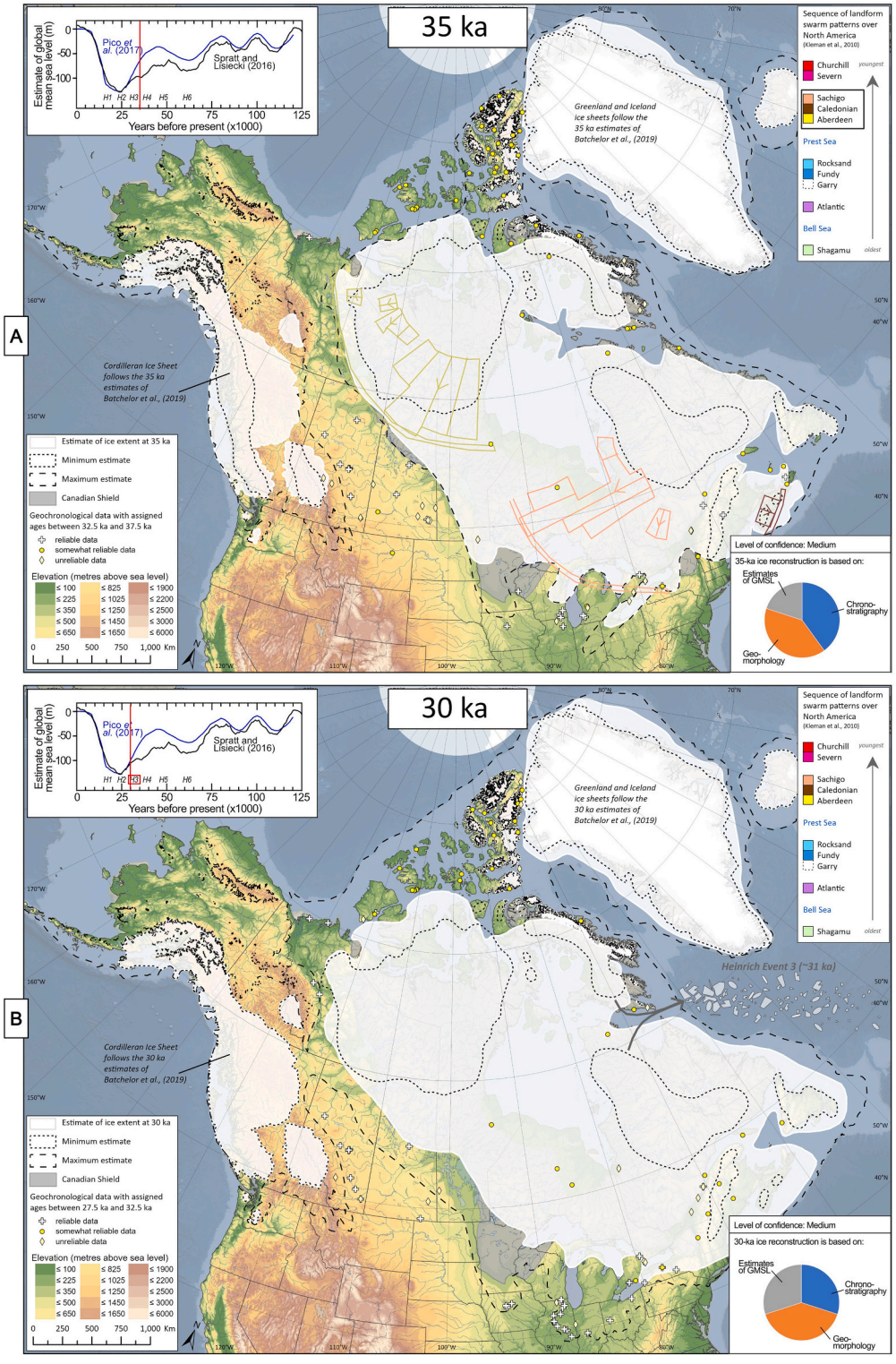

Fig. 12. Reconstructed North American ice at 35 ka (panel A) and 30 ka (panel B).

follows the "Aberdeen" landform swarm patterns (Kleman et al., 2010). Following the dating of shells (McMartin et al., 2019) we show a small ice-free region of eastern Keewatin as an extension of an ice-free Hudson Strait.

Our 35-ka ice configuration is supported in the Interior Plains by 13 radiocarbon ages on charcoal from a paleosol in central Saskatchewan (Bélanger et al., 2014). These data effectively restrict the Keewatin Dome to the Canadian Shield at 35 ka (with the possible exception of Manitoba; see below). Furthermore, in central Alberta, seven radiocarbon ages from bones (horse, deer, bison) located in a pre-LGM valley fill deposit were dated between 37 ka and 33 ka (McNeely, 2002; Young et al., 1994). Nearby, a radiocarbon age of 33.8 ± 0.4 ka was obtained from bones in a prairie dog burrow (TO-1304; Young et al., 1999). An ice-free southern Plains is also supported by a radiocarbon age on wood from a borehole dating to 36.7 ± 1.1 ka (TO-10545; Paulen et al., 2005) and wood contained in a gravel and sand unit dating to 36.6 ± 2 ka (GSC-5359; McNeely, 2002). Along the coastal areas of the Northern Interior Plains, conifer cones contained in a non-glacial sand were dated to ~35 ka (Beta-77432; McNeely, 2006). Banks Island was also ice-free between 36 ka and 35 ka as suggested by two shells located in till on the east coast (UCI-60269 and UCI-60273; Lakeman, 2012).

Regarding the northern region of the Labrador Dome at 35 ka, we assume ice extended westward over Hudson Bay, represented by the Sachigo landform swarm pattern of Kleman et al. (2010). In Hudson Strait, we show an elongated embayment (ice margin drawn after McMartin et al., 2019) extending into northern Hudson Bay as suggested by the dating of shells located in the Rae Isthmus ice stream dated to 37.3 ka and 35.4 ka (Beta-339716 and Keck-122338; McMartin et al., 2019). An ice-free Hudson Strait is also support by five radiocarbon ages on bulk sediment from Pingualuit Crater, northern Quebec, which suggest local ice-free conditions between 37.5 ka and 32.5 ka, although the original authors attributed this mid-Wisconsinan age to a mixture of Holocene and older sediments (Guyard et al., 2011). Along the Atlantic coast of Labrador, McNeely and McCuaig (1991) report a radiocarbon age on a shell in till of 37.5 ± 1.7 ka (GSC-3950).

Our 35-ka ice margin along the northern and eastern coast of Baffin Island is supported by several radiocarbon ages on shells contained in raised marine beds have yielded ages between 37 ka and 34 ka (QL-136, GSC-1964, GSC-1153 and GSC-5214; Lowdon and Blake, 1975; Lowdon et al., 1971; McNeely and Atkinson, 1995; Miller et al., 1977). On southernmost Baffin Island adjacent to the Labrador Strait, Manley and Jennings (1996) and Lowdon et al. (1967) presented three radiocarbon ages on shells in till at ~34 ka (GSC-414, AA-11450, AA-10252) suggesting ice-free conditions in the Labrador Strait at this time.

At 35 ka in Atlantic Canada, we show a significant calving bay into the Laurentian Channel and extend ice to cover most of the mainland (following the "Mid Wisconsinan" ice exent of Stea et al., 2011), which aligns with two radiocarbon ages on shells and bones suggesting ice-free conditions at that time (GSC-1220-2 and GSC-5978; Blake, 1984; McNeely, 2006). This ice advance may have resulted in the "Caledonian" landform swarm patterns in this region (Kleman et al., 2010). An ice-free Anticosti Island and Magdalen Islands between 35 ka and 33 ka is suggested by two radiocarbon ages from shells (UQ-510 and GSC-5978; Gratton et al., 1984; McNeely, 2006). Moreover, four radiocarbon ages on wood, bones and shell from Cape Breton Island have also been dated to between 37 ka and 35 ka (GSC-1220, GSC-1220-2, GSC-1408 and GSC-3381; Blake, 1984). Nearby, in the Saint Lawrence Lowlands, two radiocarbon ages on shell fragments and wood pieces suggest ice-free conditions may have existed between 34 ka and 32.5 ka (Beta-54140 and I-13549; Brodeur and Allard, 1985; Dionne and Occhietti, 1996).

Geochronological constraints are also available for the Great Lakes area at ~35 ka. Near Lake Ontario, ice-free conditions are confirmed by radiocarbon ages on wood and organic materials from various sites, notably boreholes (A2449; Mulligan and Bajc, 2018), organic material contained in lacustrine sediment (AA-57450 and AA-57447; Young and Burr, 2006) and sub-till wood on the north shore of Lake Erie (L-185B, W-177 and GSC-2126; Dreimanis et al., 1966; Lowdon et al., 1977). South of Lake Ontario, four radiocarbon ages from organics in sub-till lacustrine sediments suggest ice-free conditions between 37.5 ka and 34 ka (AA-8639, AA-34317, AA-57448 and AA-57453; Young and Burr, 2006). Eight radiocarbon ages from sub-till wood surrounding southern Lake Michigan suggest this region was ice-free between 37.5 ka and 33 ka (Buckley and Willis, 1972; Eschman, 1980; Kehew et al., 2005; Rubin and Alexander, 1960; Rubin and Berthold, 1961; Vogel and Waterbolk, 1972). Similar to our proposed 38-ka ice margin, we show oscillation of the ice margin into Lake Erie, which was potentially responsible for depositing the extensive, silt-rich buried moraines (also known as "overridden moraines") that characterize the stratigraphic record around Lake Erie (e.g. Bleuer, 1974; Totten, 1969; White et al., 1969), as well as the Mogadore, Titusville, Millbrook and Jelloway tills (Frolking and Szabo, 1998; White, 1968; White, 1984; White et al., 1969).

Our 35-ka ice margin also shows the western portion of the Labrador Dome extended over northern Lake Michigan into Wisconsin. This advance fits with evidence of an ice advance over Lake Michigan at some point between 39.1 ± 0.4 ka and 30.4 ± 0.9 ka (Carlson et al., 2018). We assume this advance terminated at the Arnott moraine where it remained until the moraine was abandoned at ~35 ka (10Be dating of Arnott Moraine; Ceperley et al., 2018). It is possible that the western-most extent of the Labrador Dome reached beyond the Canadian Shield into the Southern Interior Plains, causing the anomalous Labradorean till that was deposited in southern Manitoba (Senkiw Formation; Fenton, 1974; Teller and Fenton, 1980), as well as glaciolacustrine deposits in the Rainy River area that have been associated with a large ice advance from the Labrador sector (p. 50 in Bajc, 1991; two sites where glaciolacustrine sediments underly Whiteshell till).

As a minimum ice extent at 35 ka, we show the Keewatin Dome restricted to the Canadian Shield and covering much of mainland Nunavut and the Northwest Territories (Fig. 12A), similar to the mid-Wisconsinan Hypothesis 2 of Dredge and Thorleifson (1987). A reduced southern and eastern Keewatin margin aligns with the wealth of geochronological data suggesting ice-free conditions in the southern Interior Plains and eastern Keewatin. Furthermore, this minimum ice extent takes into account geochronological data from fluviolacustrine sediments in northern Manitoba (EKN-3; Berger and Nielsen, 1990), as well as two separate radiocarbon ages from shells located in till dated to 34.1 ± 0.4 ka and 36.7 ± 0.9 ka (TO-1892 TO-1893; McNeely, 2002). This minimal ice extent shows ice-free conditions near the Pingualuit Crater, northern Quebec (Guyard et al., 2011) as well as along the Hudson Strait (McMartin et al., 2019). It also allows for ice-free conditions and a marine incursion in the Saint Lawrence Lowlands (marine shells dated between 39 ka and 32 ka; Dionne and Occhietti, 1996; Parent et al., 2015). This marine interval may have occurred by widening of the Saint Lawrence estuary as the result of increased glacial meltwater owing to the growing LIS elsewhere on the continent (Dionne and Occhietti, 1996). The final stage of the LGM ice advance likely blocked the St Lawrence River, leading to the development of the St. Maurice Rhythmites.

Our maximum 35-ka estimate (Fig. 12A) shows Keewatin ice largely restricted to the Canadian Shield with the western margin based on Hypothesis 2 of Dredge and Thorleifson (1987). Keewatin ice is shown merged with the Labrador Dome over Hudson Bay. This maximum ice extent, showing long-lasting coverage over central Canada, satisfies criticisms of MIS 3 geochronological data from the Hudson Bay Lowlands (Miller and Andrews, 2019). Our maximum ice extent also considers evidence suggesting a short-lived, dramatic extension of the Keewatin Dome southward into the continental United States via a low-lying topographic corridor in Manitoba. The timing and extent of this advance (between ~34 ka and ~30 ka; known as the Lehigh Advance) is based on radiocarbon dating of wood contained within, overlying and underlying this till unit associated with the Keewatin Dome (Kerr et al., 2021). Along the Atlantic coastline, the ice margin is drawn at midway

between the present-day coastline and the continental shelf edge. Near Lake Ontario, the maximum estimate assumes scenario "F" of Mulligan and Bajc (2018). We show a lobe extending through Lake Erie in a southwest direction to the LGM extent in Indiana to align with OSL dating of lacustrine cave sediments in this area that suggest drainage blocked by a nearby ice margin (Wood et al., 2010). Finally, we show the Labrador and Keewatin domes joined over Hudson Bay; this maximum ice extent, showing long-lasting coverage over central Canada, satisfies criticisms of MIS 3 geochronological data from the Hudson Bay Lowlands (Miller and Andrews, 2019).

Various radiocarbon ages provide constraints on the Innuitian Ice Sheet at 35 ka. On Ellesmere Island and neighboring Axel Heiberg Island, more than 20 radiocarbon ages from shells and organic material, largely in shoreline areas, have been dated to between 37.5 ka and 32.5 ka (England, 1990; England, 1996; England et al., 2000; Ó Cofaigh et al., 2000). To the west on Melville and Banks islands, 13 radiocarbon ages on shell fragments (largely contained in tills) suggest local ice-free conditions between 37.5 ka and 32.5 ka (England et al., 2009; Nixon and England, 2014). To depict our best estimate of Innuitian ice at 35 ka, we show the present-day ice extent for the region (Fig. 12A). We consider this to be the minimum ice extent at that time. The maximum ice extent assumes full overage of Innuitian ice over the eastern Queen Elizabeth Islands.

3.18. Laurentide and Innuitian ice sheets at 30 ka

Our 30-ka map shows the continuation of ice growth toward the LGM, based largely on evidence from the chronostratigraphic record, geomorphological data and estimates of GMSL. We assume ice broadly extended southward from the Canadian Shield (Fig. 12B; medium confidence), following the overall growth pattern suggested by the "Churchill" and "Severn" landform swarm patterns (Kleman et al., 2010) as well as glacial flow set F (Boulton and Clark, 1990). In the Southern Interior Plains, the advance of the ice margin can be inferred from the youngest sub-till radiocarbon ages; notably an age of 32.2 ± 0.8 ka from charcoal records in Saskatchewan (SacA27173; Bélanger et al., 2014) and 29.4 ± 1.5 ka from a bone from a valley fill deposit in Alberta (AECV:1201c; Young et al., 1994). Accordingly, we show the 30-ka ice margin overlying the charcoal site and not yet advanced to the valley fill deposit in central Alberta. On the northwest margins, we assume ice-free conditions at 30 ka. However, starting at 30 ka, we infer growth of the Keewatin Dome in a northwestward direction, ultimately reaching the local LGM at 27 ka. This pattern of ice advance generally follows geomorphological mapping and radiocarbon dating of marine shells in this region (Lakeman and England, 2013).

Regarding the Keewatin Dome, various geochronological data offer insight into its position at 30 ka (Fig. 3). In northern Manitoba, a TL age from fluviolacustrine sediments was dated to 32 ± 2 ka (EKN-5; Berger and Nielsen, 1990). Farther west, in the Southern Interior Plains, 13 radiocarbon ages on charcoal from a paleosol in central Saskatchewan provide evidence for ice-free conditions continuously between ~50 ka and ~32 ka (Bélanger et al., 2014). These data effectively restrict the Keewatin Dome to the Canadian Shield at 35 ka (with the possible exception of Manitoba; see below). Nearby, in Alberta, six radiocarbon ages on bones contained in a valley fill deposit suggest ice-free conditions between 32 ka and 29 ka (Young et al., 1994). Also in Alberta, ice-free conditions are suggested by a radiocarbon age on sub-till wood fragments of 29.1 ± 1.6 ka (GSC-1370; Lowdon et al., 1971) as well as bones from a prairie dog burrow dated to 31.8 ± 0.7 ka (TO-782; Young et al., 1999). In the Northern Interior Plains, two pieces of wood in sand were dated to ~31 ka suggesting regional ice-free conditions at this time (TO-1188 and TO-1192; Smith, 1992). Regional ice-free conditions are supported by an OSL age on a fluvial deposit on the northwest coast of 31 ± 2.7 ka (Shfd06062; Murton et al., 2017) and an OSL age of 29.6 ± 1.6 ka (Shfd02062; Bateman and Murton, 2006) from aeolian dunes. Lastly, on Banks Island, a U-series age from a shell contained in deltaic sediments suggests ice-fee conditions at 31.8 ± 3.8 ka (UQT-142_A1; Causse and Vincent, 1989). Three radiocarbon ages on bulk sediment from Pingualuit Crater, northern Quebec, suggest local ice-free conditions between 31.5 and 28.6 ka (UCI-75737, UCI-76679, Beta-275125), although the original authors attributed this mid-Wisconsinan age to a mixture of Holocene and older sediments (Guyard et al., 2011).

Regarding the Labrador Dome, at 30 ka, we show ice covering most of Quebec and Labrador. Ice is extended eastward to Newfoundland, southward to the Great Lakes and merged with the Keewatin Ice Sheet over the Hudson Bay Lowlands. Along coastal Labrador we draw the ice margin located 100 km seaward to show an intermediate stage of growth to the continental shelf break following the analysis of sediment cores, radiocarbon dates and seismic profiles (Roger et al., 2013). In Atlantic Canada, we show ice similarly extended toward the continental shelf break, as well as a calving bay into the Laurentian Channel (following the "Mid Wisconsinan" ice exent of Stea et al., 2011). Few constraints for the 30-ka ice margin are available in New England or around the Great Lakes, thus users of these maps should take into consideration the minimum and maximum errors. In the Great Lakes, we show ice covering all of Lake Ontario and the northernmost parts of Lake Huron and Lake Michigan (after Dyke et al., 2002). Overall, the ice configuration at 30 ka is supported by estimates of GMSL, which suggest -100 m compared to present-day (Pico et al., 2017; Spratt and Lisiecki, 2016).

In Atlantic Canada, a radiocarbon age from a shell in glaciolacustrine sediment on Anticosti Island suggests the absence of Labrador ice at 31.4 ± 0.4 ka (UQ-509; Gratton et al., 1984), and a shell in till on the southwest coast of Newfoundland suggests ice-free conditions at 30.3 ± 1 ka (GSC-4563; McNeely and McCuaig, 1991). This calving bay may have extended into the Saint Lawrence Lowlands where ice-free conditions at ~32 ka are supported by two IRSL ages in this interval (M011_feldspar; Caron, 2013; Munroe et al., 2016) as well as two radiocarbon ages on shell fragments and wood pieces (Beta-54140 and I-13549; Brodeur and Allard, 1985; Dionne and Occhietti, 1996). To the east of the Appalachian Range, organic material in a lake core suggests local ice-free conditions at 28.5 ± 0.4 ka (OS-3170; Dorion, 1997).

Finally, our depiction of 30-ka ice shows the Keewatin and Labrador domes merged over Hudson Bay and extending part-way to the Great Lakes. Ice-free conditions around Lake Ontario and Lake Erie are confirmed by radiocarbon ages on wood and organic materials from various sites in the region, for example boreholes (A2449; Mulligan and Bajc, 2018), organic material contained in lacustrine sediment (AA-57450 and AA-57447; Young and Burr, 2006) and sub-till wood on the north shore of Lake Erie (L-185B, W-177 and GSC-2126; Dreimanis et al., 1966; Lowdon et al., 1977). South of Lake Michigan >20 radiocarbon ages suggest local ice-free conditions at ~30 ka (see Heath et al., 2018; Liu et al., 1986 and references therein). Finally, two radiocarbon ages from peat and shells in the Hudson Bay Lowlands suggest local ice-free conditions at 30.6 ± 0.4 ka (UOC-0593; Dalton et al., 2016).

As a minimum ice extent at 30 ka (Fig. 12B), we assume Keewatin ice was restricted to the Canadian Shield, moderate in size, and covering much of mainland Nunavut and the Northwest Territories, similar to the mid-Wisconsinan Hypothesis 2 of Dredge and Thorleifson (1987). A reduced southern and eastern Keewatin margin aligns with the wealth of geochronological data suggesting ice-free conditions in the southern Interior Plains and eastern Keewatin. This minimum ice extent takes into account geochronological data from fluviolacustrine sediments in northern Manitoba (EKN-5; Berger and Nielsen, 1990), showing an ice-free Hudson Bay. It also allows for ice-free conditions near the Pingualuit Crater, northern Quebec (Guyard et al., 2011). This minimal ice extent also allows for ice-free conditions along coastal Newfoundland and Anticosti Island, and a potential extension of this calving bay into the Saint Lawrence Lowlands as suggested by two IRSL ages in this interval (M011_feldspar; Caron, 2013; Munroe et al., 2016) as well as two radiocarbon ages on shell fragments and wood pieces (Beta-54140 and I-13549; Brodeur and Allard, 1985; Dionne and Occhietti, 1996).

Our maximum Keewatin ice extent shows an ice margin within the

southern Interior Plains as constrained by the dating of organic materials in this region (Fig. 12B). Keewatin ice is shown merged with the Labrador Dome over Hudson Bay. This maximum ice extent, showing long-lasting coverage over central Canada, satisfies criticisms of MIS 3 geochronological data from the Hudson Bay Lowlands (Miller and Andrews, 2019). Our maximum ice extent also considers evidence suggesting a short-lived, dramatic extension of the Keewatin Dome southward into the continental United States via a low-lying topographic corridor in Manitoba. The timing and extent of this advance (between ~34 ka and ~30 ka; known as the Lehigh Advance) is based on radiocarbon dating of wood contained within, overlying and underlying this till unit associated with the Keewatin Dome (Kerr et al., 2021). Along the Atlantic coastline, the ice margin roughly follows the continental shelf break and is based largely on seismic analyses and mapping of glaciomarine landforms (Josenhans et al., 1986; Piper and Macdonald, 2001; Shaw et al., 2006). In New England, the maximum ice extent follows the uppermost till unit (Sevon and Braun, 2000; Stone et al., 2005), and south of the Great Lakes, the maximum ice extent corresponds to the Shelbyville morainic system (Johnson et al., 1971) and Bloomington moraines (Frye et al., 1969).

Regarding the Innuitian Ice Sheet, numerous radiocarbon ages constrain the 30-ka extent. On Ellesmere Island and neighboring Axel Heiberg Island, radiocarbon ages from shells and organic material, largely in shoreline areas, have been dated to between 32.5 ka and 27.5 ka (England, 1978; England, 1990; England, 1996; England et al., 2000; Ó Cofaigh et al., 2000). To the west on Melville and Banks islands, radiocarbon ages on shell fragments (largely contained in tills) suggest local ice-free conditions between 32.5 ka and 27.5 ka (England et al., 2009; Nixon and England, 2014) prior to being overrun by ice. Following these data, our estimate of Innuitian ice assumes present-day ice extent over the Queen Elizabeth Islands, which we also consider as the minimum ice extent. The maximum ice extent is the edge of the continental shelf, assuming an early growth to the LGM.

On Fig. 12B, we also show Heinrich Event 3, which took place at ~31 ka (Hemming, 2004). However, similar to H5 at ~60 ka, it remains unclear whether H3 was a true increase in ice-rafted debris, an interval where foraminiferal dissolution occurred (Gwiazda et al., 1996), or a freshwater influx into the North Atlantic (Hemming, 2004). We show that expansion of continental ice toward the LGM was well-underway at 30 ka, a scenario that would provide ample ice cover to drive rafting events into the North Atlantic.

3.19. Laurentide and Innuitian ice sheets at 25 ka

The 25-ka interval is broadly assumed as the LGM in most regions of North America (Clark et al., 2009). At that time, GMSL was around -130 m compared to present-day (Pico et al., 2017; Spratt and Lisiecki, 2016). Accordingly, we show the Keewatin Dome expanded southward beyond the Canada/United States border, westward to join with the Cordilleran Ice Sheet, north to merge with the Innuitian Ice Sheet and east to cover Hudson Bay (Fig. 13; high confidence). Our estimate of the Labrador Dome at 25 ka (Fig. 13) approximates the "Churchill" and "Severn" landform swarm patterns (Kleman et al., 2010). While our work broadly supports this assertion by showing the maximum ice extent at 25 ka, we stress that many regions in the periphery of the glaciated region show evidence of ice advance (e.g. sediment cores and seismic mapping of the continental shelf; Brouard and Lajeunesse, 2017; Lévesque et al., 2020) but the timing is poorly constrained. In most cases in the marine environment, the LGM ice position is assumed to be 25 ka but might have occurred earlier or later. Evidence in support of this 25-ka ice configuration (including considerations for minimum and maximum ice extent) is outlined below.

Regarding the 25-ka extent of the Keewatin Dome, we show the southern boundary in the United States following the location of surface tills (Fullerton and Colton, 1986; Horberg and Anderson, 1956; Wright Jr., 1962) in a similar position to the LGM proposed by Dyke and Prest (1987) and Dyke (2004). As a minimum ice extent at 25 ka, we show the southern margin of the Keewatin Dome at ~300 km from its LGM extent (assumed). To the west, the Keewatin Dome is merged with the Cordilleran Ice Sheet at the LGM for the only time during the Pleistocene

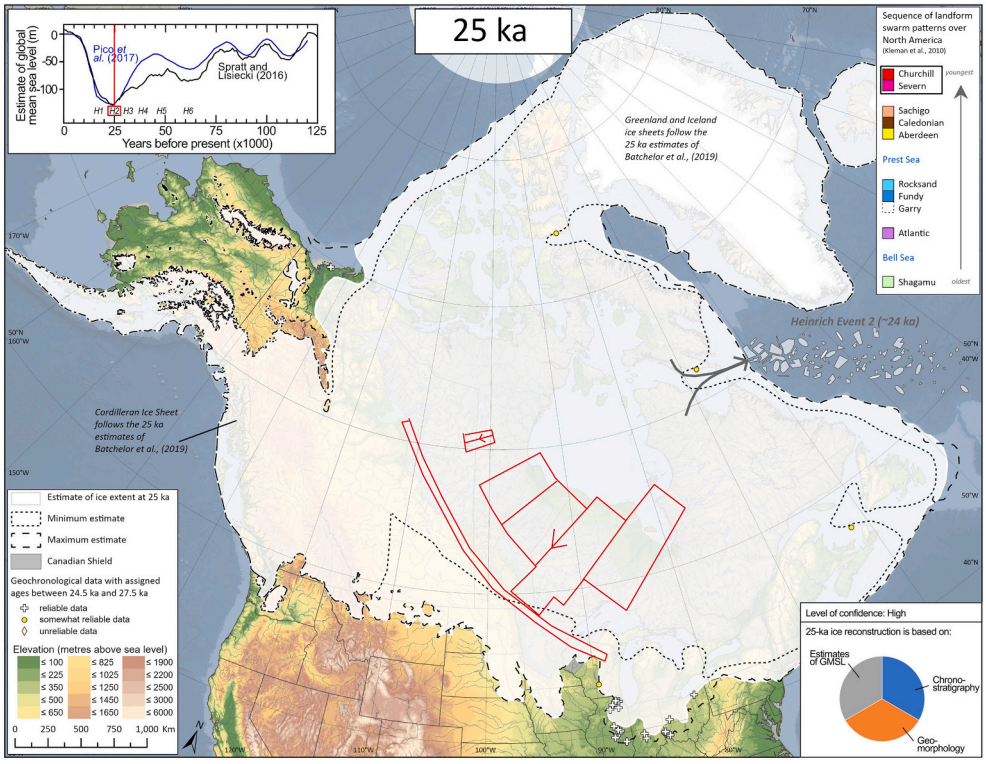

Fig. 13. Reconstructed North American ice at 25 ka.

(Young et al., 1994). In the northwestern margin, the local LGM was only reached between 18.5 ka and 15 ka (Lacelle et al., 2007) and no constraints are available for the 25-ka interval. In the Canadian Beaufort Sea, the local LGM (Toker Point Stade), during which an ice stream advanced to the continental shelf break beyond the Mackenzie Delta, was attained later than ~27 ka (Murton et al., 2017), perhaps as recently as ~16 ka (Fritz et al., 2012; Murton, 2009). We therefore draw the 25-ka ice margin ~200 km (assumed) from the LGM extent. Farther north, we show ice to the shelf break; this follows geochronological evidence for ice covering Banks Island sometime between ~31 ka and ~24 ka (Evans et al., 2014; Lakeman and England, 2013), and marine geomorphological and sedimentological evidence for extensive ice streams in Amundsen Gulf and M'Clure Strait during the local LGM (MacLean et al., 2015; Stokes et al., 2005; Stokes et al., 2009). We consider the shelf break to be the largest possible extent of the ice sheet at 25 ka (maximum estimate). On Baffin Island, the ice sheet is shown at the shelf break as is inferred from undated marine geomorphological evidence (Brouard and Lajeunesse, 2017), along with seismic-stratigraphic and sedimentological age constraints (Jenner et al., 2018; Li et al., 2011). Also on Baffin Island, the minimum ice extent approximates the coastline to account for a shell located in a till deposit that suggests marine conditions in Hudson Strait at 27.5 ± 0.4 ka (AA-10647; Manley and Jennings, 1996).

Regarding the 25-ka extent of the Labrador Dome, along the Atlantic coastline, we show the ice margin at the continental shelf break following the analysis of sediment cores, radiocarbon dates and seismic profiles (Roger et al., 2013). Offshore of Atlantic Canada, we show ice at the edge of the continental shelf between 29 ka and 25 ka, when ice began to retreat from this maximum position (King, 1996). As a minimum ice extent of the Labrador Dome, we show the ice margin roughly along the coastline of Labrador and Atlantic Canada, allowing the possibility of ice-free conditions on the Magdalen Islands at 25 ± 2 ka (OSL58; Rémillard et al., 2017). As a maximum ice extent of ice at 25 ka, along the Atlantic coastline, the ice margin roughly follows the continental shelf break and is based largely on seismic analyses and mapping of glaciomarine landforms (Josenhans et al., 1986; Piper and Macdonald, 2001; Shaw et al., 2006). In New England, the location and timing of the 25-ka ice margin of the Labrador Dome is derived from cosmogenic dating of ice marginal boulders (Balco et al., 2002) which have been recently re-calculated to between 27 ka and 25 ka using an updated production rate and scaling (Heath et al., 2018). In this region, the maximum ice extent follows the uppermost till unit (Sevon and Braun, 2000; Stone et al., 2005).

South of the Great Lakes, at 25 ka, we show ice retreating from an earlier glacial maximum, which occurred potentially around ~27 ka (Loope et al., 2018). This is supported by >40 radiocarbon ages are available spanning ~27 ka to ~24 ka (see Heath et al., 2018 and references therein). Accordingly, we show the Lake Erie lobe at a southwestern extent that is ~30 km less than its LGM extent (Heath et al., 2018). We also place the Lake Michigan Lobe south of Lake Michigan and ~120 km from the outermost LGM moraine as suggested by the work of Heath et al. (2018). The existence of ice-free areas south of the Great Lakes is confirmed by three radiocarbon ages from organic materials in Illinois, Indiana and Ohio (Heath et al., 2018; Lowell et al., 1990). South of Lake Superior, however, we place the ice margin at its LGM extent because few constraints on ice growth are available for this region; the only constraints are cosmogenic nuclide ages (Balco et al., 2002) that date the abandonment of the LGM ice position to ~23 ka (age re-calculated using an updated production rate and scaling; Heath et al., 2018). South of the Great Lakes, the maximum ice extent corresponds to the Shelbyville morainic system (Johnson et al., 1971) and Bloomington moraines (Frye et al., 1969).

Regarding the Innuitian Ice Sheet, at 25 ka, the sole geochronological constraint is on the southern coast of Devon Island; a radiocarbon age from a shell located in till was dated to 27.1 ± 0.6 ka (GSC-5848; Dyke, 1999). Overall, the shortage of geochronological constraints suggest the Innuitian Ice Sheet was extensive at 25 ka, and our estimate accordingly follows the continental shelf edge (Fig. 13) based on analysis of geomorphological records suggesting ice streams were active to the shelf edge at the LGM (England et al., 2006; Margold et al., 2015). As a minimum estimate of ice extent at 25 ka, we show ice covering all of Ellesmere, Axel Heiberg, and Devon islands. This minimum ice extent accounts for the suggestion that major Innuitian Ice Sheet build-up did not occur until perhaps as late as ~19 ka (England et al., 2006). This minimum ice extent also allows for the shell age from Devon Island (GSC-5848; Dyke, 1999). The maximum ice extent is assumed to be the edge of the continental shelf edge.

On Fig. 13, we also show Heinrich Event 2, which took place at ~24 ka (Hemming, 2004). This event is likely associated with LGM ice in the vicinity of Hudson Bay and/or Hudson Strait.

4. Discussion

Our reconstructions of the Laurentide and Innuitian ice sheets through the build-up phase of the last glacial cycle until the LGM represent a series of testable hypotheses based on interpretation from the geomorphic record, chronostratigraphic data, and inferences from the GMSL record and numerical ice sheet modelling. These maps allow relatively rapid changes in the ice marginal position to be empirically constrained and visualised, which is important for understanding and predicting the response of ice sheets to climate variability. In some cases, the ice margin is highly precise (e.g. at 75 ka aligned with the Lévrard Till in the Saint Lawrence Lowlands; Lamothe et al., 1992), whereas in other cases, the extent is highly generalized or approximated (e.g. aligning the ice margin in the southern Interior Plains to the Canadian Shield at 45 ka; Fig. 11A). For any given interval, our estimates of minimum and maximum ice extent seek to capture a combination of the lack of geochronological constraints (especially prior to 40 ka); discrepancies in estimates of GMSL; contradictions in geochronological data and/or ice sheet interpretations; and low precision of geochronological data.

Calculations of areal extent, including Greenland and the Cordilleran ice sheets which are from Batchelor et al. (2019), are shown in Fig. 14. Our work suggests that a maximum ice coverage of ~20,000,000 km^2 was reached at 25 ka and possibly also between 70 ka and 60 ka, which reflects ice build-up during MIS 4 and MIS 2, respectively. These intervals correspond to relative lows in GMSL (see Fig. 2). To contrast, minimal North American ice coverage of ~5,000,000 km^2 was possibly reached at 100 ka, 80 ka and 45 ka, which is supported by relative highs in GMSL (see Fig. 2). The significant range between the maximum and minimum hypothesised extent during MIS 3 (45 ka; Fig. 14) reflects the ongoing debate about ice presence or absence in Hudson Bay (Dalton et al., 2019; Miller and Andrews, 2019; discussed in Section 4.2).

A key advantage of our new reconstructions over previous work (Clark et al., 1993; Dredge and Thorleifson, 1987; St-Onge, 1987; Vincent and Prest, 1987) is the use of 5-ka increments, made possible because of advances in geochronology and improved study of key sites in the glaciated region. A recent model of global ice extent over the past 80 ka (Gowan et al., 2021) presents 2.5-kyr time-steps, but this work was based primarily on assumptions of sea level, glacioisostatic adjustment and ice sheet modelling, with less overall emphasis on geochronological data. Accordingly, we expect our maps to provide a definitive, empirically constrained overview of the former configurations of North American ice sheets that will be of critical interest for validating ice-sheet models similar to Gowan et al. (2021).

4.1. Asynchronous response of northern versus southern margins

Our work suggests that some areas of the Laurentide Ice Sheet underwent several cycles of advance and retreat (e.g. Saint Lawrence Lowlands), whereas others remained largely ice-free prior to growth toward the LGM (notably, some regions of the Southern Interior Plains).

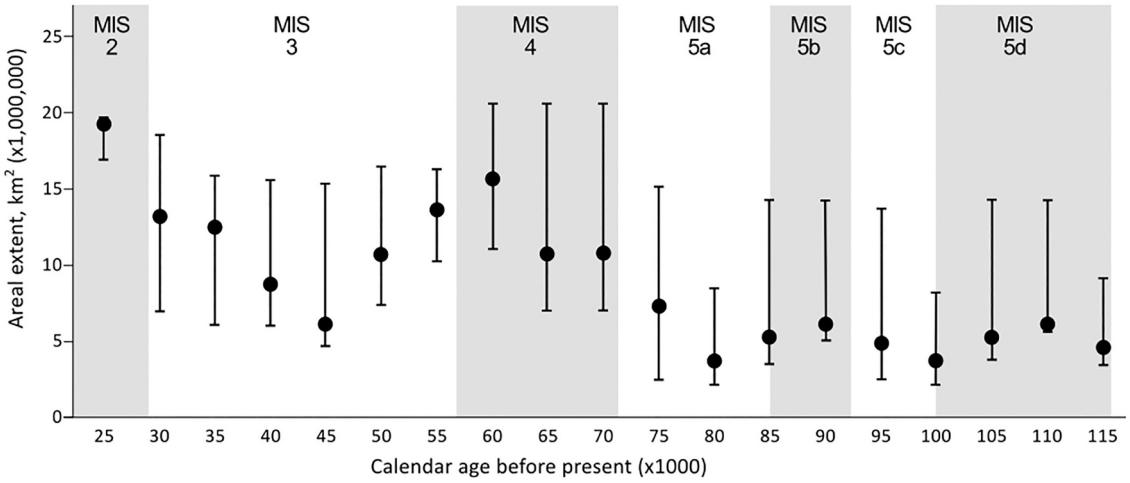

Fig. 14. Areal extent of North American ice sheets from 115 ka to 25 ka. Minimum and maximum estimates are also shown. These totals include our new reconstructions and the outlines of the Cordilleran and Greenland ice sheets from Batchelor et al. (2019).

Ice remained continuously through most of the build-up phase of the last glacial cycle until the LGM at the centre of some of the key ice sheet nucleation areas (e.g. high-altitude regions of northern Quebec, Labrador and Baffin Island; Andrews and Barry, 1978; Bahadory et al., 2021; Ives, 1957; Koerner, 1980; Marshall et al., 2000).

Also noteworthy is the marked variability between the northern and southern margins of the Laurentide and Innuitian ice sheets. Throughout the build-up phase of the last glacial cycle until the LGM, the northernmost Laurentide and the Innuitian ice margins underwent relatively small advance/retreat cycles, whereas the southern margin of the Laurentide underwent much greater fluctuations, with retreat rates of the order of ~50 to 80 m/yr. This is not surprising given the likely warmer and wetter conditions at the southern margin, compared to the less sensitive colder and drier regions further north. Indeed, recent modelling of the Laurentide Ice Sheet during the last deglaciation shows a marked spatial gradient in surface mass balance, with the southern margins thinning by up to 10 m/year while the northern margins thickened slightly (Ullman et al., 2015). Similar gradients in surface mass balance are likely during the warm periods of the pre-LGM period and explain the rapid retreat of the southern and western margins and relative stability further north.

Our reconstructions allow us to estimate the rate of advance/retreat as the ice sheet transitioned through the climate variations of the last build-up phase of the last glacial cycle until the LGM, which provides a useful context for assessing rates of change during the last deglaciation (e.g. Bentley et al., 2014; Dalton et al., 2020; Hughes et al., 2016; Scourse et al., 2021) as well as present-day ice marginal changes in Greenland and Antarctica (e.g. Miles et al., 2016). The greatest change in ice sheet area within the last build-up phase of the last glacial cycle until the LGM took place between peak MIS 3 (45 ka) and peak MIS 4 (60 ka), when the ice sheets expanded from minimal ice coverage (~5,000,000 km^2) to at or close to its maximum (~20,000,000 km^2; Fig. 14). Considering our uncertainties for each time-step, we estimate that the rate of ice retreat between 60 ka and 45 ka varied from 37 m/year to 80 m/year across several southern and western ice sheet sectors, with the highest possible retreat rate over these transects estimated at 87 m/year (Table 1). Thus, our work builds upon growing empirical (Boulton and Clark, 1990; Kleman et al., 2010) and modelled (Stokes et al., 2012) evidence that support a highly dynamic North American ice sheet complex prior to the LGM. Although our estimated retreat rates are long-term averages and as such may mask shorter episodes of higher retreat, they highlight that some modern rates of outlet glacier/ice sheet retreat of >100 m/yr (e.g. Carr et al., 2017) are similar or higher than those experienced during past episodes of major ice sheet deglaciation.

Table 1
Approximate retreat rates between 60 ka and 45 ka. In each transect, the minimum possible ice retreat is 0 m/year (i.e. the minimum extent at 60 ka overlaps with the maximum extent at 45 ka). Transect locations are shown on Fig. 1.

Transect	Most probable	Maximum possible
South to Keewatin Dome (Fig. 1 Transect A)	1200 km (80 m/year)	1200 km (80 m/year)
South to Labrador Dome (Fig. 1 Transect B)	550 km (37 m/year)	1300 km (87 m/year)
Northeast to Labrador Dome (Fig. 1 Transect C)	680 km (45 m/year)	700 km (47 m/year)

Recent modelling work offers a largely independent analysis with which to compare our ice sheet reconstructions through the last glacial cycle to the LGM. A significant difference is that modelled results are often highly generalized and do not include several of the regional-scale changes that we show here (e.g. dramatic lobes pulsing into Lake Erie as supported by geochronological data). Another key difference relates to the relatively small ice sheet that we reconstruct at 110 ka, with ice restricted to the Keewatin and Labrador domes and Hudson Bay ice-free (Fig. 5B). This is significantly different to the modelling work of Stokes et al. (2012), who describe 'explosive' ice growth and a relatively large North American ice sheet at that time. Instead, our 110 ka best-estimate reconstruction is more closely aligned with the modelled ice sheet extent of Bahadory et al. (2021), who show a pronounced build-up of ice southward over Keewatin to the boundary of the Canadian Shield. In addition, our ice sheet extent at 80 ka (informed by estimates of GMSL, numerical modelling, chronostratigraphy and geomorphology; Fig. 7B) is significantly smaller than the modelled reconstruction of Stokes et al. (2012) that showed the Keewatin and Labrador domes joined over northern Hudson Bay at that time. Our ice estimate at 80 ka is also smaller than that presented by Gowan et al. (2021), especially with respect to the Labrador Dome, which is depicted in Gowan et al. (2021) as covering most of the Canadian Shield. Finally, both Gowan et al. (2021) and Stokes et al. (2012) show maximum MIS 4 ice at 65 ka, whereas our work suggests it occurred closer to 60 ka.

4.2. *The MIS 3 enigma*

A topic of longstanding debate is whether Hudson Bay was glaciated or ice-free between 50 ka and 40 ka, during MIS 3. First formally proposed by Dredge and Thorleifson (1987), this reduced ice hypothesis was recently revived by new geochronological dating (OSL, radiocarbon, U-Series) of material from this region, along with a critical

analysis of pre-existing geochronological data (Dalton et al., 2016). In that paper, Dalton et al. (2016) devised a ranking system to assess the quality of geochronological data, which resulted in the removal of many radiocarbon ages owing to suspected modern-day contamination. However, the MIS 3 age assignment of several key sites (based on radiocarbon ages on wood along with OSL dating of fluvial sediments) was determined to be reliable. Moreover, the feasibility of an ice-free Hudson Bay Lowlands during MIS 3 is corroborated by recent work that suggests higher-than-expected GMSL during that time (Pico et al., 2016), and an ice-free Hudson Bay region has been reconciled with this GMSL estimate (Dalton et al., 2019; Pico et al., 2017). For these reasons, our best estimate at 45 ka shows an entirely ice-free Hudson Bay and surrounding region, with remnant ice domes over Keewatin and Labrador (drawn after Dredge and Thorleifson, 1987). However, this hypothesis has been questioned by Miller and Andrews (2019), who argue that radiocarbon data from the Hudson Bay Lowlands are unreliable owing to modern-day contamination. Instead, Miller and Andrews (2019) suggest that Hudson Bay was fully glaciated during MIS 3 and was perhaps required to source Heinrich Events 4 and 5. Recent modelling work on global ice sheet dynamics over the past 80 ka, constrained by some geochronological data from the glaciated region, suggests that both scenarios can be reconciled with estimates of GMSL through that interval (Gowan et al., 2021). Thus, the glaciated scenario of Miller and Andrews (2019) is accounted for in our 'maximum' ice estimate and resolving the ice extent around this issue should be a key priority for future work (see Section 4.4).

There is evidence of significantly reduced ice sheets during MIS 3 elsewhere in the Northern Hemisphere. For example, the Olympia Interglaciation was an interval spanning ~45 ka to 20 ka when ice was absent from much of the Cordillera of western North America (Armstrong and Clague, 1977; Armstrong et al., 1965; Hickin et al., 2016). Moreover, recent mapping and chronological work in Fennoscandia suggests that the Eurasian Ice Sheet was extremely reduced at this time, possibly holding only ~1 m of sea level equivalent (Kleman et al., 2021). This work is supported by extensive radiocarbon and OSL datasets from Fennoscandian and surrounding areas (Helmens, 2014; Johansson et al., 2011; Olsen et al., 2001; Wohlfarth, 2010). However, ice volume reduction in these regions would have had significantly less impact on GMSL compared to reduction of the Laurentide Ice Sheet (e.g. Pico et al., 2016).

4.3. Implications for continental runoff and drainage routes

Because North American ice sheets straddle the continental drainage divide, their evolution (e.g. timing and extent of growth and recession) are critical for testing hypotheses related to meltwater discharge and the potential connection to climate events (e.g. Condron and Winsor, 2012; Leydet et al., 2018). Although we do not reconstruct pre-LGM evolution of major proglacial lakes, there is evidence for their existence (e.g. Karig and Miller, 2013) and our maps, in combination with GIA modelling, could be used to explore their evolution and possible impact on ocean circulation. For example, at the LGM, North American ice sheets extended into the Mississippi River watershed and drained meltwater southward into the Gulf of Mexico (Wickert et al., 2013). Recession from the LGM position led to shifting water to more northern watersheds (Wickert, 2016), which disrupted the Atlantic Meridional Overturning Circulation, potentially causing the Younger Dryas cold reversal (Broecker et al., 1989).

One of our key findings is that the MIS 4 ice advance at 60 ka (Fig. 9B) was the first major advance of Late Pleistocene ice over North America and the first time in the last glacial cycle that the Labrador and Keewatin domes became confluent. This aligns with the work of Rittenour et al. (2007), who documented a pronounced shift in the Mississippi River basin toward a braided regime (Dudley braid belt) that was attributed to increased sediment input and meltwater from continental ice encroaching on the northern reaches of the Mississippi River watershed sometime between 77 ka to 50 ka. A similar event possibly occurred between 42 ka and 35 ka (Melville Ridge braid belt; Rittenour et al., 2007). This second event also broadly aligns with the position of our maximum ice sheet margin into the Mississippi River watershed at 40 ka and 35 ka (Figs. 11B, 12A). These ice advances are (NB: these advances into the Mississippi River watershed are shown as maximum ice estimates because they are believed to be short-lived, see; Kerr et al., 2021). Proxy records also document increased sediment discharge and freshwater influx into the Gulf of Mexico intermittently from 60 ka to 30 ka (Tripsanas et al., 2007), which could reflect the successive filling and draining of lakes beyond the southern ice sheet margin during this time (Figs. 9 to 12).

4.4. Future work

We identify three key regions where future work on the stratigraphic record of ice sheet change during the build-up phase of the last glacial cycle until the LGM is critical for reducing uncertainties in North American ice reconstructions. First, additional dating of the stratigraphic record in the Hudson Bay Lowlands would provide insight into whether ice was present or absent during MIS 3 (Dalton et al., 2019; Miller and Andrews, 2019; see Section 4.2). Advancing research in this area should come from constraining the age of non-glacial deposits via multiple, reproducible geochronological methods. Further work on the potential of paleoclimate indicators (e.g. pollen) to differentiate between stratigraphically different non-glacial deposits could also help resolve this issue (Dalton et al., 2017; Dredge et al., 1990). Renewed stratigraphy analyses may also prove useful in the Hudson Bay Lowlands, as a generalized stratigraphic framework is not yet established for this region, owing to the similarities in most till units and also between interglacial units (see Thorleifson et al., 1992). Compounded with these issues is the shortage of sites where multiple non-glacial deposits are exposed.

Secondly, future ice sheet reconstructions would also benefit from additional work in the Ontario Basin. While a stratigraphic framework detailing the Wisconsinan history of this region exists (Karrow et al., 2000), the timing of key events remains debated. Most pre-40 ka ages come from the TL work of Berger and Eyles (1994), often with low precision, and no additional luminescence techniques have been attempted to refine these estimates. Regarding the pre-LGM record in this region, it may also be worthwhile to further investigate the Pottery Road Formation, an event where large fluvial-like channels eroded into the Scarborough Formation tills implying a dramatic lowering of base levels at this time (Karrow, 1974). This could suggest a dramatic shift in ice position (temporarily re-established continental drainage toward the Saint Lawrence Lowlands?) during the retreat of MIS 4 ice from the region, which would be critical for understanding changes to continental drainage over that time. However, it has also been argued that these channels may have been caused by subglacial erosion, thus implying that the ice sheet never left (Sharpe and Barnett, 1985).

Finally, future research could build upon the detailed investigations into the Quaternary stratigraphy of the Saint Lawrence Lowlands that have occurred since the early 1970s (Gadd, 1971). Situated in a topographically varied area ranging from an estuary to the Appalachian Mountains, this region was subjected to a complex assortment of marine incursions, peatland development, and fluvial systems draining the entire Great Lakes basin and ice-marginal proglacial lakes prior to the LGM. Determining a stratigraphic framework as well as the age of non-glacial intervals in this region remains a topic of ongoing work. From the perspective of North American ice sheets, a key issue in need of resolving is the timing of ice advance(s) into this region from MIS 5a until the end of MIS 3. Currently, geochronological data are of low abundance and precision through this interval.

5. Conclusion

Understanding the history of North American ice sheets, which held the largest global ice mass to grow and decay over the past ~115 ka, is critical for reconciling the impact of large continental ice sheets on sea level change and offers a useful analogue for studying their behaviour in relation to the climate system. Here we synthesise a large ensemble of geochronological, modelling, and empirical datasets, and show that the build-up of North American ice toward the LGM was highly dynamic, rather than slow and gradual. During this interval, some areas of North America remained largely ice-free (e.g. Great Lakes region), others remained continuously glaciated (high-elevation regions of Labrador and Baffin Island) and others, particularly along the highly dynamic southern ice sheet margin, underwent multiple cycles of rapid ice sheet growth and decay (e.g. >80 m/year averaged over thousands of years). Our use of best, minimum, and maximum ice extent estimates at each time-step allows us to capture a range of uncertainties that are inherent to dealing with a diverse ensemble of data. Significant uncertainties in our maps often accompany intervals of low precision of geochronological data, discrepancies in GMSL, and different data interpretations. A key interval of contention is the presence or absence of ice over Hudson Bay during MIS 3 (Dalton et al., 2019; Miller and Andrews, 2019). Future work should be focussed on dating the stratigraphic record in key regions (notably, the Hudson Bay Lowlands and Saint Lawrence Lowlands) using non-radiocarbon methods such as OSL. Despite these uncertainties, our new empirically constrained maps represent both a series of testable hypotheses and a benchmark dataset for several disciplines that rely on the position of former continental ice sheets; as such, they are key for refining global paleoclimate models.

Data availability

Supplementary Information contains:

- A zip file containing the 19 ice margin reconstructions (including 'best', 'minimum' and 'maximum' ice estimate for each time slice) as GIS shapefiles.
- Individual maps showing the 19 ice margin reconstructions in PDF format.
- Excel table containing the geochronological dataset.

Declaration of Competing Interest

None.

Acknowledgements

ASD was funded by the DIFeREns2 Junior Research Fellowship (grant no. 609412; funded by European Union / Durham University). CLB was funded by a Norwegian Vista scholarship (project 6273) and CRS acknowledges funding from the NERC (NE/J00782X/1). We thank the following individuals for helpful conversations on pre-LGM regional stratigraphy: Dave Evans, Brandon Curry, Michel Lamothe, Phil Kerr, Henry Loope, Riley Mulligan, Isabelle McMartin, Harvey Thorleifson, Brent Ward, Roger Paulen. We also thank John Andrews for conversations about Heinrich Events, as well as Johan Kleman and an anonymous reviewer for constructive feedback

Appendix A. Supplementary data

Supplementary data to this article can be found online at https://doi.org/10.1016/j.earscirev.2021.103875.

References

Allard, G., Roy, M., Ghaleb, B., Richard, P.J.H., Larouche, A.C., Veillette, J.J., Parent, M., 2012. Constraining the age of the last interglacial–glacial transition in the Hudson Bay lowlands (Canada) using U–Th dating of buried wood. Quat. Geochronol. 7, 37–47.
Andrews, J.T., Barry, R.G., 1978. Glacial inception and disintegration during the last glaciation. Annu. Rev. Earth Planet. Sci. 6, 205–228.
Armstrong, J.E., Clague, J.J., 1977. Two major Wisconsin lithostratigraphic units in southwest British Columbia. Can. J. Earth Sci. 14 (7), 1471–1480.
Armstrong, J.E., Crandell, D.R., Easterbrook, D.j. and Noble, J.B., 1965. Late Pleistocene stratigraphy and chronology in southwestern British Columbia and northwestern Washington. Geol. Soc. Am. Bull. 76 (3), 321–330.
Asmerom, Y., Polyak, V.J., Burns, S.J., 2010. Variable winter moisture in the southwestern United States linked to rapid glacial climate shifts. Nat. Geosci. 3 (2), 114–117.
Bahadory, T., Tarasov, L., Andres, H., 2021. Last glacial inception trajectories for the Northern Hemisphere from coupled ice and climate modelling. Clim. Past 17 (1), 397–418.
Bajc, A.F., 1991. Glacial and Glaciolacustrine History of the Fort Frances-Rainy River Area, Ontario, Canada.
Bajc, A.F., Karrow, P.F., Yansa, C.H., Curry, B.B., Nekola, J.C., Seymour, K.L., Mackie, G. L., 2015. Geology and paleoecology of a Middle Wisconsin fossil occurrence in Zorra Township, southwestern Ontario, Canada. Can. J. Earth Sci. 52 (6), 386–404.
Balco, G., Stone, J.O.H., Porter, S.C., Caffee, M.W., 2002. Cosmogenic-nuclide ages for New England coastal moraines, Martha's Vineyard and Cape Cod, Massachusetts, USA. Quat. Sci. Rev. 21 (20), 2127–2135.
Balescu, S., Lamothe, M., 1994. Comparison of TL and IRSL age estimates of feldspar coarse grains from waterlain sediments. Quat. Sci. Rev. 13 (5-7), 437–444.
Batchelor, C.L., Margold, M., Krapp, M., Murton, D.K., Dalton, A.S., Gibbard, P.L., Stokes, C.R., Murton, J.B., Manica, A., 2019. The configuration of Northern Hemisphere ice sheets through the quaternary. Nat. Commun. 10 (1), 3713.
Bateman, M.D., Murton, J.B., 2006. The chronostratigraphy of Late Pleistocene glacial and periglacial aeolian activity in the Tuktoyaktuk Coastlands, NWT, Canada. Quat. Sci. Rev. 25 (19-20), 2552–2568.
Becerra-Valdivia, L., Higham, T., 2020. The timing and effect of the earliest human arrivals in North America. Nature 584 (7819), 93–97.
Bednarski, J.M., 1995. Glacial advances and stratigraphy in Otto Fiord and adjacent areas, Ellesmere Island, Northwest Territories. Can. J. Earth Sci. 32 (1), 52–64.
Bélanger, N., Carcaillet, C., Padbury, G.A., Harvey-Schafer, A.N., Van Rees, K.J., 2014. Periglacial fires and trees in a continental setting of Central Canada, Upper Pleistocene. Geobiology 12 (2), 109–118.
Bell, T., 1992. Glacial and Sea Level History of Western Fosheim Peninsula, Ellesmere Island, Arctic Canada. University of Alberta. PhD thesis.
Bennett, M.R., Bustos, D., Pigati, J.S., Springer, K.B., Urban, T.M., Holliday, V.T., Reynolds, S.C., Budka, M., Honke, J.S., Hudson, A.M., Fenerty, B., Connelly, C., Martinez, P.J., Santucci, V.L., Odess, D., 2021. Evidence of humans in North America during the Last Glacial Maximum. Science 373 (6562), 1528–1531.
Bentley, M.J., Ócofaigh, C., Anderson, J.B., Conway, H., Davies, B., Graham, A.G.C., Hillenbrand, C.-D., Hodgson, D.A., Jamieson, S.S.R., Larter, R.D., Mackintosh, A., Smith, J.A., Verleyen, E., Ackert, R.P., Bart, P.J., Berg, S., Brunstein, D., Canals, M., Colhoun, E.A., Crosta, X., Dickens, W.A., Domack, E., Dowdeswell, J.A., Dunbar, R., Ehrmann, W., Evans, J., Favier, V., Fink, D., Fogwill, C.J., Glasser, N.F., Gohl, K., Golledge, N.R., Goodwin, I., Gore, D.B., Greenwood, S.L., Hall, B.L., Hall, K., Hedding, D.W., Hein, A.S., Hocking, E.P., Jakobsson, M., Johnson, J.S., Jomelli, V., Jones, R.S., Klages, J.P., Kristoffersen, Y., Kuhn, G., Leventer, A., Licht, K., Lilly, K., Lindow, J., Livingstone, S.J., Massé, G., McGlone, M.S., McKay, R.M., Melles, M., Miura, H., Mulvaney, R., Nel, W., Nitsche, F.O., O'Brien, P.E., Post, A.L., Roberts, S. J., Saunders, K.M., Selkirk, P.M., Simms, A.R., Spiegel, C., Stolldorf, T.D., Sugden, D. E., van der Putten, N., van Ommen, T., Verfaillie, D., Vyverman, W., Wagner, B., White, D.A., Witus, A.E., Zwartz, D., 2014. A community-based geological reconstruction of Antarctic Ice Sheet deglaciation since the Last Glacial Maximum. Quat. Sci. Rev. 100, 1–9.
Berger, G.W., Eyles, N., 1994. Thermoluminescence chronology of Toronto-area Quaternary sediments and implications for the extent of the midcontinent ice sheet (s). Geology 22, 31–34.
Berger, A., Loutre, M.F., 1991. Insolation values for the climate of the last 10 million years. Quat. Sci. Rev. 10 (4), 297–317.
Berger, G.W., Nielsen, E., 1990. Evidence from thermoluminescence dating for Middle Wisconsinan deglaciation in the Hudson Bay Lowland of Manitoba. Can. J. Earth Sci. 28, 240–249.
Bernier, F., Occhietti, S., 1991. Nouvelle séquence glaciaire antérieure aux Sédiments de Saint-Pierre, Sainte-Anne-de-la-Perade, Québec. Géog. Phys. Quatern. 45 (1), 101–110.
Berti, A.A., 1975. Paleobotany of Wisonsinan Insterstadials, Eastern Great Lakes Region, North America. Quat. Res. 5, 591–619.
Bintanja, R., van de Wal, R.S.W., Oerlemans, J., 2005. Modelled atmospheric temperatures and global sea levels over the past million years. Nature 437, 125–128.
Blake, W.J., 1984. Geological Survey of Canada Radiocarbon Dates XXIV. Geological Survey of Canada, Paper 84-7, p. 35.
Blake, W.J., 1986. Geological Survey of Canada Radiocarbon Dates XXV. Geological Survey of Canada, Paper 85-7, p. 32.
Blake, W.J., 1993. Holocene emergence along the Ellesmere Island coasts of northernmost Baffin Bay. Nor. Geol. Tidsskr. 73, 147–160.
Bleuer, N.K., 1974. Buried Till Ridges in the Fort Wayne Area, Indiana, and their Regional Significance. Geol. Soc. Am. Bull. 85 (6), 917–920.

Boulton, G.S., Clark, C.D., 1990. A highly mobile Laurentide ice sheet revealed by satellite images of glacial lineations. Nature 346, 813–817.
Briner, J.P., Axford, Y., Forman, S.L., Miller, G.H., Wolfe, A.P., 2007. Multiple generations of interglacial lake sediment preserved beneath the Laurentide Ice Sheet. Geology 35 (10), 887–890.
Brodeur, D., Allard, M., 1985. Stratigraphie et Quaternaire de l'île aux Coudres, estuaire moyen du Saint-Laurent, Québec. Géog. Phys. Quatern. 39 (2), 183–197.
Broecker, W.S., Kennett, J.P., Flower, B.P., Teller, J.T., Trumbore, S., Bonani, G., Wolfli, W., 1989. Routing of meltwater from the Laurentide Ice Sheet during the Younger Dryas cold episode. Nature 341 (6240), 318–321.
Brouard, E., Lajeunesse, P., 2017. Maximum extent and decay of the Laurentide Ice Sheet in Western Baffin Bay during the Last glacial episode. Sci. Rep. 7 (1), 10711.
Buckley, J., Willis, E.H., 1972. Isotopes' radiocarbon measurements IX. Radiocarbon 14 (1), 114–139.
Calkin, P.E., Muller, E.H., Barnes, J.H., 1982. The Gowanda hospital interstadial site, New York. Am. J. Sci. 282 (7), 1110–1142.
Campbell, J.E., Little, E.C., Utting, D., McMartin, I., 2013. Surficial geology, Nanuraqtalik Lake, Nunavut; CGM-P60. Geol. Surv. Canada 1, 50, 000 scale.
Carlson, A.E., Tarasov, L., Pico, T., 2018. Rapid Laurentide ice-sheet advance towards southern Last Glacial Maximum limit during marine isotope stage 3. Quat. Sci. Rev. 196, 118–123.
Caron, O., 2013. Synthèse et modèle cartographique 3D des formations quaternaires pour les bassins-versants des rivières Chaudière et Saint-François: Géochronologie, stratigraphie et paléogéographie wisconsinienne du sud du Québec. Université du Québec à Montréal, 358 pp.
Carr, J.R., Stokes, C.R., Vieli, A., 2017. Threefold increase in marine-terminating outlet glacier retreat rates across the Atlantic Arctic: 1992–2010. Ann. Glaciol. 58 (74), 72–91.
Causse, C., Vincent, J.S., 1989. Th-U disequilibium dating of Middle and Late Pleistocene wood and shells from Banks and Victoria islands, Arctic Canada. Can. J. Earth Sci. 26 (12), 2718–2723.
Ceperley, E.G., Marcott, S.A., Rawling, J.E., 2018. A 10be Based Chronology for the Arnott Moraine of the Laurentide Ice Sheet, Central Wisconsin.
Ceperley, E.G., Marcott, S.A., Rawling, J.E., Zoet, L.K., Zimmerman, S.R.H., 2019. The role of permafrost on the morphology of an MIS 3 moraine from the southern Laurentide Ice Sheet. Geology 47 (5), 440–444.
Clark, P.U., Clague, J.J., Curry, B.B., Dreimanis, A., Hicock, S.R., Miller, G.H., Berger, G. W., Eyles, N., Lamothe, M., Miller, B.B., Mott, R.J., Oldale, R.N., Stea, R.R., Szabo, J. P., Thorleifson, L.H., Vincent, J.S., 1993. Initiation and development of the Laurentide and Cordilleran Ice Sheets following the last interglaciation. Quat. Sci. Rev. 12 (2), 79–114.
Clark, P.U., Dyke, A.S., Shakun, J.D., Carlson, A.E., Clark, J., Wohlfarth, B., Mitrovica, J. X., Hostetler, S.W., McCabe, A.M., 2009. The Last Glacial Maximum. Science 325 (5941), 710–714.
Clayton, L., Moran, S.R., 1982. Chronology of Late Wisconsinan Glaciation in Middle North America. Quat. Sci. Rev. 1, 55–82.
Clet, M., Occhietti, S., 1994. Palynologie et paléoenvironnements des épisodes du Sable de Lotbinière et des Varves de Deschaillons (Pléistocène supérieur) de la vallée du Saint-Laurent. Can. J. Earth Sci. 31 (9), 1474–1485.
Colgan, P.M., Vanderlip, C.A., Braunschneider, K.N., 2015. Athens Subepisode (Wisconsin Episode) non-glacial, and older glacial sediments in the subsurface of southwestern Michigan, USA. Quat. Res. 84 (3), 382–397.
Condron, A., Winsor, P., 2012. Meltwater routing and the Younger Dryas. Proc. Natl. Acad. Sci. 109 (49), 19928–19933.
Dalton, A.S., Finkelstein, S.A., Barnett, P.J., Forman, S.L., 2016. Constraining the Late Pleistocene history of the Laurentide Ice Sheet by dating the Missinaibi Formation, Hudson Bay Lowlands, Canada. Quat. Sci. Rev. 146, 288–299.
Dalton, A.S., Väliranta, M., Barnett, P.J., Finkelstein, S.A., 2017. Pollen and macrofossil-inferred paleoclimate at the Ridge Site, Hudson Bay Lowlands, Canada: Evidence for a dry climate and significant recession of the Laurentide Ice Sheet during Marine Isotope Stage 3. Boreas 46 (3), 388–401.
Dalton, A.S., Finkelstein, S.A., Barnett, P.J., Väliranta, M., Forman, S.L., 2018. Late Pleistocene chronology, palaeoecology and stratigraphy at a suite of sites along the Albany River, Hudson Bay Lowlands, Canada. Palaeogeogr. Palaeoclimatol. Palaeoecol. 492, 50–63.
Dalton, A.S., Finkelstein, S.A., Forman, S.L., Barnett, P.J., Pico, T., Mitrovica, J.X., 2019. Was the Laurentide Ice Sheet significantly reduced during Marine Isotope Stage 3? Geology 47 (2), 111–114.
Dalton, A.S., Margold, M., Stokes, C.R., Tarasov, L., Dyke, A.S., Adams, R.S., Allard, S., Arends, H.E., Atkinson, N., Attig, J.W., Barnett, P.J., Barnett, R.L., Batterson, M., Bernatchez, P., Borns, H.W., Breckenridge, A., Briner, J.P., Brouard, E., Campbell, J. E., Carlson, A.E., Clague, J.J., Curry, B.B., Daigneault, R.-A., Dubé-Loubert, H., Easterbrook, D.J., Franzi, D.A., Friedrich, H.G., Funder, S., Gauthier, M.S., Gowan, A.S., Harris, K.L., Hétu, B., Hooyer, T.S., Jennings, C.E., Johnson, M.D., Kehew, A.E., Kelley, S.E., Kerr, D., King, E.L., Kjeldsen, K.K., Knaeble, A.R., Lajeunesse, P., Lakeman, T.R., Lamothe, M., Larson, P., Lavoie, M., Loope, H.M., Lowell, T.V., Lusardi, B.A., Manz, L., McMartin, I., Nixon, F.C., Occhietti, S., Parkhill, M.A., Piper, D.J.W., Pronk, A.G., Richard, P.J.H., Ridge, J.C., Ross, M., Roy, M., Seaman, A., Shaw, J., Stea, R.R., Teller, J.T., Thompson, W.B., Thorleifson, L.H., Utting, D.J., Veillette, J.J., Ward, B.C., Weddle, T.K., Wright, H.E., 2020. An updated radiocarbon-based ice margin chronology for the last deglaciation of the North American Ice Sheet Complex. Quat. Sci. Rev. 234, 106223.
Dansgaard, W., Johnsen, S.J., Clausen, H.B., Dahl-Jensen, D., Gundestrup, N.S., Hammer, C.U., Hvidberg, C.S., Steffensen, J.P., Sveinbjörnsdottir, A.E., Jouzel, J., Bond, G., 1993. Evidence for general instability of past climate from a 250-kyr ice-core record. Nature 364, 218–220.
deVries, H., Dreimanis, A., 1960. Finite radiocarbon dates of the port talbot interstadial deposits in Southern Ontario. Science 131 (3415), 1738–1739.
Dionne, J.-C., Occhietti, S., 1996. Aperçu du Quaternaire à l'embouchure du Saguenay, Québec. Géog. Phys. Quatern. 50 (1), 5–34.
Dorale, J.A., Onac, B.P., Fornós, J.J., Ginés, J., Ginés, A., Tuccimei, P., Peate, D.W., 2010. Sea-level highstand 81,000 years ago in Mallorca. Science 327, 860–863.
Dorion, C.C., 1997. An Updated High Resolution Chronology of Deglaciation and Accompanying Marine Transgression in Maine. University of Maine. MSc thesis, 147 pp.
Dredge, L.A., Thorleifson, L.H., 1987. The Middle Wisconsinan history of the Laurentide Ice Sheet. Géog. Phys. Quatern. 41 (2), 215–235.
Dredge, L.A., Morgan, A.V., Nielsen, E., 1990. Sangamon and pre-sangamon interglaciations in the Hudson Bay Lowlands of Manitoba. Géog. Phys. Quatern. 44 (3), 319–336.
Dreimanis, A., Terasmae, J., McKenzie, G.D., 1966. The Port Talbot Interstade of the Wisconsin Glaciation. Can. J. Earth Sci. 3 (3), 305–325.
Dubé-Loubert, H., Roy, M., Allard, G., Lamothe, M., Veillette, J.J., 2013. Glacial and nonglacial events in the eastern James Bay lowlands, Canada. Can. J. Earth Sci. 50 (4), 379–396.
Dyke, A.S., 1999. Last Glacial Maxiumm and deglaciation of Devon Island, Arctic Canada: support for an Innuitian ice sheet. Quat. Sci. Rev. 18 (3), 393–420.
Dyke, A.S., 2004. An outline of North American deglaciation with emphasis on central and northern Canada. In: Ehlers, J., Gibbard, P.L. (Eds.), Quaternary Glaciations - Extent and Chronology, Part II. Elsevier, pp. 373–424.
Dyke, A.S., Prest, V.K., 1987. Late Wisconsinan and Holocene History of the Laurentide Ice Sheet. Géog. Phys. Quatern. 41 (2), 237–263.
Dyke, A.S., Andrews, J.T., Clark, P.U., England, J.H., Miller, G.H., Shaw, J., Veillette, J. J., 2002. The Laurentide and Innuitian ice sheets during the Last Glacial Maximum. Quat. Sci. Rev. 21 (1-3), 9–31.
Engels, J.L., Edwards, M.H., Polyak, L., Johnson, P.D., 2008. Seafloor evidence for ice shelf flow across the Alaska–Beaufort margin of the Arctic Ocean. Earth Surf. Process. Landf. 33 (7), 1047–1063.
England, J., 1978. The glacial geology of northeastern Ellesmere Island, N.W.T, Canada. Can. J. Earth Sci. 15 (4), 603–617.
England, J., 1990. The late Quaternary history of Greely Fiord and its tributaries, west-central Ellesmere Island. Can. J. Earth Sci. 27 (2), 255–270.
England, J., 1996. Glacier dynamics and paleoclimatic change during the last glaciation of eastern Ellesmere Island, Canada. Can. J. Earth Sci. 33 (5), 779–799.
England, J., Smith, I.R., Evans, D.J.A., 2000. The last glaciation of east-central Ellesmere Island, Nunavut: ice dynamics, deglacial chronology, and sea level change. Can. J. Earth Sci. 37 (10), 1355–1371.
England, J., Atkinson, N., Bednarski, J., Dyke, A.S., Hodgson, D.A., Cofaigh, Ó., C., 2006. The Innuitian Ice Sheet: configuration, dynamics and chronology. Quat. Sci. Rev. 25 (7–8), 689–703.
England, J.H., Furze, M.F.A., Doupé, J.P., 2009. Revision of the NW Laurentide Ice Sheet: implications for paleoclimate, the northeast extremity of Beringia, and Arctic Ocean sedimentation. Quat. Sci. Rev. 28 (17-18), 1573–1596.
Eschman, D.F., 1980. Some evidence of Mid-Wisconsinan Events in Michigan. Mich. Acad. 12, 423–436.
Evans, D.J.A., Campbell, I.A., 1992. Glacial and postglacial stratigraphy of Dinosaur Park and surrounding plains, southern Alberta, Canada. Quat. Sci. Rev. 11 (5), 535–555.
Evans, D.J.A., England, J.H., La Farge, C., Coulthard, R.D., Lakeman, T.R., Vaughan, J. M., 2014. Quaternary geology of the Duck Hawk Bluffs, southwest Banks Island, Arctic Canada: a re-investigation of a critical terrestrial type locality for glacial and interglacial events bordering the Arctic Ocean. Quat. Sci. Rev. 91, 82–123.
Eyles, C.H., Eyles, N., 1983. Sedimentation in a large lake: a reinterpretation of the late Pleistocene stratigraphy at Scarborough Bluffs, Ontario, Canada. Geology 11 (3), 146–152.
Eyles, N., Williams, N.E., 1992. The sedimentary and biological record of the last interglacial-glacial transition at Toronto, Canada. Geol. Soc. Am. Spec. Pap. 270, 119–137.
Fenton, M.M., 1974. The Quaternary stratigraphy of a portion of southeastern Manitoba, Canada. University of Western Ontario, London, Ontario, Canada.
Ferland, P., Occhietti, S., 1990. L'Argile de La Pérade : nouvelle unité marine antérieure au Wisconsinien supérieur, vallée du Saint-Laurent, Québec. Géogr. Phys. Q. 44 (2), 159.
Fisher, T.G., Waterson, N., Lowell, T.V., Hajdas, I., 2009. Deglaciation ages and meltwater routing in the Fort McMurray region, northeastern Alberta and northwestern Saskatchewan, Canada. Q. Sci. Rev. 28 (17-18), 1608–1624.
Flint, R.F., 1943. Growth of North American ice sheet during the Wisconsin age. Geol. Soc. Am. Bull. 54 (3), 325–362.
Forman, S.L., Bettis II, E.A., Kemmis, T.J., Miller, B.B., 1992. Chronologic evidence for multiple periods of loess deposition during the Late Pleistocene in the Missouri and Mississippi River Valley, United States: Implications for the activity of the Laurentide ice sheet. Palaeogeogr. Palaeoclimatol. Palaeoecol. 93 (1-2), 71–83.
Fréchette, B., Wolfe, A.P., Miller, G.H., Richard, P.J.H., de Vernal, A., 2006. Vegetation and climate of the last interglacial on Baffin Island, Arctic Canada. Palaeogeogr. Palaeoclimatol. Palaeoecol. 236 (1-2), 91–106.
Fritz, M., Wetterich, S., Schirrmeister, L., Meyer, H., Lantuit, H., Preusser, F., Pollard, W. H., 2012. Eastern Beringia and beyond: Late Wisconsinan and Holocene landscape dynamics along the Yukon Coastal Plain, Canada. Palaeogeogr. Palaeoclimatol. Palaeoecol. 319-320, 28–45.
Frolking, T.A., Szabo, J.P., 1998. Quaternary Geology along the Eastern Margin of the Scioto Lobe in Central Ohio. Dept. of Natural Resources, Division of Geological Survey, Columbus, State of Ohio, 40 pp.

Frye, J.C., Glass, H.D., Kempton, J.P., Willman, H.B., 1969. Glacial tills of Northwestern Illinois. Illinois State Geol. Surv. Circ. 437, 47.
Fullerton, D.S., Colton, R.B., 1986. Stratigraphy and correlation of the glacial deposits on the Montana Plains. Quat. Sci. Rev. 5, 69–82.
Fulton, R.J.E., 1989. Quaternary geology of Canada and Greenland.
Gadd, N.R., 1971. Pleistocene geology of the Central St. Lawrence Lowland. Geological Survey of Canada. Memoir 359, 153.
Ganopolski, A., Calov, R., 2011. The role of orbital forcing, carbon dioxide and regolith in 100 kyr glacial cycles. Clim. Past 7 (4), 1415–1425.
Gephart, G.D., Monaghan, G.W., Larson, G.J., 1982. A mid-Wisconsinan event in the Lake Michigan Basin [abstract]. Geol. Soc. Am. Abstr. Programs 14 (5), 260.
Godfrey-Smith, D.I., Huntley, D.J., Chen, W.H., 1988. Optical dating studies of quartz and feldspar sediment extracts. Quat. Sci. Rev. 7 (3-4), 373–380.
Govin, A., Capron, E., Tzedakis, P.C., Verheyden, S., Ghaleb, B., Hillaire-Marcel, C., St-Onge, G., Stoner, J.S., Bassinot, F., Bazin, L., Blunier, T., Combourieu-Nebout, N., El Ouahabi, A., Genty, D., Gersonde, R., Jimenez-Amat, P., Landais, A., Martrat, B., Masson-Delmotte, V., Parrenin, F., Seidenkrantz, M.S., Veres, D., Waelbroeck, C., Zahn, R., 2015. Sequence of events from the onset to the demise of the Last Interglacial: Evaluating strengths and limitations of chronologies used in climatic archives. Quat. Sci. Rev. 129, 1–36.
Gowan, E.J., Zhang, X., Khosravi, S., Rovere, A., Stocchi, P., Hughes, A.L.C., Gyllencreutz, R., Mangerud, J., Svendsen, J.I., Lohmann, G., 2021. Global ice sheet reconstruction for the past 80000 years. Nat. Commun. 12 (1199).
Gratton, D., Gwyn, Q.H.J., Dubois, M., J.M., 1984. Les paléoenvironnements sédimentaires au Wisconsinien moyen et supérieur, île d'Anticosti, golfe du Saint-Laurent, Québec. Géog. Phys. Quatern. 38 (3), 229–242.
Grootes, P.M., Stuiver, M., White, J.W.C., Johnsen, S., Jouzel, J., 1993. Comparison of oxygen isotope records from the GISP2 and GRIP Greenland ice cores. Nature 366 (6455), 552–554.
Guyard, H., St-Onge, G., Pienitz, R., Francus, P., Zolitschka, B., Clarke, G.K.C., Hausmann, S., Salonen, V.-P., Lajeunesse, P., Ledoux, G., Lamothe, M., 2011. New insights into Late Pleistocene glacial and postglacial history of northernmost Ungava (Canada) from Pingualuit Crater Lake sediments. Quat. Sci. Rev. 30 (27-28), 3892–3907.
Gwiazda, R.H., Hemming, S.R., Broecker, W.S., 1996. Provenance of icebergs during Heinrich Event 3 and the contrast to their sources during other Heinrich episodes. Paleoceanography 11 (4), 371–378.
Heath, S.L., Loope, H.M., Curry, B.B., Lowell, T.V., 2018. Pattern of southern Laurentide Ice Sheet margin position changes during Heinrich Stadials 2 and 1. Quat. Sci. Rev. 201, 362–379.
Helmens, K.F., 2014. The Last Interglacial–Glacial cycle (MIS 5–2) re-examined based on long proxy records from central and northern Europe. Quat. Sci. Rev. 86, 115–143.
Hemming, S.R., 2004. Heinrich events: Massive late Pleistocene detritus layers of the North Atlantic and their global climate imprint. Rev. Geophys. 42 (1). RG1005, 1-43.
Hickin, A.S., Lian, O.B., Levson, V.M., 2016. Coalescence of late Wisconsinan Cordilleran and Laurentide ice sheets east of the Rocky Mountain Foothills in the Dawson Creek region, northeast British Columbia, Canada. Quat. Res. 85 (3), 409–429.
Hillaire-Marcel, C., Causse, C., 1989. Chronologie Th/U des concrétions calcaires des varves du lac glaciaire de Deschaillons (Wisconsinien inférieur). Can. J. Earth Sci. 26 (5), 1041–1052.
Hillaire-Marcel, C., Page, P., 1981. Paléotempératures Isotopiques du Lac Glaciaire de Deschaillons. In: Mahaney, W.C. (Ed.), Quaternary Paleoclimate. Geo Abstracts Ltd., Norwich, pp. 273–298.
Horberg, L., Anderson, R.C., 1956. Bedrock Topography and Pleistocene Glacial Lobes in Central United States. J. Geol. 64 (2), 101–116.
Hughes, O.L., Tarnocai, C., Schweger, C.E., 1993. Pleistocene stratigraphy, paleopedology, and paleoecology of a multiple till sequence exposed on the Little Bear River, Western District of Mackenzie, N.W.T., Canada. Can. J. Earth Sci. 30 (4), 851–866.
Hughes, A.L.C., Gyllencreutz, R., Lohne, Ø.S., Mangerud, J., Svendsen, J.I., 2016. The last Eurasian ice sheets – a chronological database and time-slice reconstruction, DATED-1. Boreas 45, 1–45.
Huntley, D., Mills, A., Paulen, R., 2008. Surficial deposits, landforms, glacial history, and reconnaissance drift sampling in the Trout Lake map area, Northwest Territories. Geol. Surv. Can. Curr. Res. 2008-14.
Ives, J.D., 1957. Glaciation of the Torngat Mountains. North. Labrador. Arctic 10 (2), 67–87.
Jackson, L.E., Andriashek, L.D., Phillips, F.M., 2011. Chapter 45: Limits of Successive Middle and Late Pleistocene Continental Ice Sheets, Interior Plains of Southern and Central Alberta and Adjacent Areas. In: Ehlers, J., Gibbard, P.L., Hughes, P.D. (Eds.), Developments in Quaternary Science, vol. 15. Elsevier, pp. 575–589.
Jass, C.N., Beaudoin, A.B., 2014. Radiocarbon Dates of Late Quaternary Megafauna and Botanical Remains from Central Alberta, Canada. Radiocarbon 56 (3), 1215–1222.
Jenner, K.A., Campbell, D.C., Piper, D.J.W., 2018. Along-slope variations in sediment lithofacies and depositional processes since the Last Glacial Maximum on the northeast Baffin margin, Canada. Mar. Geol. 405, 92–107.
Johansson, P., Lunkka, J.P., Sarala, P., 2011. Chapter 9 - The Glaciation of Finland. In: Ehlers, J., Gibbard, P.L., Hughes, P.D. (Eds.), Developments in Quaternary Sciences. Elsevier, pp. 105–116.
Johnsen, S.J., Clausen, H.B., Dansgaard, W., Fuhrer, K., Gundestrup, N., Hammer, C.U., Iversen, P., Jouzel, J., Stauffer, B., steffensen, J.P., 1992a. Irregular glacial interstadials recorded in a new Greenland ice core. Nature 359 (6393), 311–313.
Johnsen, S.J., Clausen, H.B., Dansgaard, W., Fuhrer, K., Gundestrup, N., Hammer, C.U., Iversen, P., Jouzel, J., Stauffer, B., Steffensen, J.P., 1992b. Irregular glacial interstadials recorded in a new Greenland ice core. Nature 359, 311–313.
Johnson, W.H., Glass, H.D., Gross, D.L., Moran, S.R., 1971. Glacial drift of the Shelbyville Moraine at Shelbyville, Illinois. Illinois Geol. Surv. Circ. 459, 22.
Josenhans, H.W., Zevenhuizen, J., Klassen, R.A., 1986. The Quaternary geology of the Labrador shelf. Can. J. Earth Sci. 23 (8), 1190–1213.
Karig, D.E., Miller, N.G., 2013. Middle Wisconsin glacial advance into the Appalachian Plateau, Sixmile Creek, Tompkins Co., NY. Quat. Res. 80 (3), 522–533.
Karrow, P.F., 1963. Pleistocene Geology of the Hamilton-Galt Area. Ontario Department of Mine Geological Report No. 16: 68 + maps.
Karrow, P.F., 1967. Pleistocene geology of the Scarborough Area. Ontario Geol. Surv. Rep. 46, 108.
Karrow, P.F., 1974. Till stratigraphy in parts of Southwestern Ontario. Geol. Soc. Am. Bull. 85 (5), 761–768.
Karrow, P.F., Dreimanis, A., Barnett, P.J., 2000. A proposed diachronic revision of late quaternary time-stratigraphic classification in the Eastern and Northern Great Lakes Area. Quat. Res. 54 (1), 1–12.
Karrow, P.F., Bloom, A.L., Haas, J.N., Heiss, A.G., McAndrews, J.H., Miller, B.B., Morgan, A.V., Seymour, K.L., 2009. The Fernbank interglacial site near Ithaca, New York, USA. Quat. Res. 72 (1), 132–142.
Kaufman, D.S., Williams, K.M., 1992. Radiocarbon Date List VII: Baffin Island, N.W.T., Canada. Institute of Arctic and Alpine Research Occasional Paper No. 48.
Kehew, A.E., Beukema, S.P., Bird, B.C., Kozlowski, A.L., 2005. Fast flow of the Lake Michigan Lobe: evidence from sediment-landform assemblages in southwestern Michigan, USA. Quat. Sci. Rev. 24 (22), 2335–2353.
Kerr, P.J., Tassier-Surine, S.A., Kilgore, S.M., Bettis III, E.A., Dorale, J.A., Cramer, B.D., 2021. Timing, provenance, and implications of two MIS 3 advances of the Laurentide Ice Sheet into the Upper Mississippi River Basin, USA. Quat. Sci. Rev. 261, 106926.
King, L.H., 1996. Late Wisconsinan ice retreat from the Scotian Shelf. Geol. Soc. Am. Bull. 108 (8), 1056–1067.
Kleman, J., Jansson, K., De Angelis, H., Stroeven, A.P., Hättestrand, C., Alm, G., Glasser, N., 2010. North American Ice Sheet build-up during the last glacial cycle, 115–21kyr. Quat. Sci. Rev. 29 (17-18), 2036–2051.
Kleman, J., Hättestrand, M., Borgström, I., Fabel, D., Preusser, F., 2021. Age and duration of a MIS 3 interstadial in the Fennoscandian Ice Sheet core area – Implications for ice sheet dynamics. Quat. Sci. Rev. 264, 107011.
Koerner, R.M., 1980. Instantaneous glacierization, the rate of albedo change, and feedback effects at the beginning of an ice age. Quat. Res. 13 (2), 153–159.
Lacelle, D., Lauriol, B., Clark, I.D., Cardyn, R., Zdanowicz, C., 2007. Nature and origin of a Pleistocene-age massive ground-ice body exposed in the Chapman Lake moraine Complex, central Yukon Territory, Canada. Q. Res. 68 (2), 249–260.
Lakeman, T.R., 2012. Quaternary Glaciation of Central Banks Island, NT, Canada. University of Alberta, Edmonton, Alberta. PhD thesis. 203 pp.
Lakeman, T.R., England, J.H., 2013. Late Wisconsinan glaciation and postglacial relative sea-level change on western Banks Island, Canadian Arctic Archipelago. Q. Res. 80 (1), 99–112.
Lambeck, K., Chappell, J., 2001. Sea level change through the last glacial cycle. Science 292, 679–686.
Lamothe, M., 1984. Apparent thermoluminescence ages of St-Pierre Sediments at Pierreville, Quebec, and the problem of anomalous fading. Can. J. Earth Sci. 21 (12), 1406–1409.
Lamothe, M., 1985. Lithostratigraphy And Geochronology Of The Quaternary Deposits Of The Pierreville And St-pierre Les Becquets Areas, Quebec. University of Western Ontario, London, Ontario, Canada. PhD thesis. 224 pp.
Lamothe, M., 1989. A new framework for the pleistocene stratigraphy of the Central St. Lawrence Lowland, Southern Québec. Géog. Phys. Quatern. 43 (2), 119.
Lamothe, M., Huntley, D.J., 1988. Thermoluminescence Dating of Late Pleistocene Sediments, St. Lawrence Lowland, Québec. Géog. Phys. Quatern. 42 (1), 33.
Lamothe, M., Parent, M., Shilts, W.W., 1992. Sangamonian and early Wisconsinan events in the St. Lawrence Lowland and Appalachians of southern Quebec, Canada. Geol. Soc. Am. Spec. Pap. 270, 171–184.
Lévesque, Y., St-Onge, G., Lajeunesse, P., Desiage, P.-A., Brouard, E., 2020. Defining the maximum extent of the Laurentide Ice Sheet in Home Bay (eastern Arctic Canada) during the Last Glacial episode. Boreas 49, 52–70.
Leydet, D.J., Carlson, A.E., Teller, J.T., Breckenridge, A., Barth, A.M., Ullman, D.J., Sinclair, G., Milne, G.A., Cuzzone, J.K., Caffee, M.W., 2018. Opening of glacial Lake Agassiz's eastern outlets by the start of the Younger Dryas cold period. Geology 46 (2), 155–158.
Li, G., Piper, D.J.W., Campbell, D.C., 2011. The Quaternary Lancaster Sound trough-mouth fan, NW Baffin Bay. J. Quat. Sci. 26 (5), 511–522.
Linsley, B.K., 1996. Oxygen-isotope record of sea level and climate variations in the Sulu Sea over the past 150,000 years. Nature 380 (6571), 234–237.
Lisiecki, L.E., Raymo, M.E., 2005. A Pliocene-Pleistocene stack of 57 globally distributed benthic $\delta^{18}O$ records. Paleoceanography 20, PA1003.
Liu, C.-L., Riley, K.M., Coleman, D.D., 1986. Illinois State Geological Survey radiocarbon dates IX. Radiocarbon 28 (1), 110–133.
Liverman, D.G.E., Catto, N.R., Rutter, N.W., 1989. Laurentide glaciation in west-central Alberta: a single (Late Wisconsin) event. Can. J. Earth Sci. 26 (2), 266–274.
Löfverström, M., Lora, J.M., 2017. Abrupt regime shifts in the North Atlantic atmospheric circulation over the last deglaciation. Geophys. Res. Lett. 44 (15), 8047–8055.
Loope, H.M., Antinao, J.L., Lowell, T.V., Curry, B.B., Monaghan, G.W., 2018. Chronology of Laurentide Ice Sheet fluctuations surrounding the Last Glacial Maximum, Central Indiana, USA. In: Geological Society of America 130th Annual Meeting, Indianapolis, Indiana.
Lowdon, J.A., Blake, W.J., 1970. Geological survey of Canada radiocarbon dates IX. Radiocarbon 12 (1), 46–86.

Lowdon, J.A., Blake, W.J., 1975. Geological survey of Canada radiocarbon dates XV. Geol. Surv. Canada Pap. 75-7.
Lowdon, J.A., Fyles, J.G., Blake, W.J., 1967. Geological survey of Canada radiocarbon dates VI. Radiocarbon 9, 156–197.
Lowdon, J.A., Robertson, I.M., Blake, W.J., 1971. Geological survey of Canada radiocarbon dates XI. Radiocarbon 13 (2), 255–324.
Lowdon, J.A., Robertson, I.M., Blake, W.J., 1977. Geological survey of Canada radiocarbon dates XVII. Geol. Surv. Canada 77-7, 25.
Lowell, T.V., Savage, K.M., Scott Brockman, C., Stuckenrath, R., 1990. Radiocarbon analyses from Cincinnati, Ohio, and their implications for glacial stratigraphic interpretations. Quat. Res. 34 (1), 1–11.
MacDonald, B.G., 1971. Late Quaternary Stratigraphy and Deglaciation in Eastern Canada, The Late Cenozoic Glacial Ages. Yale Univeristy Press, pp. 331–353.
MacLean, B., Blasco, S., Bennett, R., Lakeman, T., Hughes-Clarke, J., Kuus, P., Patton, E., 2015. New marine evidence for a Late Wisconsinan ice stream in Amundsen Gulf, Arctic Canada. Quat. Sci. Rev. 114, 149–166.
MacNeill, R.H., 1969. Some dates relating to the dating of the last major ice sheet in Nova Scotia. Marit. Sed. 5 (1), 3.
Manley, W.F., Jennings, A.E., 1996. Radiocarbon Date List VIII: Eastern Canadian Arctic, Labrador, Northern Quebec, East Greenland Shelf, Iceland Shelf, and Antarctica. University of Colorado, Institute of Arctic and Alpine Research.
Margold, M., Stokes, C.R., Clark, C.D., 2015. Ice streams in the Laurentide Ice Sheet: Identification, characteristics and comparison to modern ice sheets. Earth Sci. Rev. 143, 117–146.
Marshall, S.J., 2002. Modelled nucleation centres of the Pleistocene ice sheets from an ice sheet model with subgrid topographic and glaciologic parameterizations. Quat. Int. 95-96, 125–137.
Marshall, S.J., Tarasov, L., Clarke, G.K.C., Peltier, W.R., 2000. Glaciological reconstruction of the Laurentide Ice Sheet: physical processes and modelling challenges. Can. J. Earth Sci. 37 (5), 769–793.
McDonald, B.C., Shilts, W.W., 1971. Quaternary stratigraphy and events in Southeastern Quebec. Geol. Soc. Am. Bull. 82 (3), 683.
McMartin, I., Campbell, J.E., Dredge, L.A., 2019. Middle Wisconsinan marine shells near Repulse Bay, Nunavut, Canada: implications for Marine Isotope Stage 3 ice-free conditions and Laurentide Ice Sheet dynamics in north-west Hudson Bay. J. Quat. Sci. 34 (1), 64–75.
McNeely, R., 2002. Geological survey of Canada radiocarbon dates XXXIII. Geol. Surv. Canada Curr. Res. 2001, 1–51.
McNeely, R., 2006. Geological survey of Canada radiocarbon dates XXXV. Geol. Surv. Can. Pap. 2006-G, 1–156.
McNeely, R., Atkinson, D.E., 1995. Geological survey of Canada radiocarbon dates XXXII. Geol. Surv. Can. Pap. 1995-G, 1–92.
McNeely, R., Jorgensen, P.K., 1992. Geological survey of Canada radiocarbon dates XXX. Geol. Surv. Can. Pap. 90-7, 1–84.
McNeely, R., Jorgensen, P.K., 1993. Geological survey of Canada radiocarbon dates XXXI. Geol. Surv. Canada Pap. 91-7, 1–85.
McNeely, R., McCuaig, S., 1991. Geological survey of Canada radiocarbon dates XXIX. Geol. Surv. Can. Pap. 89-7, 1–134.
Miles, B.W.J., Stokes, C.R., Jamieson, S.S.R., 2016. Pan–ice-sheet glacier terminus change in East Antarctica reveals sensitivity of Wilkes Land to sea-ice changes. Sci. Adv. 2 (5), e1501350.
Miller, G.H., Andrews, J.T., 2019. Hudson Bay was not deglaciated during MIS-3. Quat. Sci. Rev. 225, 105944.
Miller, G.H., Andrews, J.T., Short, S.K., 1977. The last interglacial-glacial cycle, Clyde foreland, Baffin Island, N.W.T.: stratigraphy, biostratigraphy, and chronology. Can. J. Earth Sci. 14 (12), 2824–2857.
Miller, G.H., Mode, W.N., Wolfe, A.P., Sauer, P.E., Bennike, O., Forman, S.L., Short, S.K., Stafford, T.W.J., 1999. Stratified interglacial lacustrine sediments from Baffin Island, Arctic Canada: chronology and paleoenvironmental implications. Quat. Sci. Rev. 18 (6), 789–810.
Monaghan, G.W., Larson, G.J., 1986. Late Wisconsinan drift stratigraphy of the Saginaw Ice Lobe in south-central Michigan. Geol. Soc. Am. Bull. 97, 324–328.
Monaghan, G.W., Larson, G.J., Gephart, G.D., 1986. Late Wisconsinan drift stratigraphy of the Lake Michigan Lobe in southwestern Michigan. Geol. Soc. Am. Bull. 97 (3), 329–334.
Mosher, D.C., Piper, D.J.W., Vilks, G.V., Aksu, A.E., Fader, G.B., 1989. Evidence for Wisconsinan glaciations in the Verrill Canyon area, Scotian Slope. Quat. Res. 31 (1), 27–40.
Mulligan, R.P.M., Bajc, A.F., 2018. The pre-Late Wisconsin stratigraphy of southern Simcoe County, Ontario: implications for ice sheet buildup, decay, and Great Lakes drainage evolution. Can. J. Earth Sci. 55 (7), 709–729.
Munroe, J.S., Perzan, Z.M., Amidon, W.H., 2016. Cave sediments constrain the latest Pleistocene advance of the Laurentide Ice Sheet in the Champlain Valley, Vermont, USA. J. Quat. Sci. 31 (8), 893–904.
Murton, J.B., 2009. Stratigraphy and palaeoenvironments of Richards Island and the eastern Beaufort Continental Shelf during the last glacial-interglacial cycle. Permafr. Periglac. Process. 20 (2), 107–125.
Murton, J.B., Bateman, M.D., Telka, A.M., Waller, R., Whiteman, C., Kuzmina, S., 2017. Early to mid Wisconsin Fluvial Deposits and Palaeoenvironment of the Kidluit Formation, Tuktoyaktuk Coastlands, Western Arctic Canada. Permafr. Periglac. Process. 28 (3), 523–533.
Nixon, F.C., England, J.H., 2014. Expanded Late Wisconsinan ice cap and ice sheet margins in the western Queen Elizabeth Islands, Arctic Canada. Quat. Sci. Rev. 91, 146–164.
Ó Cofaigh, C., England, J., Zreda, M., 2000. Late Wisconsinan glaciation of southern Eureka Sound: evidence for extensive Innuitian ice in the Canadian High Arctic during the Last Glacial Maximum. Quat. Sci. Rev. 19 (13), 1319–1341.
Occhietti, S., Balescu, S., Lamothe, M., Clet, M., Cronin, T., Ferland, P., Pichet, P., 1996. Late Stage 5 Glacio-isostatic Sea in the St. Lawrence Valley, Canada and United States. Q. Res. 45 (2), 128–137.
Olsen, L., Sveian, H., Berstrøm, B., Selvik, S.F., Lauritzen, S.-E., Stokland, Ø., Grøsfjeld, G., 2001. Methods and stratigraphies used to reconstruct Mid- and Late Weichselian palaeoenvironmental and paeloclimatic changes in Norway. Norges Geol. Undersøgelse Bull. 438, 21–46.
Packalen, M.S., Finkelstein, S.A., McLaughlin, J.W., 2014. Carbon storage and potential methane production in the Hudson Bay Lowlands since mid-Holocene peat initiation. Nat. Commun. 5, 4078.
Parent, M., Paradis, S.J., Bolsvert, E., 1995. Ice-flow patterns and glacial transport in the eastern Hudson Bay region: implications for the late Quaternary dynamics of the Laurentide Ice Sheet. Can. J. Earth Sci. 32 (12), 2057–2070.
Parent, M., Lefebvre, R., Rivard, C., Lavoie, M., Guilbault, J.-P., 2015. Midwisconsinan fluvial and marine sediments in the Central St Lawrence Lowlands- implications for glacial and deglacial events in the Appalachian Uplands. In: Geological Society of America Northeastern Section - 50th Annual Meeting. Bretton Woods, New Hampshire, USA.
Paulen, R., Beaudoin, A.B., Pawlowicz, J.G., 2005. An interstadial site in the Birch Mountains, North-Central Alberta [poster]. In: Canadian Quaternary (CANQUA) Conference, Winnipeg, Manitoba.
Paulen, R.C., Smith, I.R., Hickin, A.S., 2019. GEM-2 Southern Mackenzie Surficial activity 2018 report: surficial geology and heavy mineral studies in southern Northwest Territories. In: Paulen, R.C., Smith, I.R., Day, S.J.A. (Eds.), Geological Survey of Canada Open File, vol. 8477, pp. 62–70.
Pico, T., Mitrovica, J.X., Ferrier, K.L., Braun, J., 2016. Global ice volume during MIS 3 inferred from a sea-level analysis of sedimentary core records in the Yellow River Delta. Quat. Sci. Rev. 152, 72–79.
Pico, T., Creveling, J.R., Mitrovica, J.X., 2017. Sea-level records from the U.S. mid-Atlantic constrain Laurentide Ice Sheet extent during Marine Isotope Stage 3. Nat. Commun. 8, 15612.
Pico, T., Willenbring, J., Dalton, A.S., Hemming, S., 2021. Was there a glacial outburst flood in the Torngat Mountains during Marine Isotope Stage 3? Clim. Past Discuss. https://doi.org/10.5194/cp-2021-132.
Pigati, J.S., 2002. On correcting 14C ages of gastropod shell carbonate for fractionation. Radiocarbon 44 (3), 755–760.
Piper, D., Macdonald, A., 2001. Timing and position of Late Wisconsinan ice-margins on the upper slope seaward of Laurentian Channel. Géog. Phys. Quatern. 55 (2), 131–140.
Polyak, L., Darby, D.A., Bischof, J.F., Jakobsson, M., 2007. Stratigraphic constraints on late Pleistocene glacial erosion and deglaciation of the Chukchi margin, Arctic Ocean. Quat. Res. 67 (2), 234–245.
Prest, V.K., Hode-Keyser, J., 1977. Geology ants, Montreal Island and vicinity, Quebec. Geol. Surv. Can. Pap. 75-27, 29p.
Rampton, V.N., 1988. Quaternary Geology of the Tuktoyaktuk Coastlands, Northwest Territories. Geological Survey of Canada Memoir 423.
Rashid, H., Piper, D.J.W., Drapeau, J., Marin, C., Smith, M.E., 2019. Sedimentology and history of sediment sources to the NW Labrador Sea during the past glacial cycle. Quat. Sci. Rev. 221, 105880.
Reimer, P.J., Bard, E., Bayliss, A., Beck, J.W., Blackwell, P.G., Bronk Ramsey, C., Buck, C. E., Cheng, H., Edwards, R.L., Friedrich, M., Grootes, P.M., Guilderson, T.P., Haflidason, H., Hajdas, I., Hatté, C., Heaton, T.J., Hoffmann, D.L., Hogg, A.G., Hughen, K.A., Kaiser, K.F., Kromer, B., Manning, S.W., Niu, M., Reimer, R.W., Richards, D.A., Scott, E.M., Southon, J.R., Staff, R.A., Turney, R.S.M., van der Plicht, J., 2013. IntCal13 and Marine13 Radiocarbon Age Calibration Curves 0–50,000 Years cal BP. Radiocarbon 55 (4), 1869–1887.
Rémillard, A.M., St-Onge, G., Bernatchez, P., Hétu, B., Buylaert, J.-P., Murray, A.S., Vigneault, B., 2016. Chronology and stratigraphy of the Magdalen Islands archipelago from the last glaciation to the early Holocene: new insights into the glacial and sea-level history of eastern Canada. Boreas 45 (4), 604–628.
Rémillard, A.M., St-Onge, G., Bernatchez, P., Hétu, B., Buylaert, J.-P., Murray, A.S., Lajeunesse, P., 2017. Relative sea-level changes and glacio-isostatic adjustment on the Magdalen Islands archipelago (Atlantic Canada) from MIS 5 to the late Holocene. Quat. Sci. Rev. 171, 216–233.
Rieck, R.L., Winters, H.A., 1980. Distribution and significance of glacially buried organic matter in Michigan's Southern Peninsula. Phys. Geogr. 1 (1), 74–89.
Rittenour, T.M., Blum, M.D., Goble, R.J., 2007. Fluvial evolution of the lower Mississippi River valley during the last 100 k.y. glacial cycle: Response to glaciation and sea-level change. Geol. Soc. Am. Bull. 119 (5-6), 586–608.
Roger, J., Saint-Ange, F., Lajeunesse, P., Duchesne, M.J., St-Onge, G., Trenhaile, A., 2013. Late quaternary glacial history and meltwater discharges along the Northeastern Newfoundland Shelf. Can. J. Earth Sci. 50 (12), 1178–1194.
Rubin, M., Alexander, C., 1960. U.S. geological survey radiocarbon dates V. Am. J. Sci. Radiocarbon Suppl. 2, 129–185.
Rubin, M., Berthold, S.M., 1961. U. S. geological survey radiocarbon dates VI. Radiocarbon 3, 86–98.
Scourse, J.D., Chiverrell, R.C., Smedley, R.K., Small, D., Burke, M.J., Saher, M., Van Landeghem, K.J.J., Duller, G.A.T., Cofaigh, C.Ó., Bateman, M.D., Benetti, S., Bradley, S., Callard, L., Evans, D.J.A., Fabel, D., Jenkins, G.T.H., McCarron, S., Medialdea, A., Moreton, S., Ou, X., Praeg, D., Roberts, D.H., Roberts, H.M., Clark, C. D., 2021. Maximum extent and readvance dynamics of the Irish Sea Ice Stream and Irish Sea Glacier since the Last Glacial Maximum. J. Quat. Sci. https://doi.org/10.1002/jqs.3313.

Sevon, W.D., Braun, D.D., 2000. Glacial deposits of Pennsylvania, Map 59. In: D.o.C.a.N. R. Commonwealth of Pennsylvania, Bureau of Topographic and Geologic Survey.
Shapiro, B., Drummond, A.J., Rambaut, A., Wilson, M.C., Matheus, P.E., Sher, A.V., Pybus, O.G., Gilbert, M.T.P., Barnes, I., Binladen, J., Willerslev, E., Hansen, A.J., Baryshnikov, G.F., Burns, J.A., Davydov, S., Driver, J.C., Froese, D.G., Harington, C. R., Keddie, G., Kosintsev, P., Kunz, M.L., Martin, L.D., Stephenson, R.O., Storer, J., Tedford, R., Zimov, S., Cooper, A., 2004. Rise and Fall of the Beringian Steppe Bison. Science 306, 1561–1564.
Sharpe, D.R., Barnett, P.J., 1985. Significance of sedimentological studies on the Wisconsinan Stratigraphy of Southern Ontario. Géog. Phys. Quatern. 39 (3), 255.
Shaw, J., Piper, D.J.W., Fader, G.B.J., King, E.L., Todd, B.J., Bell, T., Batterson, M.J., Liverman, D.G.E., 2006. A conceptual model of the deglaciation of Atlantic Canada. Quat. Sci. Rev. 25 (17-18), 2059–2081.
Shilts, W.W., 1981. Surficial geology of the Lac Mégantic area, Québec. Geol. Surv. Can. Mem. 397, 102.
Slomka, J.M., Hartman, G.M.D., 2018. Sedimentary Architecture of a Glaciolacustrine Braidplain Delta: Proxy Evidence of a Pre-Middle Wisconsinan Glaciation (Grimshaw Gravels, Interior Plains, Canada). Boreas.
Small, D., Clark, C.D., Chiverrell, R.C., Smedley, R.K., Bateman, M.D., Duller, G.A.T., Ely, J.C., Fabel, D., Medialdea, A., Moreton, S.G., 2017. Devising quality assurance procedures for assessment of legacy geochronological data relating to deglaciation of the last British-Irish Ice Sheet. Earth Sci. Rev. 164, 232–250.
Smith, D.G., 1992. Glacial Lake Mackenzie, Mackenzie Valley, Northwest Territoties, Canada. Can. J. Earth Sci. 29 (8), 1756–1766.
Smith, I.R., 1999. Late Quaternary glacial history of Lake Hazen Basin and eastern Hazen Plateau, northern Ellesmere Island, Nunavut, Canada. Can. J. Earth Sci. 36 (9), 1547–1565.
Spratt, R.M., Lisiecki, L.E., 2016. A Late Pleistocene sea level stack. Clim. Past 12 (4), 1079–1092.
Stea, R.R., Seaman, A.A., Pronk, T., Parkhill, M.A., Allard, S., Utting, D., 2011. The Appalachian Glacier Complex in Maritime Canada. In: Ehlers, J., Gibbard, P.L., Hughes, P.D. (Eds.), Developments in Quaternary Science, vol. 15, pp. 631–659. Amsterdam.
Steig, E.J., Wolfe, A.P., Miller, G.H., 1998. Wisconsinan refugia and the glacial history of eastern Baffin Island, Arctic Canada: coupled evidence from cosmogenic isotopes and lake sediments. Geology 26 (9), 835–838.
Stokes, C.R., 2017. Deglaciation of the Laurentide Ice Sheet from the Last Glacial Maximum. Cuadernos Invest. Geogr. 43 (2), 377–428.
Stokes, C.R., Clark, C.D., Darby, D.A., Hodgson, D.A., 2005. Late Pleistocene ice export events into the Arctic Ocean from the M'Clure Strait Ice Stream, Canadian Arctic Archipelago. Glob. Planet. Chang. 49 (3), 139–162.
Stokes, C.R., Clark, C.D., Storrar, R., 2009. Major changes in ice stream dynamics during deglaciation of the north-western margin of the Laurentide Ice Sheet. Quat. Sci. Rev. 28 (7), 721–738.
Stokes, C.R., Tarasov, L., Dyke, A.S., 2012. Dynamics of the North American Ice Sheet Complex during its inception and build-up to the Last Glacial Maximum. Quat. Sci. Rev. 50, 86–104.
Stone, J.R., Schafer, J.P., London, E.H., DiGiacomo-Cohen, M.L., Lewis, R.S., Thompson, W.B., 2005. Quaternary geologic Map of Connecticut and Long Island Sound Basin, Scale 1:100,000. United States Geological Survey.
St-Onge, D.A., 1987. The Sangamonian Stage and the Laurentide Ice Sheet. Géog. Phys. Quatern. 41 (2), 189–198.
Stroup, J.S., Lowell, T.V., Breckenridge, A., 2013. A model for the demise of large, glacial Lake Ojibway, Ontario and Quebec. J. Paleolimnol. 50 (1), 105–121.
Tarasov, L., Dyke, A.S., Neal, R.M., Peltier, W.R., 2012. A data-calibrated distribution of deglacial chronologies for the North American ice complex from glaciological modeling. Earth Planet. Sci. Lett. 315-316, 30–40.
Teller, J.T., Fenton, M.M., 1980. Late Wisconsinan glacial stratigraphy and history of southeastern Manitoba. Can. J. Earth Sci. 17, 19–35.
Terasmae, J., 1960. A palynological study of Pleistocene interglacial beds at Toronto, Ontario. Geol. Surv. Canada Bull. 56, 23–48.
Thorleifson, L.H., Wyatt, P.H., Shilts, W.W., 1992. Hudson Bay lowlands Quaternary Stratigraphy: Evidence for Early Wisconsinan Glaciation Centred in Quebec. Geological Society of America.
Totten, S.M., 1969. Overridden Recessional Moraines of North-Central Ohio. Geol. Soc. Am. Bull. 80, 1931–1946.
Treat, C.C., Kleinen, T., Broothaerts, N., Dalton, A.S., Dommain, R., Douglas, T.A., Drexler, J., Finkelstein, S.A., Grosse, G., Hope, G., Hutchings, J., Jones, M.C., Kuhry, P., Lacourse, T., Lähteenoja, O., Loisel, J., Notebaert, B., Payne, R., Peteet, D. M., Sannel, A.B.K., Stelling, J.M., Strauss, J., Swindles, G.T., Talbot, J., Tarnocai, C., Verstarten, G., Williams, C.J., Xia, Z., Yu, Z., Väliranta, M., Hättestrand, M., Alexanderson, H., Brovkin, V., 2019. Widespread global peatland establishment and persistence over the last 130,000 y. Proc. Natl. Acad. Sci. 116 (11), 4822–4827.
Tripsanas, E.K., Bryant, W.R., Slowey, N.C., Bouma, A.H., Karageorgis, A.P., Berti, D., 2007. Sedimentological history of Bryant Canyon area, northwest Gulf of Mexico, during the last 135 kyr (Marine Isotope Stages 1–6): A proxy record of Mississippi River discharge. Palaeogeogr. Palaeoclimatol. Palaeoecol. 246 (1), 137–161.
Tulenko, J.P., Lofverstrom, M., Briner, J.P., 2020. Ice sheet influence on atmospheric circulation explains the patterns of Pleistocene alpine glacier records in North America. Earth Planet. Sci. Lett. 534, 116115.
Tyrrell, J.B., 1898. The glaciation of north Central Canada. J. Geol. 6 (2), 147–160.
United States Geological Survey's Center for Earth Resources Observation and Science (EROS), 2010. 30 Arc-Second DEM of North America. https://databasin.org/datasets/d2198be9d2264de19cb93fe6a380b69c.
Veillette, J.J., 1995. New evidence for northwestward glacial ice flow, James Bay region, Quebec. In: Geological Survey of Canada Current Research 1995-C; Canadian Shield, pp. 249–258.
Veillette, J.J., Pomares, J.-S., 1991. Older ice flows in the Matagami-Chapais area Quebec. In: Geological Survey of Canada, Paper 91-1C, Current Research, Part C, pp. 143–148.
Veillette, J.J., Dyke, A.S., Roy, M., 1999. Ice-flow evolution of the Labrador Sector of the Laurentide Ice Sheet: a review, with new evidence from northern Quebec. Quat. Sci. Rev. 18 (8-9), 993–1019.
de Vernal, A., Causse, C., Hillaire-Marcel, C., Mott, R., Occhietti, S., 1986. Palynostratigraphy and Th/U ages of upper Pleistocene interglacial and interstadial deposits on Cape Breton Island, eastern Canada. Geology 14 (7), 554–557.
Vincent, J.-S., Prest, V.K., 1987. The early Wisconsinan history of the Laurentide ice sheet. Géog. Phys. Quatern. 41 (2), 199–213.
Vogel, J.C., Waterbolk, H.T., 1972. Groningen radiocarbon dates X. Radiocarbon 14 (1), 6–110.
Wang, Y.J., Cheng, H., Edwards, R.L., An, Z.S., Wu, J.Y., Shen, C.-C., Dorale, J.A., 2001. A high-resolution absolute-dated late Pleistocene monsoon record from Hulu Cave, China. Science 294, 2345–2348.
Whipple, K.X., Kirby, E., Brocklehurst, S.H., 1999. Geomorphic limits to climate-induced increases in topographic relief. Nature 401 (6748), 39–43.
White, G.W., 1968. Age and correlation of Pleistocene deposits at Garfield Heights (Cleveland), Ohio. Geol. Soc. Am. Bull. 79 (6), 749–752.
White, G.W., 1984. Glacial Geology of Summit County, Ohio. State of Ohio Department of Natural Resources Division of Geological Survey. Report of Investigations No. 123.
White, G.W., Totten, S.M., Gross, D.L., 1969. Pleistocene Stratigraphy of Northwestern Pennsylvania.
Wickert, A.D., 2016. Reconstruction of North American drainage basins and river discharge since the Last Glacial Maximum. Earth Surf. Dyn. 4 (4), 831–869.
Wickert, A.D., Mitrovica, J.X., Williams, C., Anderson, R.S., 2013. Gradual demise of a thin southern Laurentide ice sheet recorded by Mississippi drainage. Nature 502 (7473), 668–671.
Winters, H.A., Rieck, R.L., 1991. Late Glacial Terrain Transformation in Michigan. Mich. Acad. 23, 137–148.
Wohlfarth, B., 2010. Ice-free conditions in Sweden during Marine Oxygen Isotope Stage 3? Boreas 39 (2), 377–398.
Wolfe, A.P., Fréchette, B., Richard, P.J.H., Miller, G.H., Forman, S.L., 2000. Paleoecology of a >90,000-year lacustrine sequence from Fog Lake, Baffin Island, Arctic Canada. Quat. Sci. Rev. 19 (17-18), 1677–1699.
Wood, J.R., Forman, S.L., Everton, D., Pierson, J., Gomez, J., 2010. Lacustrine sediments in Porter Cave, central Indiana, USA and possible relation to Laurentide ice sheet marginal positions in the middle and late Wisconsinan. Palaeogeogr. Palaeoclimatol. Palaeoecol. 298 (3-4), 421–431.
Wright Jr., H.E., 1962. Role of the Wadena Lobe in the Wisconsin Glaciation of Minnesota. Geol. Soc. Am. Bull. 73, 73–100.
Young, R.A., Burr, G.S., 2006. Middle Wisconsin glaciation in the Genesee Valley, NY: A stratigraphic record contemporaneous with Heinrich Event, H4. Geomorphology 75 (1-2), 226–247.
Young, R.R., Burns, J.A., Smith, D.G., Arnold, L.D., Rains, R.B., 1994. A single, late Wisconsin, Laurentide glaciation, Edmonton area and southwestern Alberta. Geology 22, 683–686.
Young, R.R., Burns, J.A., Rains, R.B., Schowalter, D.B., 1999. Late Pleistocene glacial geomorphology and environment of the Hand Hills region and southern Alberta, related to Middle Wisconsin fossil prairie dog sites. Can. J. Earth Sci. 36 (9), 1567–1581.